



**University of
Zurich^{UZH}**

Department of Geography

The Weissmies Hanging Glacier

Analysis of its Evolution and the Underlying Destabilisation Processes

GEO 511 Master's Thesis

Author

Michael Peneder
09-932-088

Supervised by

Dr. Jérôme Faillietaz
jerome.faillettaz@geo.uzh.ch

Faculty representative

Prof. Dr. Andreas Vieli
andreas.vieli@geo.uzh.ch

Date of Submission: 29.09.2016
Department of Geography, University of Zurich

Summary

A part of the Triftgletscher on the north-west slope of Weissmies (4017 m a.s.l.) in the valley of Saas (canton of Valais, Switzerland) has recently become unstable. In summer 2014 it was feared that a large part of this hanging glacier could break off and lead to a large ice avalanche endangering mountaineering routes, ski runs and even the town of Saas Grund on the valley bottom. In this thesis, the long-term evolution of Triftgletscher as well as the recent evolution of the instability (called Instabil 1) were studied to assess why and how the glacier has reached the present dangerous situation.

Hanging glacier instabilities can be divided into three groups according to their conditions at the ice / bedrock interface: cold, mixed and temperate. The break off of cold glacier instabilities can be predicted with measurements of the velocity and seismic activity. For the second type, this is not possible: The instability develops due to an extending temperate zone without any clear precursory signs. For temperate glacier instabilities, some critical conditions are known that can promote a break off: A pulse of subglacial water runoff together with a less efficient drainage system can increase the water pressure at the bed and lead to a break off. In this context it is important to know that water at the bed of a glacier can either be evacuated in fast / efficient or in slow/ inefficient drainage systems. An efficient drainage system typically develops later in the melting season when high melt and higher water pressure promote the formation of channels.

An analysis of maps, aerial images and digital elevation models showed that a general trend of melting of the tongue and subsequent retreating of Triftgletscher can be observed. The results correspond well with observations from other alpine glaciers. At the tongue, the surface decreased over 60 m between 1971 and 2015. On a plateau near Instabil 1 at around 3200 m above sea level the surface decreased 15 to 30 m. With these results, the hypothesis of another study could be confirmed. Further, a surface decrease of around 40 m was detected next to Instabil 1 with the digital elevation models.

At a smaller scale, this evolution was studied with images from mountaineers from different years. The support of the ice masses below Instabil 1 decreased clearly since 1992. On the side of Instabil 1 bedrock appeared in 2004 where the surface decrease was measured with the digital elevation models. From 2004 to 2015 this zone extended massively. The geometrical changes at Instabil 1 in 2004 can be linked to the summer heat wave 2003, which led to 5-10 % total mass loss of alpine glaciers and a rise of the freezing limit above 4500 m above sea level for 10 days.

The drainage system during the summer of 2015 was analyzed by using webcam images and a semi-qualitative Drainage Efficiency Water Flow (DEWF) index. The peaks in the drainage system were strongly connected to positive temperatures. In addition to that, the temporal evolution from a slow to a fast drainage system could be observed.

In a next step, GPS velocity measurements were compared with the DEWF index and temperature measurements. The GPS velocities followed the temperature changes most of the time. From the data, it was not possible to determine if the type of drainage system influenced the velocities in summer 2015. In general, the GPS velocities were clearly lower than in summer 2014 (around 12 cm / d compared to over 20 cm / d). The GPS velocities showed that in winter 2015 / 2016 the measured velocities were only half as high as the values of summer 2015. This provides evidence that the temperatures and / or the drainage system influence the velocities at Instabil 1.

It was shown that in summer 2014 the subglacial drainage system was not equally developed. Due to lower temperatures at the beginning of the melting period this is not surprising. Increased icefall activity in the summer of 2014 were linked to increased temperature and precipitation peaks. As the weather station of Grächen is relatively far away, the influence of the precipitation peaks has still to be approved with future research. Subglacial drainage systems could also be confirmed for the years 2003, 2004 and from 2009 to 2013. Therefore, the thermal transition at the glacier bed is eventually more advanced than previously assumed.

In the long run the ice / bedrock interface will be fully temperate because future temperatures and the frequency of summer heat waves like 2003 are expected to increase. Such a temperate state could be better assessed as break offs are coupled with rapid changes of the subglacial water runoff. Local temperature and precipitation measurements can help to detect such phases and could then together with velocity measurements be used for an early warning system. Larger break offs will probably more likely occur in spring or towards the end of the melting season when the drainage system is not efficient enough and a pulse of subglacial water flow could trigger a rupture event. In winter, the cold glacier instability conditions can be applied to the Weissmies case. Consequently, the velocity monitoring of Instabil 1 with GPS sensors is still essential to detect changes of the dynamic behavior and to predict larger break offs.

Contents

Abbreviations.....	I
List of Figures and Tables.....	II
Preface.....	IV
1. Introduction.....	1
1.1 Background	1
1.2 General Aim and Research Questions.....	1
1.3 Structure of the Thesis.....	2
2. Theoretical Background.....	3
2.1 Definition of a Hanging Glacier.....	3
2.2 Types of Avalanching Glacier Instabilities.....	5
2.3 Subglacial Drainage Systems	7
2.4 Hanging Glacier as a Hazard.....	9
2.5 Study Site	11
2.6 Previous Studies	13
3. Long-term Evolution	16
3.1 Material and Methods.....	16
3.1.1 Data.....	16
3.1.2 Map Comparison	18
3.1.3 Position of the Tongue.....	18
3.1.4 Aerial Images Comparison	19
3.1.5. Surface Change.....	19
3.2 Results	22
3.2.1 Map Comparison	22
3.2.2 Position of the Tongue.....	23
3.2.3 Aerial Images Comparison	26
3.2.4 Surface Change.....	28
3.3 Discussion	36
3.4 Summary of Results	40
4. Recent Evolution	41
4.1 Material and Methods.....	41
4.1.1 Data.....	41

4.1.2 Geometric Changes of Instabil 1	42
4.1.3 Hydrology	42
4.1.4 Weather Data	43
4.1.5 Velocities	46
4.2 Results	48
4.2.1 Geometric Changes of Instabil 1	48
4.2.2 Hydrology, Weather Data and Velocities	51
4.3 Discussion	60
4.4 Summary of Results	63
5. Synthesis	65
5.1 Conclusion	65
5.2 Future Evolution and Hazard Assessment	65
5.3 Open Questions and Limitations	66
Acknowledgement	68
References	69
6. Appendix	72
Personal Declaration	125

Abbreviations

In this section, some important abbreviations of this thesis are shortly explained.

- a.s.l. = above sea level, used for altitudes.
- DEM = Digital Elevation Model, model or 3D representation of the surface of a terrain.
- ELA = Equilibrium Line Altitude, represents the altitude where the annual accumulation and ablation of a glacier are equal.
- GPS = Global Positioning System, a global navigation satellite system that determines the location in reference to multiple satellites.

List of Figures and Tables

Figures

Figure 1: Classification of avalanching glaciers.....	5
Figure 2: Overview of the subglacial drainage system elements.....	8
Figure 3: Arborescent and non-arborescent drainage systems	9
Figure 4: Large-scale overview of the study area.....	12
Figure 5: Instabilities at the Weissmies	13
Figure 6: Profiles for the determination of the surface change.....	20
Figure 7: Reference points for aligning and georeferencing of the DEM1982	21
Figure 8: Longitudinal profile II.....	22
Figure 9: Comparison of pixel maps 1:25'000	23
Figure 10: Position of the tongue of Triftgletscher over time	24
Figure 11: Observed absolute length changes of Triftgletscher	25
Figure 12: Calculated mean yearly length changes of Triftgletscher	25
Figure 13: Oblique aerial photograph from 1919 and position of tongue 1881	26
Figure 14: Orthogonal aerial image composite.....	27
Figure 15: DHM25 (1995) compared to the pixel map 1:25'000 (1995)	28
Figure 16: swissALTI ^{3D} (2009) compared to pixel map 1:25'000 (2009)	29
Figure 17: 3D visualization of the DEM1982 solid model.....	30
Figure 18: 3D visualization of the DEM1982 textured model	30
Figure 19: Results of the longitudinal profile in west-east direction.....	32
Figure 20: Results of the longitudinal profile II	32
Figure 21: Results of the longitudinal profile in north-south direction	33
Figure 22: Surface change 1982 — 2009.....	34
Figure 23: Surface change 2009 — 2014.....	35
Figure 24: Surface change 2014 — 2015.....	36
Figure 25: Swiss alpine glacier observations over time.....	37
Figure 26: Ice avalanche recorded on the 27.08.2014	39
Figure 27: Locations of the weather stations Grächen and Gornergrat	44
Figure 28: Position of the GPS sensors WM01 and WM02	47
Figure 29: Instabil 1 1955, 1985 and 1992	49
Figure 30: Instabil 1 2003, 2009, 2011 and 2015	50

Figure 31: Visible changes of the ice surface at Instabil 1 between 1985 and 2015	51
Figure 32: Drainage system of Instabil 1 in summer 2015 compared to weather data.....	53
Figure 33: Cumulative degree hours and DEWF index for summer 2015	54
Figure 34: GPS measurements, DEWF index and temperatures for summer 2015.....	55
Figure 35: Weather of summer 2014 compared to the weather of summer 2015.....	56
Figure 36: Ice on the bedrock besides Instabil 1 on the 17.07.2014.....	57
Figure 37: Assumed small channel below Instabil 1 on the 05.08.2014	57
Figure 38: Observable subglacial drainage systems before 2014.....	59
Figure 39: Polygons of the stable areas for the Co-registration.....	73
Figure 40: Orthogonal view of the DEM1982 solid model	74
Figure 41: Length changes of Allalingsletscher between 1881 and 2015.....	74
Figure 42: DEWF index and positive degree hours for summer 2015	80
Figure 43: GPS 3D velocities of WM01 June 2015 to September 2016	80
Figure 44: GPS 3D velocities of WM02 June 2015 to September 2016	81
Figure 45 to Figure 87: Historical archive of Instabil 1.....	82 – 124

Tables

Table 1: Data overview for the assessment of the long-term evolution	16
Table 2: Data overview for the assessment of the recent evolution	41
Table 3: DEWF Index	43
Table 4: Correction factors for the weather stations Grächen and Gornergrat.....	46
Table 5: Overview of the supplementary digital results on DVD	72
Table 6: Software configuration of Agisoft PhotoScan.....	72
Table 7: Georeferencing points for the DEM1982	72
Table 8: Description and area of the Co-registration polygons	73
Table 9: Observation protocol for the DEWF index.....	75

Preface

During my studies, I have always been interested in alpine processes and hazards. Together with my passion for hiking and mountaineering, I was looking for a topic that combined my interests. The Weissmies case allowed me to work on an important case study with connections to the actual practice of observation and managements of alpine hazards. Especially how and why such hanging glacier instabilities can evolve fascinated me.

1 Introduction

1.1 Background

A part of the Triftgletscher on the north-west slope of Weissmies (4017 m a.s.l.) showed an increased ice fall activity in summer 2014. For this reason, it has been monitored since then by Geopraevent AG with an interferometric radar and a webcam on behalf of the community Saas Grund, the mountain railways Hohsaas and the canton of Valais [geopraevent.ch, 2015]. It was feared that a large part of the hanging glacier could break off. Such ice falls or ice avalanches can pose a severe threat to humans, settlements and infrastructure [Pralong and Funk, 2006].

In the case of the Weissmies hanging glacier, ski runs in winter and mountaineering routes in summer are endangered. Ice avalanches can entrain snow that leads to larger run out distances [Margreth *et al.*, 2011]. This means that the situation is likely more dangerous in winter when more snow is available so that large break off events could even reach the town of Saas Grund (see 2.5 Study Site). On the unstable part of the glacier, additional monitoring devices (GPS sensors, Doppler radar, infrasound array and seismometers) have been installed in summer 2015 which could give a more detailed insight of the dynamic processes [Preiswerk *et al.*, 2016]. In summer 2015 the observed velocities were surprisingly much slower than in the colder summer 2014. After Preiswerk *et al.* [2016] an explanation for this could be a change in the subglacial drainage system.

1.2 General Aim and Research Questions

The general aim of this study is to explain why and how the glacier has reached this dangerous situation and how it could further evolve as a hazard.

To answer this general question, the three following points are studied:

- I. What is the long-term evolution of the Triftgletscher since 1862?
- II. What is the recent (since 1985) evolution of the unstable part?
- III. Which type of instability after Faillettaz *et al.* [2015] is likely? The following questions help to assess the type of instability: Does the unstable part of the glacier show a seasonal variation in velocity? Is there an influence of water?

This study sets its focus explicitly only on Instabil 1 (see also 2.5 Study Site) and does not discuss any changes of Instabil 2. This decision was made due to data availability, the larger volume of Instabil 1 and also the occurrence of observable subglacial water drainage systems (see *Preiswerk et al.* [2016] and this thesis). The thesis also aims to fill some of the information gaps from *Preiswerk et al.* [2016]. As described more detailed in 2.5 Study Site (see page 14) the evolution of the instability as well as the subglacial drainage system still lack some essential data background.

1.3 Structure of the Thesis

In a first step, the theoretical background of hanging glacier instabilities and the study site is enlightened in chapter 2. Then the long-term evolution of Triftgletscher and its implications for the instability are reconstructed with maps and other data in chapter 3, followed by the recent evolution of the unstable part in chapter 4 including velocity measurements and hydrological observations. In chapter 5 an elaboration and synthesis of the results is conducted. Chapter 6 is the appendix that also includes a historical image archive.

In addition to the printed version of this master's thesis also a digital copy with supplementary digital results is provided on DVD. In the corresponding chapters the reference to these digital results is made and they are listed in the appendix (see Table 5).

All orthogonal aerial images and maps are oriented north if not indicated differently. Please be aware that especially the maps and aerial images from swisstopo are protected by copyright. The usage rights of pictures from various photographers are only valid for this master thesis and have to be verified again before used in other publications. The date format used in this thesis is dd.mm.yyyy, where d stands for day, m for month and y for year.

2

Theoretical Background

In this section, three different types of hanging glacier instabilities are discussed based on scientific literature. This is important to understand the different rupture mechanisms and the hazard assessment for each type. Further, the theoretical background helps to categorize the Weissmies hanging glacier in terms of a possible rupture mechanism.

2.1 Definition of a Hanging Glacier

The encyclopedia of earth sciences from Spektrum gives a rather simple definition that defines a hanging glacier as a glacier located in a rock wall or a glacier flowing into an escarpment [*Earth Sciences Spektrum*, 2016]. The distinction to ice frozen to the rock is made with the presence of an accumulation area in flatter terrain higher up.

According to the U.S. Geological Survey a hanging glacier originates high on the wall of a glacier valley and descends only part of the way to the surface of the main glacier [*USGS*, 2016]. The main mechanisms for ice and snow transfer to the valley floor below are avalanches and ice falls.

These two short definitions are not very precise as they do not implement any temporal changes and the mass transfer is not described in depth.

A more detailed and well-founded definition is given by *Pralong and Funk* [2006] who define hanging glaciers as unbalanced avalanching glaciers. Avalanching glaciers (see *Figure 1, page 5*) are dry calving glaciers lying on a steep slope or terminating on a bedrock cliff. In this context, dry calving means that the glaciers are not in contact with a water body, which excludes all glaciers calving into the ocean (e.g. in Greenland and Antarctica). Calving is induced by gravity-driven ruptures as the glacier front is no longer able to support its own weight [*Faillettaz et al.*, 2015]. The steep slope / bedrock cliff criteria assures that ice chunks fall away from the calving zone and lead to a mass loss. The observed critical slope for slab fractures is dependent on the altitude because in higher altitudes the fraction of ice frozen to the bed is higher which increases the basal adhesion and therefore allows steeper slopes [*Alean*, 1985].

The unstable part is built up by snow accumulation and its transformation into glacier ice over time. The term “unbalanced” means that such avalanching glaciers calve under

constant climatic conditions to maintain a finite size geometry which is observable through reoccurring icefalls with a return period longer than a hydrological year (several years to decades) [*Pralong and Funk*, 2006]. Such unbalanced hanging glaciers lie entirely above the equilibrium line altitude (ELA), which means they are entirely located in the accumulation zone. The cyclic behaviour is characterized by accumulation of mass and the subsequent rupture events.

According to *Pralong and Funk* [2006] the steady state geometry should therefore be related to an entire icefall cycle. Ramp glaciers lie on a steep and relatively uniform bed and lead to much larger instabilities than terrace glaciers as the calving area is a significant part of the whole glacier so that very large ice volumes (typically 10^5 – 10^6 m³) can be released. But sometimes the identification of avalanching glaciers is demanding as some show only very few icefalls. Furthermore, changing climatic conditions can lead to glacier changes that also have an influence on the stability conditions.

However, the classification presented above is also incomplete as it does not account for the influence of subglacial water, which is after *Faillietaz et al.* [2015] a key parameter for the assessment of avalanching glaciers. In the next section the three main types of hanging glacier instabilities are therefore characterized. This extends the definition of *Pralong and Funk* [2006] and incorporates water as an important parameter for the classification of hanging glaciers instabilities.

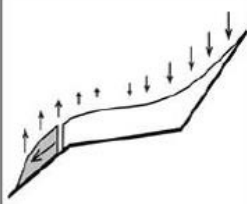
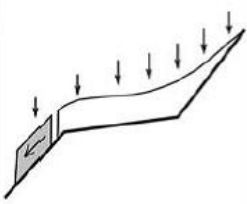
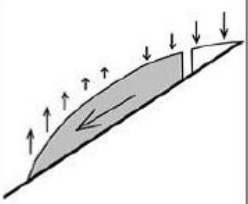
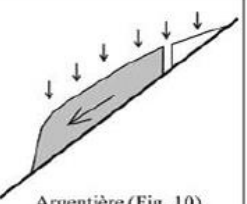
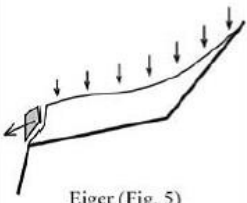
	Terrace		Ramp	
	Balanced	Unbalanced	Balanced	Unbalanced
Slab	 <p>Allalin (Fig. 3)</p>	 <p>Balmhorn (Fig. 4)</p>	 <p>Coolidge (Fig. 8) Altels (Fig. 9)</p>	 <p>Argentière (Fig. 10) Weisshorn (Fig. 11) Jorasses (Fig. 12)</p>
Wedge	<p>balanced avalanching glaciers are not subject to wedge fractures</p>		<p>ramp glaciers are not subject to wedge fractures</p>	
	 <p>Eiger (Fig. 5) Gutz (Fig. 6) Mönch (Fig. 7)</p>			

Figure 1: Classification of avalanching glaciers [Pralong and Funk, 2006]

The classifications Terrace/Ramp and Balanced/Unbalanced refer to the type of avalanching glacier and the division Wedge/Slab to the type of fracture. The unstable ice masses are depicted in gray. The massbalance regime is indicated with vertical arrows. © Pralong and Funk [2006]

2.2 Types of Avalanching Glacier Instabilities

The thermal nature of the ice/bedrock interface and the presence of liquid water in the glacier are used to distinguish between three types of avalanching glacier instabilities [Faillettaz *et al.*, 2015]:

1. Cold glaciers

These glaciers are entirely frozen to their bedrock. Changes in the glacier geometry (for example an increase in mass and therefore volume) lead to a progressive increase of the internal damage of the ice and to an unstable state. Unbalanced cold glaciers show periodical break offs when their mass and ice thickness increases until a critical geometry is reached. The rupture event of the unstable ice masses takes place within the ice and usually a few meters above bedrock. The assessment of the time of the break off is possible by using the increase in velocities and passive seismic activity.

2. Mixed conditions at the ice / bedrock interface

Some parts of these glaciers are frozen to the bedrock but there exists also a temperate zone. These glaciers can be perceived as glaciers in transition from a cold to a temperate regime. Liquid water - in the form of locally trapped meltwater - has a destabilizing impact at the ice/bedrock interface in the temperate zone because it reduces the basal resistance. The rupture event takes place directly on the bedrock in the temperate zone. The only way to assess a rupture event is the detection of a progressive warming at the bed in advance as no other clear precursory signs are known. This means that predictions of the time of break off are not yet possible with the knowledge available.

3. Temperate conditions at ice / bedrock interface

In steep terrain, temperate glacier tongues slide on the bedrock. Rapid changes of the subglacial water runoff at the ice/bedrock are the main driver of the instability. An increased subglacial water pressure decreases the basal friction which is enhanced by a distributed drainage network. Such a less efficient drainage network is developed during a phase of reduced runoff. A pulse of subglacial water flow could then trigger the rupture event which takes place directly at the bedrock. The prediction of the time of such rupture events is not possible so far, but the critical conditions described above help to assess the instability.

A progressive warming at the ice / bed interface towards a partially temperate regime (from instability type 1 to instability type 2) and the resulting destabilization process is expected to occur without visible signs until a few days before the collapse [*Faillietaz et al.*, 2015]. When the warming is relatively fast, the glacier has no time to adapt to the changes at the interface which explains the lacking precursors. Until the bed is not fully temperate, this danger of a sudden collapse is persisting.

For all types of destabilization processes, the “natural” adaption of the glacier to reach a stable state lasts longer than the destabilization process itself, which means that a potential instability can develop [*Pralong and Funk*, 2006]. The stability of avalanching glaciers is additionally also influenced by lateral abutments and the bedrock roughness which can both have a stabilizing effect.

2.3 Subglacial Drainage Systems

As we have seen in the previous chapter, water at the bed of a hanging glacier plays an important role regarding its instability and the evolution of its dynamics. For this reason, this chapter gives a short overview of the theoretical subglacial drainage concept models for alpine glaciers is. For mathematical formulas see the cited papers as they are of less importance for this thesis because no drainage system is modelled.

In the scientific literature the analysis of glacial hydrology is often divided into supraglacial (on the surface of the glacier), englacial (within the body of the glacier) and subglacial (at the base of the glacier) flow pathways [*Fountain and Walder, 1998*]. In this context, it is important to note that those phenomena are coupled and water from the surface moves in most of the cases to the drainage system at the base of the glacier.

Between 1960 and 1990 the theoretical fundament was built for the modern conceptual models of glacier drainage [*Flowers, 2015*]. The understanding of glacial hydrology is especially useful for the analysis of glacier dynamics, glacier-induced floods and also the prediction of runoff from drainage basins affected by glaciers [*Fountain and Walder, 1998*].

Crevasses are the main path for rain and surface meltwater to enter the body of a temperate glacier [*Fountain and Walder, 1998*]. Compared to moulins, crevasses are not only found in the ablation zone and allow therefore also water infiltration in the accumulation zone, where many hanging glaciers are located. At the beginning of the melt season, the meltwater penetrates the winter snowpack and is then moved along crevasses and pre-existing englacial channels. If such channels have closed in winter, the water will slowly escape through microfractures in the ice. During this process, melting occurs and the development of englacial channels starts. When the water reaches the glacier bed, it will meet impermeable bedrock or unconsolidated sediments [*Hubbard and Nienow, 1997*]. At the base, the water can be drained in different ways. *Flowers* [2015] has created an overview of the different subglacial drainage concept models that are discussed in the literature (see *Figure 2, next page*).

The subglacial flow systems can be divided into two groups, the fast / efficient / channelized systems and the slow / inefficient / distributed systems. According to *Fountain and Walder* [1998] the terms fast / efficient and slow / inefficient drainage systems should be preferred in the terminology because distributed system can also consist

to some parts of channels which would be classified into the first group. Channels can either be in the ice, see for example the Röthlisberger or R-channels [Röthlisberger, 1972], or cut into the bedrock, see the Nye or N-channels [Nye, 1976].

The fast system covers a very small fraction of the glacier bed and shows a converging flow (arborescent network) [Fountain and Walder, 1998]. In contrast to the fast system stands the slow system that covers a large fraction of the glacier bed and shows a non-arborescent network with different flow paths (see Figure 3, next page).

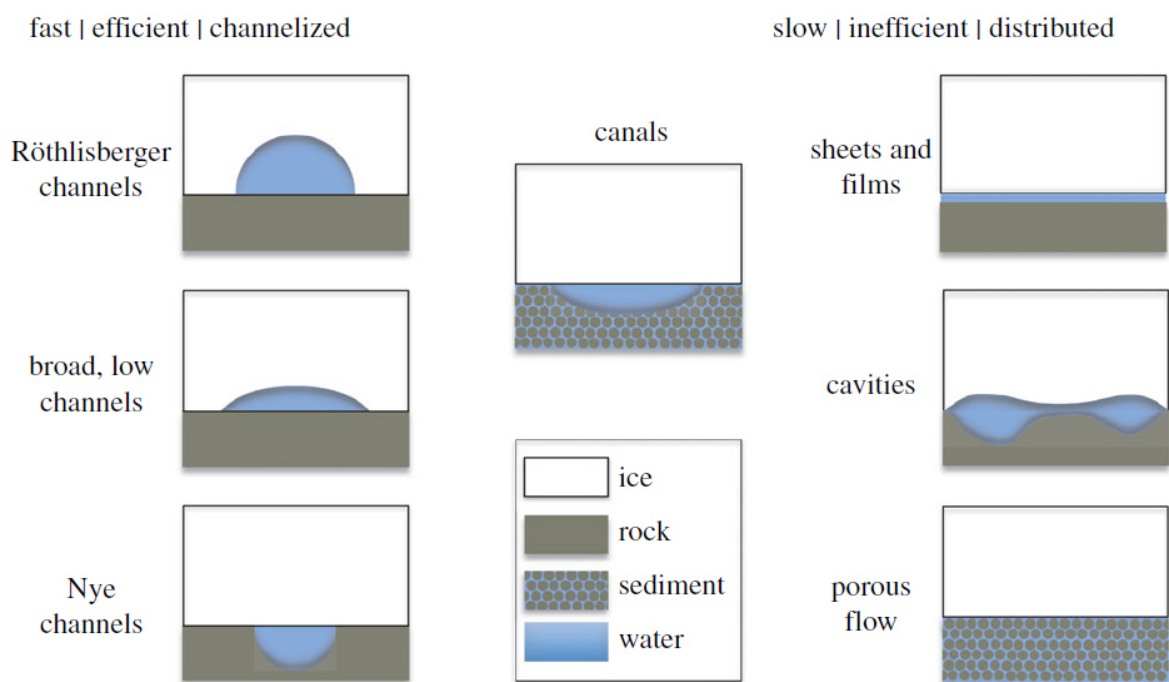


Figure 2: Overview of the subglacial drainage system elements [Flowers, 2015]

On the left side of the graph the efficient elements of subglacial drainage systems are depicted, on the right side the inefficient elements of subglacial drainage systems are shown. © Flowers [2015]

These drainage systems shown here are not steady systems, they are dynamic and a spatial and temporal transition between efficient and inefficient flow can be observed [Flowers, 2015]. At the beginning of the melting season, the subglacial drainage system should typically mainly consist of poorly connected cavities [Fountain and Walder, 1998]. The increased meltwater flux and the inefficient drainage system lead to an increase of the water pressure. This changes the stress distribution at the glacier bed and increases the glacier movement. With progressing time the water pressure and melting due to stronger water flow lead to larger cavity orifices and finally to a fast system consisting of channels.

If the water flux remains small with progressing time, the local cavity system can remain stable and no efficient system develops. In autumn, the water inputs to the subglacial hydrological system stop with the end of the melting season [Hubbard and Nienow, 1997]. The channels then gradually close by deformation of the overlying ice. Therefore, in winter a more distributed drainage system develops again. Specific local conditions can of course influence this idealized drainage cycle and lead to a different evolution.

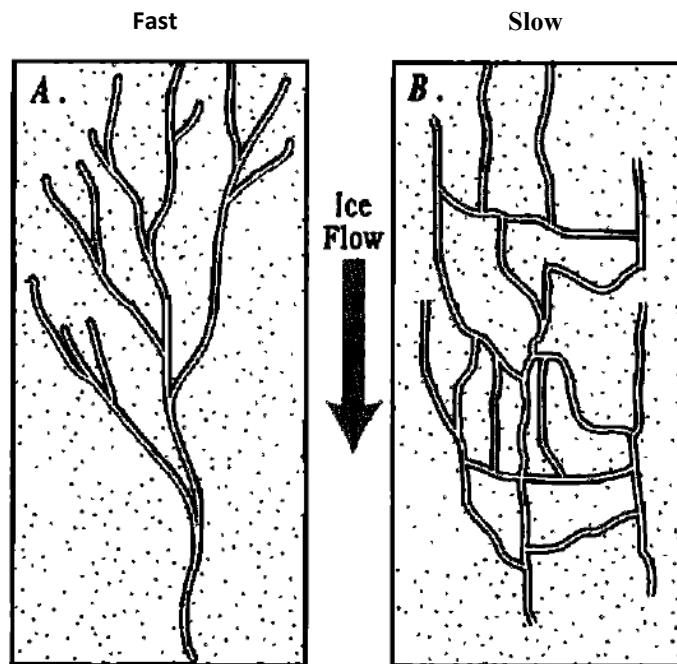


Figure 3: Arborescent and non-arborescent drainage systems [adapted from *Fountain and Walder, 1998*]
On the left the arborescent (fast) drainage system is shown, on the right the non-arborescent (slow) drainage system. © *Fountain and Walder [1998]*

2.4 Hanging Glacier as a Hazard

Break off events from hanging glacier instabilities can lead to ice avalanches that drag snow, water and / or rocks [Pralong and Funk, 2006]. The entrainment of snow increases the run out distances and the avalanche volumes [Margreth *et al.*, 2011]. Such a chain of processes involving other materials can result in major disasters like snow avalanches, floods and mudflows [Faillettaz *et al.*, 2015].

In endangered zones the inhabitants are often not aware of the potential threat of ice avalanches [Pralong and Funk, 2006]. One explanation for this is that very large ice avalanches have return periods in the order of one generation. This time span is relatively long and people lose sight of the danger. Additionally, climatic variations lead also to

adaptions of the glaciers and can therefore influence a potential hazardous situation. This means that an avalanching glacier, which would periodically give rise to ice avalanches under constant climatic conditions, could also have only one isolated catastrophic event or that new hazardous situations could develop at other locations.

Climate change and the resulting melting and retreating of glaciers affect the hazard potential of glaciers in different ways in the near future: contemporary dangerous situations will be mitigated but also new dangerous situations could emerge from new glacier geometries and temperatures at the ice/bedrock interface [Faillettaz *et al.*, 2015]. Especially successive hot summers play an important role here as they warm the still frozen ice/bedrock interface which leads to a reduced basal friction. In general, steep cold hanging glaciers below 4000 m a.s.l. are likely to reach a partly temperate bed by the end of this century [Gilbert *et al.*, 2015]. The presence of cold firn makes these cold glaciers very sensitive to warming due to the possibility of surface meltwater percolation and refreezing.

The detection of hazardous avalanching glaciers is difficult as the destabilization processes are not directly visible [Pralong and Funk, 2006]. Only their indicators (geometrical changes, crevasse formation and / or increase in velocity) can be observed. In addition, direct measurements are often complicated by the steep and heavily crevassed terrain and the danger of ice falls and avalanches. Measurements are often conducted only after clear signs of destabilization, which means that the conditions prior to the unstable state are not clear although they would be important for the assessment of the potential danger. The comparison of the surface velocities at different locations on a cold avalanching glacier helps to estimate the unstable ice volumes and time of break off [Faillettaz *et al.*, 2015].

For the assessment of the instability various difficulties emerge [Faillettaz *et al.*, 2015]. First, the heterogeneous nature of material (ice, microcracks, ice crystals) and the ice-bedrock contact as well as their characterization and measuring at different scales is challenging. Second, rupture processes are nonlinear and include the heterogeneities mentioned above. Finally, the driving force leading to a rupture can be either triggered by internal changes (e.g. damage accumulation) or external effects like earthquakes or rapid changes of the subglacial water flow regime. The physics of ice fracture and the feedback mechanisms between crevassing, ice deformation and load distribution are complex and

mostly not know [Pralong and Funk, 2006]. Together with sparse measurements, an accurate stability assessment is demanding.

A prominent and often cited rupture event in the alps is the ice avalanche at the Mattmark dam construction site in Switzerland 1965 [Röthlisberger, 1981]. The terminal part of the Allalingsletscher broke off and 88 employees were killed when it reached the construction site. In this specific case the temperate bed and the subglacial hydrology played a substantial role in the break off process [Faillettaz *et al.*, 2015]. A recent example for a chain of processes is the mudflow in the Kazbek massif in Northern Ossetia on 20.09.2002 that had its origin in an enormous rock/ice avalanche [Haeberli *et al.*, 2004]. More than 120 people died because of this tragic event.

2.5 Study Site

The Weissmies hanging glacier is located in Switzerland in the canton of Valais on the north-west slope of Weissmies (4017 m a.s.l.) and is part of the Triftgletscher (*see Figure 4, next page*). The coordinates of the Weissmies summit are the following:

- 8.01200°E / 46.12770°N (WGS 84)
- 2'644'315.52 E / 1'108'628.06 N (local Swiss coordinate system CH1903+/LV95)

In the north of Weissmies another 4000 m peak is found, the Lagginhorn (4010 m a.s.l.). Following the south-west ridge from Weissmies the Trifthorn (3396 m a.s.l.) can be reached. The south ridge of Weissmies leads via the Zwischenbergpass to the summit of Pizzo d'Andolla (3654 m a.s.l.), which marks also the southern border to Italy. Near villages in the valley of Saas (Saastal) are Saas Balen, Saas Grund, Saas Fee and Saas Almagell.

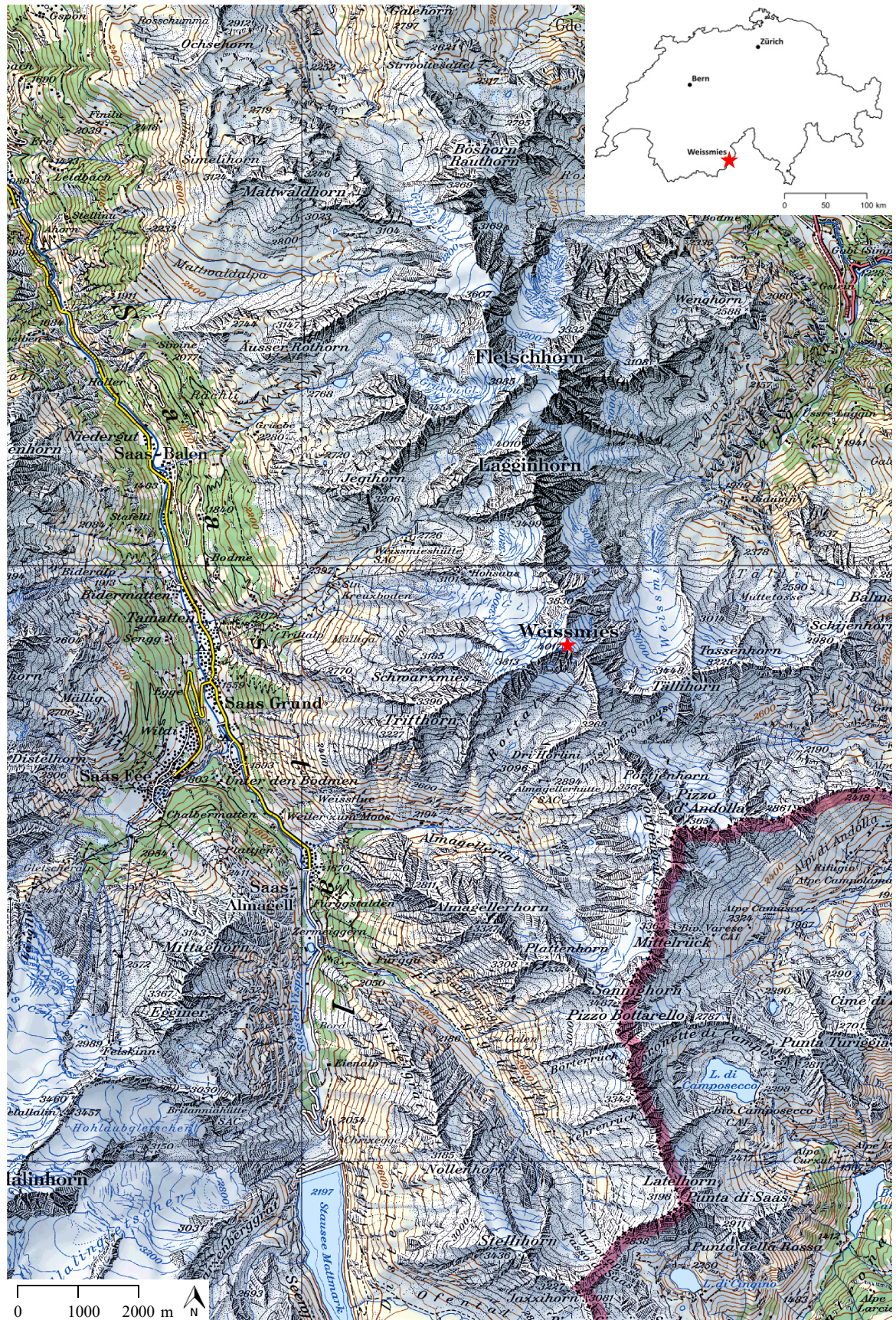


Figure 4: Large-scale overview of the study area

The map and the inset map are all based on swisstopo data (school licence number 5701106093). Base map: pixel map 1:100'000 from 2009, inset map: swissboundaries 2015. © swisstopo

2.6 Previous Studies

To the knowledge of the author, no borehole measurements have been conducted at the Weissmies hanging glacier and no information about the bed temperatures is available. Due to the steep and rough terrain, this is not surprising. *Preiswerk et al.* [2016] published a paper about the Weissmies case which included also information about a potential rupture event. They identified two different unstable parts (see *Figure 5*). As already highlighted in 1.2 General Aim and Research Questions this master thesis deals only with the evolution of Instabil 1.

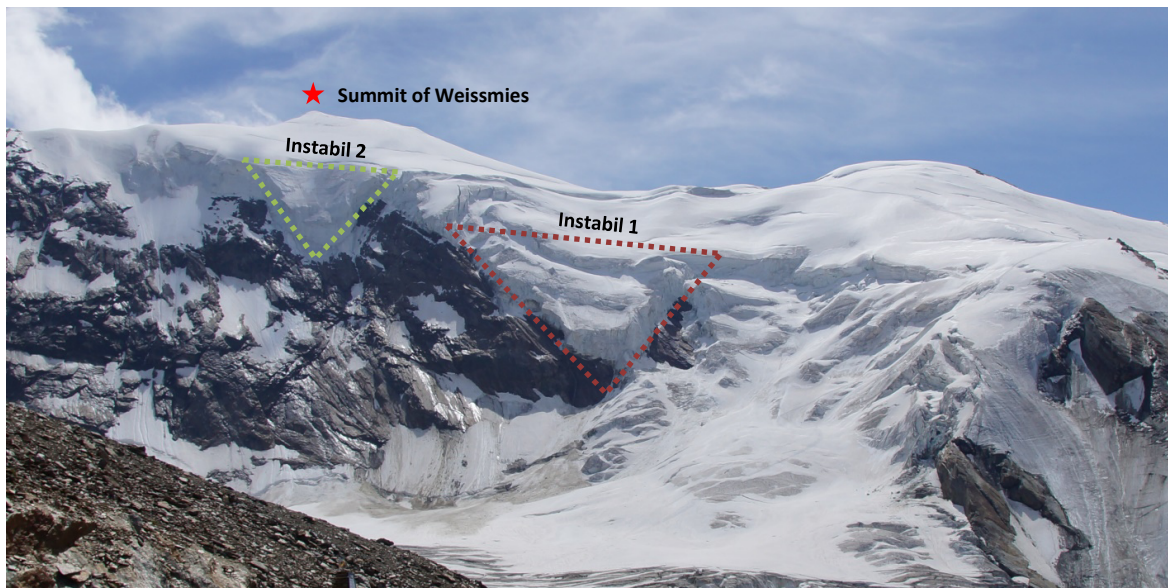


Figure 5: Instabilities at the Weissmies

Instabil 1 is highlighted with a red triangle and Instabil 2 with green triangle. The image of the Weissmies is from 06.08.2013. The viewing direction is southeast from the mountain railway station Hohsaas. © Dennis Henß, abenteuersuechtig.de

An unpublished study of the company wasser/schnee/lawinen – A. Burkard AG in Brig has calculated potential volumes and potential consequences of a rupture event (after communication from Lucas Preiswerk and *Preiswerk et al.* [2016]):

- Unstable volumes: Instabil 1 = 750'000 m³, Instabil 2 = 500'000 m³
- Events of more than 30'000 m³ ice in winter may endanger the ski resort.
- A break off of more than 200'000 m³ ice could reach the town of Saas Grund in winter.
- A break off of more than 500'000 m³ ice could reach the town of Saas Grund even without snow in the flow path.

The main results and conclusions of the study of *Preiswerk et al.* [2016] relevant for this thesis are the following:

- Glacier thinning due to climate warming has led to the destabilisation of Instabil 1 because it has almost completely removed the buttressing support from the Triftgletscher below.
- Instabil 1 is likely in a transition from cold to temperate conditions at the glacier bed.
- In October 2014, Instabil 1 was moving with velocities more than 20 cm/d.
- In summer 2015 the velocities were more or less stable around 10 cm/d. In July 2015 it even decreased to only 3 cm/d.
- The low velocities in summer 2015 were surprising as long periods above freezing enabled meltwater production and could have allowed basal sliding at the glacier bed. Summer 2015 was warmer than summer 2014.
- An explanation for the slowdown of the velocities could be a change in the subglacial drainage system. 2014 a widespread zone of wet rock was observed next to Instabil 1 whereas in 2015 it was a single channel of subglacial discharge. This more efficient drainage system could have led to reduced water pressure and therefore limited basal motion.
- Another hypothesis for the decrease in velocities could be a subglacial rock barrier.
- The study area has changing snow heights, ice topography changes and strong variations in scene illumination.

The hypothesis of glacier thinning was based on educated guesses from locals but it was not proven with data and not quantified. Especially, it is not clear if the surface of the plateau at around 3300 m a.s.l. has really subsided. Further, the subglacial hydrological system was described rather superficial and there is no information given about the condition of the hydrological system in the past and how it develops during the melting season. One part of the master thesis is the assessment of these uncertainties (*see* 1.2 General Aim and Research Questions).

As described in 2.4 Hanging Glacier as a Hazard the conditions prior to the unstable state are of high importance for the assessment of the potential danger of a hanging glacier. From the Triftgletscher no reconstruction of its past evolution has been published to the

knowledge of the author and it is not listed in the *Swiss Glacier Monitoring Network (GLAMOS)* [2016]. This is the reason why the next chapter deals first with this gap of knowledge.

3 Long-term Evolution

The understanding of the long-term evolution of Triftgletscher helps to assess how and why the present critical situation at Instabil 1 has emerged. Further, it allows together with the short-term evolution the evaluation of future risks.

3.1 Material and Methods

3.1.1 Data

For the reconstruction of the long-term evolution of the Triftgletscher a comparison of maps, aerial images and digital elevation models (DEMs) was conducted. The data specifications and their sources are presented in the table below.

Table 1: Data overview for the assessment of the long-term evolution

For the maps the scale is noted. Abbreviations: AGS = actual glacier status in the dataset, sl = school licence for the University of Zurich from the Swiss Federal Office of Topography (swisstopo, licence number 5701106093), map.geo = <https://map.geo.admin.ch> (the public accessible online geoinformation webtool from swisstopo), ETH-I = ETH (Swiss Federal Institute of Technology Zurich) Image Archive online (<http://ba.e-pics.ethz.ch/index.jsp>, last access: 22.02.2016) and VAW = Laboratory of Hydraulics, Hydrology and Glaciology of ETH

	Description of dataset	AGS	Source
Maps			
<i>Dufour map</i> 1:100'000	Sheet 23 Domo D'Ossola	1862	swisstopo sl
<i>Siegfried map</i> 1:50'000 <i>in the alps</i>	Sheet 534 Saas Different years are available: 1881, 1888, 1909, 1915, 1924 and 1933 Triftgletscher is not updated between these years.	1881	swisstopo sl
<i>Swiss map raster</i> 1:25'000	Sheet 1329 Saas Different years are available: 1970, 1977, 1985, 1990, 1998, 2003 and 2012 The pixel maps 2001 and 2009 were available with the school licence of the University. The other maps were downloaded in the Portable Document Format (PDF) from map.geo.admin.ch. The AGS of the map does not correspond to the year of publication of the maps. For the AGS see the row on the right. The number on left is the year of publication and the number on the right corresponds to the AGS on the maps.	1970 ► 1967 1977 ► 1977 1985 ► 1982 1990 ► 1988 1998 ► 1995 2003 ► 2001 2012 ► 2009	swisstopo sl map.geo
Aerial Images			
<i>Orthogonal images</i> (relatively)	The following aerial images are not georeferenced and not rectified screenshots from map.geo.admin.ch.	Year of pictures	swisstopo map.geo

	<p>Image Number and date of flight:</p> <p>19460540030094, 02.08.1946 19679990573720, 25.09.1967 19759990226474, 06.10.1975 19881080047765, 18.08.1988 19991090022702, 10.09.1999 20011090023314, 29.08.2001</p> <p>Image number and date of flight 1982 :</p> <p>19821075373989, 13.09.1982 19821075373990, 13.09.1982</p> <p>19829990134319, 16.09.1982 19829990134320, 16.09.1982 19829990134321, 16.09.1982 19829990134322, 16.09.1982 19829990144294, 16.09.1982 19829990144295, 16.09.1982 19829990144296, 16.09.1982</p> <p>The following images were available with the school licence.</p> <p>SWISSIMAGE level 2:</p> <p>si_l2_1329_11_r□□□□.tif si_l2_1329_12_r□□□□.tif</p> <p>□□□□ = 2006, 2009 and 2012</p>		swisstopo sl
<i>Oblique images</i>	<p>LBS_MH01-001036, 1919 LBS_MH01-001037, 1919 LBS_MH01-001127, 1919 LBS_H1-012338, 06.07.1949 LBS_H1-018830, 13.10.1955</p>	Year of pictures	ETH-I
DEMs			
<i>DEM1982</i>	Produced with Agisoft PhotoScan (see 3.1.5. Surface Change) using orthogonal aerial photographs from 1982 (see <i>Aerial Images, this table</i>)	1982	swisstopo Agisoft
<i>DHM25</i>	Derived from the swiss national maps 1:25'000, grid of 25 m, average deviation in map sheet 1329: 4-6 m	1995	swisstopo sl
<i>swissALTI^{3D}</i>	Digital terrain model with 2 m mesh, data status in the relevant perimeter is 2009 Above 2000 m a.s.l. mean deviation 1-3 m (stereo correlation method used at this altitudes)	2009	swisstopo sl
<i>DEM2014</i>	Digital terrain model with 2 m mesh, data status in the perimeter is 02.09.2014. The DEM was provided by the VAW for this master thesis and was produced by swisstopo with the same methods as the swissALTI ^{3D} . Above 2000 m a.s.l. mean deviation: 1-3 m	2014	swisstopo VAW
<i>DEM2015</i>	Digital terrain model with 2 m mesh, data status in the perimeter is 21.9.2015. The specifications and source information are the same as the DEM2014.	2015	swisstopo VAW

Most of the data is rather new (around 1960 – 2014). In the view of the author this data availability is suitable as the unstable part has developed in the last decades [geopraevent.ch, 2015]. Between 1862 and 1967 the data availability is rather poor because the Triftgletscher is not updated on the maps covering this period of time: The glacier outlines stay the same on all Siegfried maps, but it is very unlikely that no change has happened in around 50 years. Therefore, the actual glacier status of these maps was set to the oldest map from 1881. Due to the update cycle of swisstopo the swissALTI^{3D} from 2009 and the pixel map from 2009 are the newest data available of this kind. Additionally, two DEMs provided by the VAW from 2014 and 2015 were used. The DEM2015 was provided later in the working process so that not all analyses could be conducted with this DEM. The newest aerial image available with the swisstopo school licence is from 2012.

3.1.2 Map Comparison

The Dufour and the Siegfried map do not perfectly overlap with the more precise swiss map raster. For this reason, only the pixel maps 1:25'000 were used for the map comparison. The pixel maps, which were not available with the swisstopo school licence (see 3.1.1 Data), were downloaded from map.geo.admin.ch in the Portable Document Format (PDF) and converted into the Tagged Image File Format (TIFF) with the open source software GNU Image Manipulation Program (GIMP, version 2.8.16). These files were then further opened with ArcMap (ESRI, version 10.2.2.3552) and georeferenced on the grid intersections from the pixel map from 2009. The georeferenced TIFFs were used to create an animated Graphics Interchange Format (GIF) file (1200 ms pause between the images) with GIMP and a compiled map overview for the report.

3.1.3 Position of the Tongue

For the change of the position of the tongue of Triftgletscher the Dufour map and the Siegfried map were used in addition to the pixel maps 1:25'000. The position of the tongue was digitalized in ArcMap as a Shape-file for each map. To be consistent within all determined tongue positions, the blue contour lines were assumed to be part of the glacier, even if the map did not show glacier ice as ground cover. This allowed to integrate debris covered ice parts also into the analysis. For 2009 the position of the tongue was more difficult to assess due to the ragged tongue and blue contour lines relatively far away from the visible glacier ice symbolization (see the pixel map from 2009, for example Figure 6). For this reason the position of the tongue in the year 2009 was approximated by striking a balance between the blue ice contour lines and the glacier ice symbolization. Two

products were generated from this analysis: a map with all tongue positions for different points in time and a GIF-File where the change is visible over time.

3.1.4 Aerial Images Comparison

Five oblique aerial images of the Weissmies north-west face and the Triftgletscher from the years 1919, 1949 and 1955 were downloaded from the ETH Image Archive online in the TIFF-Format (*see Table 1*). The usage rights of these pictures are public domain. The relatively old oblique images were used to compare them with the recent evolution of the unstable part, as visualization medium for the report and as historical record for the appendix.

Orthogonal aerial images from the study area were downloaded from the map.geo.admin.ch portal as screenshots and then saved with GIMP as a TIFF-file. This method does not incorporate any spatial reference. Therefore the aerial images were georeferenced in ArcMap by using control points and the spline transformation method. This method optimizes the local accuracy of the transformation as the target control points lie exactly on the reference control points [*ArcGIS.com*, 2016]. With more control points, the accuracy of the spline transformation can be increased, but at least 10 control points are needed. As reference for the aerial images the SWISSIMAGE level 2 aerial images from 2012 were used because they were already georeferenced and rectified by swisstopo. The control points were mainly set around the tongue of the glacier, the moraines and the summit of Weissmies to reach a good accuracy in the area of interest. This was done for each picture separately. Then a compiled overview figure was created.

3.1.5. Surface Change

To determine the surface elevation changes of Triftgletscher, the height values were read out from the pixel maps 1:25'000 along two profiles in the flow direction. The profiles were positioned in an appropriate way so that they could easily be transferred by hand on the printed maps where the height values were then read out in a distance of 5 mm (which corresponds to 98 m in map scale) between the measurement points. Because the values could not always exactly be determined due to the narrow spacing of the contour lines, they were approximated with a unit of measurement of 5 m in height. For the available DEMs the height values were read along those profiles using the function *Stack Profile* in ArcMap.

Further a difference image of the swissALTI^{3D} (2009) and the DEM2014 was calculated in ArcMap using the *Raster Calculator* tool. The same procedure was conducted with the DEM2014 and the DEM2015.

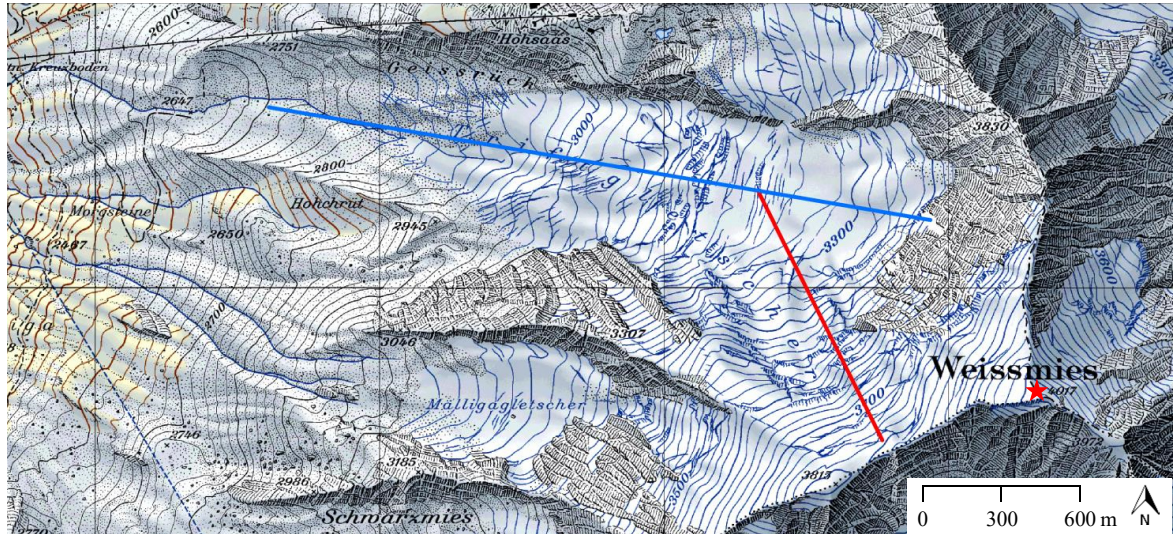


Figure 6: Profiles for the determination of the surface change

The blue line shows the longitudinal profile in west-east direction, the red line shows the longitudinal profile in the steep part of the glacier in north-south direction. The background map is the swiss map raster 1:25'000 from 2009. © swisstopo

Due to the results of the map comparison (see 3.2.1 Map Comparison) the 20 m contour lines were calculated in ArcMap for the DHM25 (1995) and the swissALTI^{3D} (2009) with the function *Contour*. The pixel map and the contour lines of the swissALTI^{3D} for the year 2009 showed relatively large height differences above 3200 m a.s.l. (see 3.2.4 Surface Change). This result left some doubts about the trustworthiness of the height information of the older maps as the swissALTI^{3D} is more precise than the DHM25.

To have more reliable height information at this altitude for a long-term analysis, a DEM was created with the software Agisoft PhotoScan (version 1.2.4.2399) from 9 aerial photographs from 1982 (see Table 1). The aerial photographs were downloaded piecewise from map.geo.admin.ch in the 4th available zoom level and then stitched together with the Microsoft software Image Composite Editor's (version 2.0.3.0) simple panorama function (camera motion is detected automatically by the software). Then Agisoft PhotoScan calculated the camera positions from common points on the photographs and aligned them [Agisoft PhotoScan Manual, 2016]. Next a dense point cloud was calculated based on the estimated camera positions and the pictures. From this point cloud a 3D polygonal mesh representing the object surface was built within the software. For presentation purposes, a texture generated from the input images was laid over the mesh. For the software parameters see Table 6 (Appendix).

Due to the complex terrain, the subsequent shadowing and the changing ground surface conditions (especially snow cover and glacier changes) it was challenging to find stable georeferencing points for the DEM1982 as the SWISSIMAGE from 2012 was used as reference image.

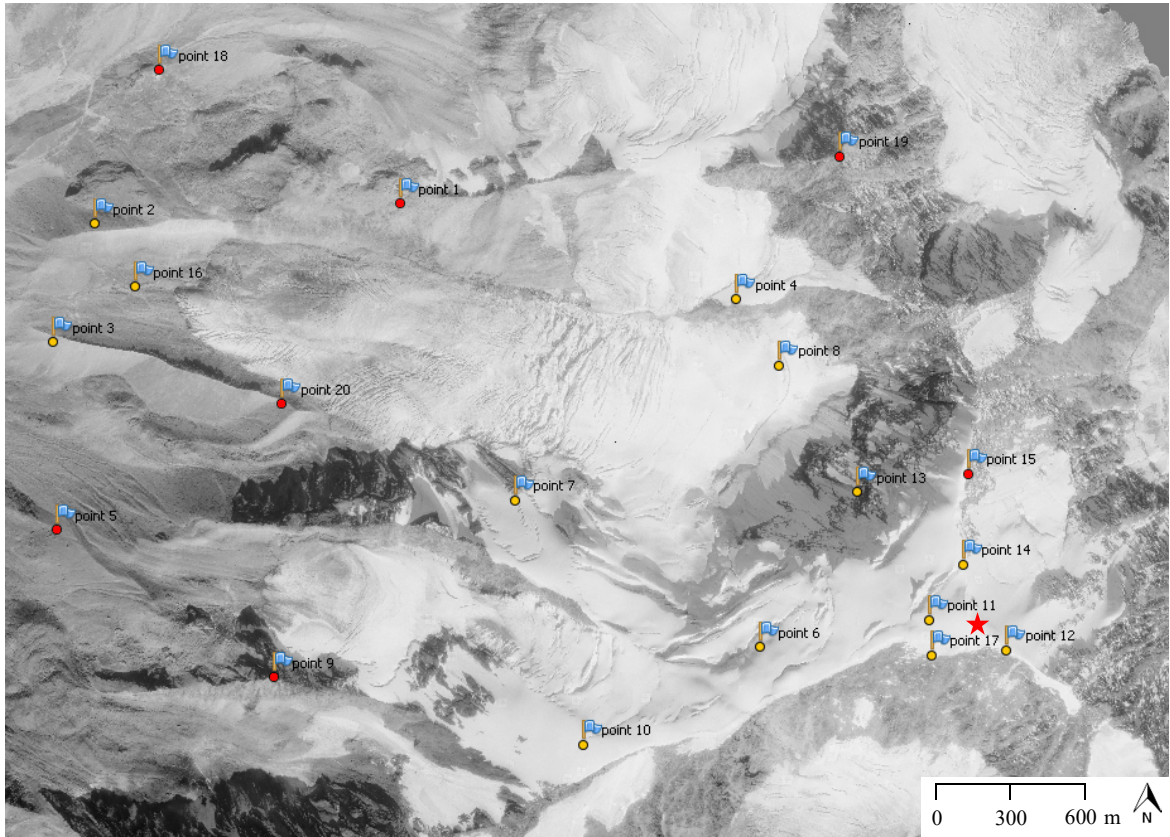


Figure 7: Reference points for aligning and georeferencing of the DEM1982

The yellow points were used as reference points for the aligning process together with the red points that were additionally used for georeferencing with the SWISSIMAGE from 2012. The aerial image in the background is a composite image of the aerial images from 1982. The coordinates of the georeferencing points are listed in the appendix (see Table 7). © swisstopo

To improve the georeferencing, the co-registration algorithmus from *Nuth and Kääb* [2011] was calculated for the generated DEM1982 and the swissALTI^{3D} from 2009. For the areas assumed to be stable for the co-registration see Figure 39 (Appendix) and the descriptive Table 8 (Appendix). The results of the co-registration led to the following offset: x-direction: 3.5 m, y-direction: 0.5 m, z-direction: 0 m. The DEM was then accordingly shifted -3.5 m in x direction and -0.5 m in y direction in ArcMap with the tool *Shift*. The DEM1982 is available in the supplementary digital results of this thesis in the GeoTIFF format.

To compare the DEM1982, the swissALTI^{3D} and the DEM2014 another longer longitudinal profile (see Figure 8) was created in ArcMap and the height values were read out with the function *Stack Profile*.

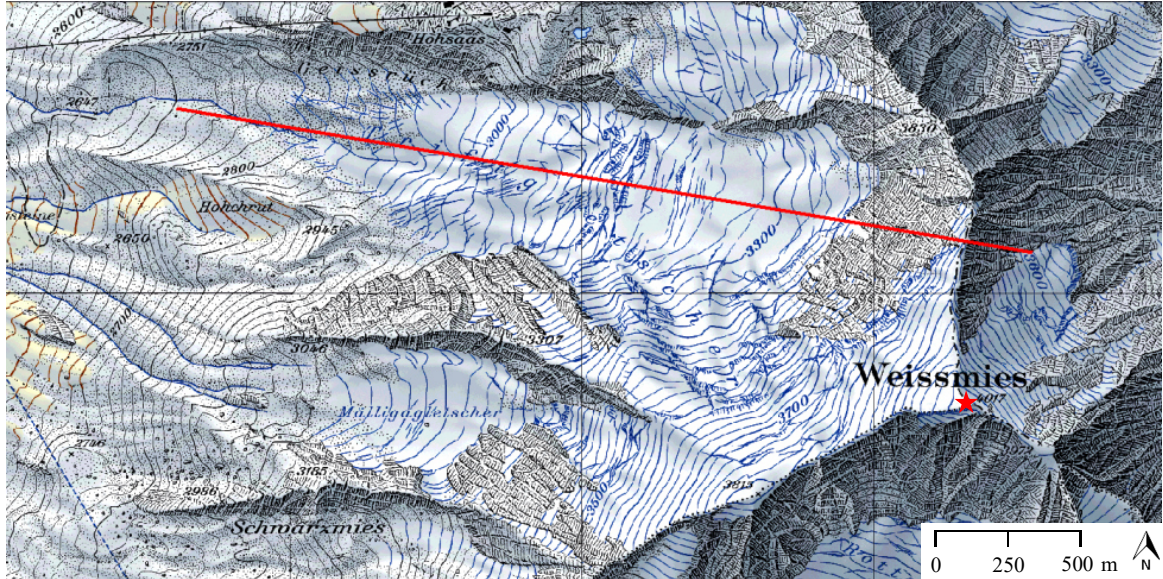


Figure 8: Longitudinal profile II

The red line shows the position of the second and longer longitudinal profile for the comparison of the DEM1982, the swissALTI^{3D} and the DEM2014. The background map is the swiss map raster 1:25'000 from 2009. © swisstopo

3.2 Results

3.2.1 Map Comparison

From 1967 to 1977 the glacier length decreased. Then from 1982 to 1988, the glacier advanced again and the tongue showed a broad and taw-like front, especially 1988. But this advance did not reach the glacier status from 1967. From 1988 to 2009, the glacier tongue has retreated again. Mülligagletscher in around 850 m horizontal distance south of Triftgletscher in a parallel oriented valley shows a similar evolution (general retreat and short advance between 1982 and 1988).

The area covered with snow and ice of the north-west facing rock walls of Weissmies has decreased between 2001 and 2009. In the accumulation area above 3300 m a.s.l. the height of the surface has not changed according to the map data. This gets even clearer when studying the animated GIF (see Table 5, Appendix): the position of the contour lines 3300 m and further upslope do not change from 1977 to 2009 (except adaptations of the ice and snow cover on the steep rock walls). 1977 the mountain station Kreuzboden appears on the map. Followed 1982 by the mountain railway to Hohsaas. 2009 the position of its mountain station Hohsaas is slightly changed to the southeast.

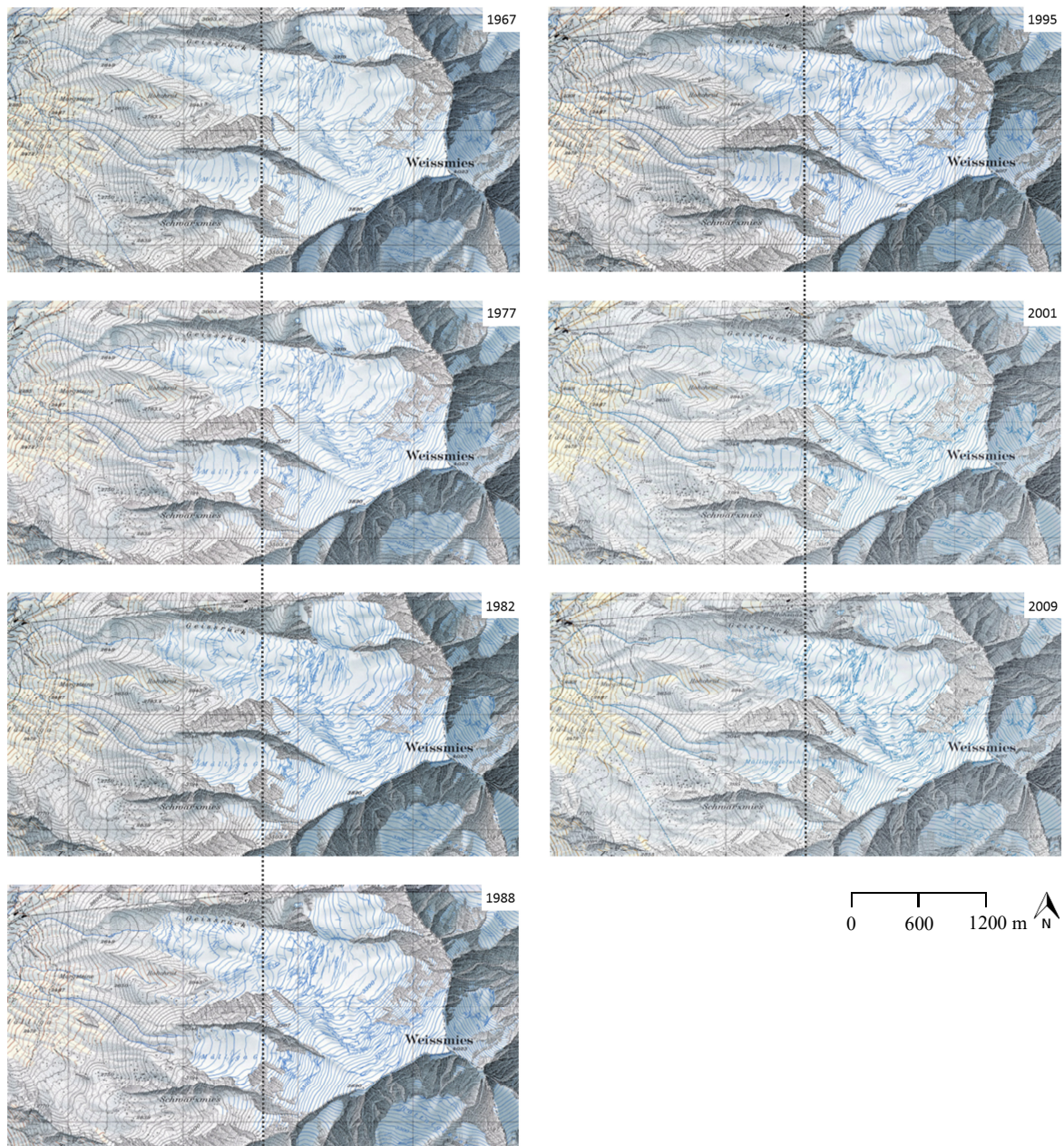


Figure 9: Comparison of pixel maps 1:25'000
On the right upper corner of each map the year of glacier status is highlighted. The black dotted line can be used as a reference for comparison. © swisstopo

3.2.2 Position of the Tongue

The additional information from the Dufour and Siegfried maps shows that the decrease in length and the subsequent retreating of the position of the tongue was also present between 1862 and 1967 (see Figure 10, next page). From 1862 to 2009 the position of the glacier tongue has moved approximately 1080 m in upslope direction.

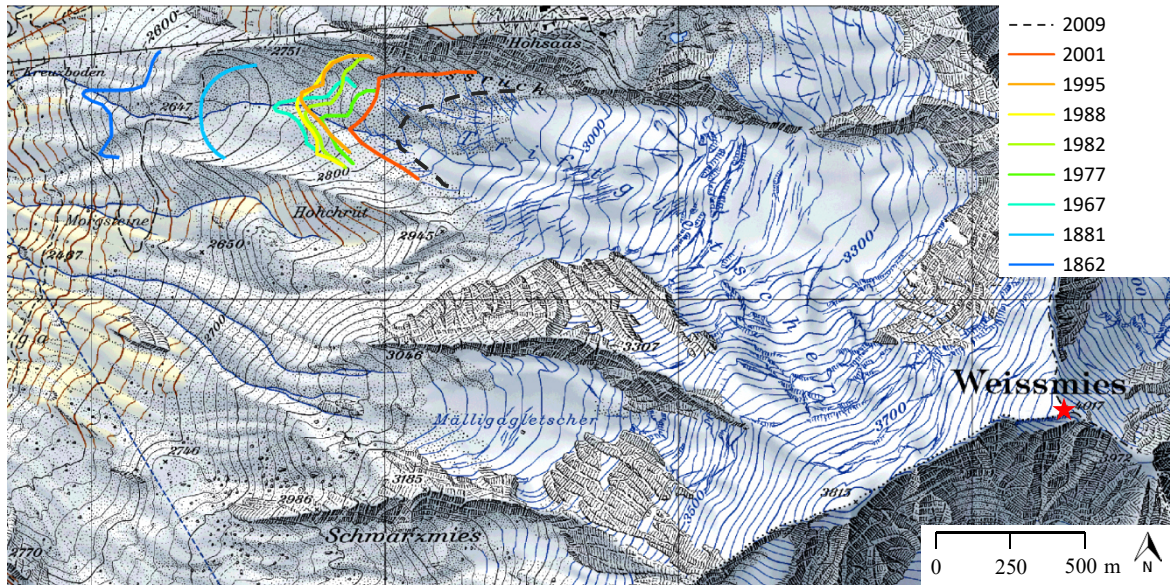


Figure 10: Position of the tongue of Triftgletscher over time

The different colored lines show the position of the tongue of Triftgletscher over time. The background map is the pixel map 1:25'000 from 2009. © swisstopo

These length changes can also be plotted for each time period (*see Figure 11, next page*). Because the time intervals are of different length, the calculated mean yearly length change shows that the strongest rate of decrease has probably occurred between 1995 and 2001 (*see Figure 12, next page*). If the calculations were conducted with the most upslope position of the tongue in 2009 and not the compromise between blue contour lines and ice symbolization, the strongest rate of decrease would be observed in the interval from 2001 to 2009. It is important to note that those values are only theoretical as the changes during one time interval are not observed and also advances could have happened during a retreat phase and vice versa.

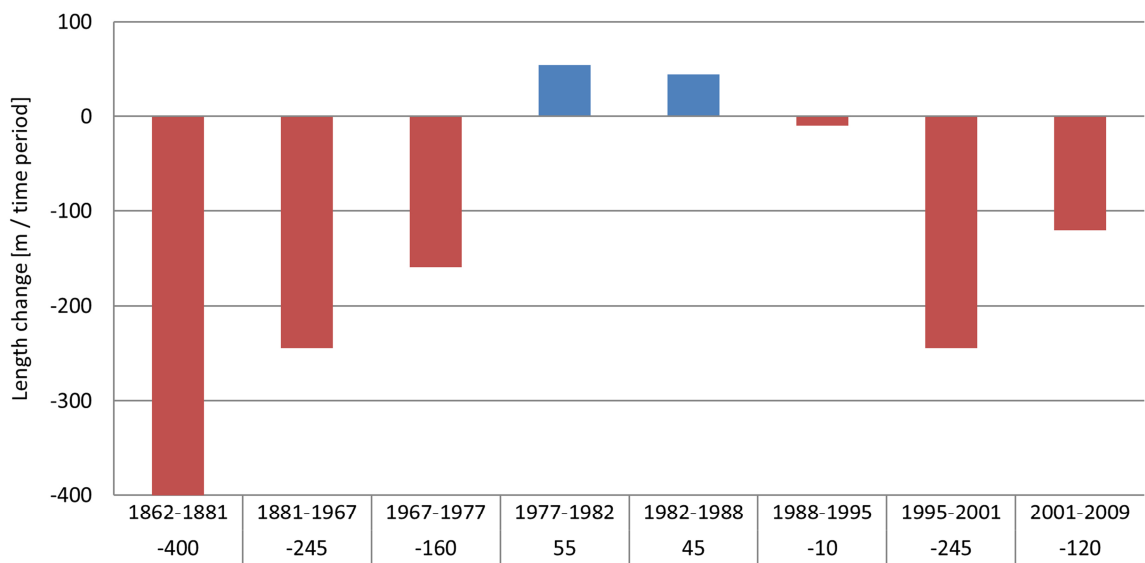


Figure 11: Observed absolute length changes of Triftgletscher

For the time periods of the map comparison the change of the position of the tongue was measured and the difference plotted. Note that the time intervals are of different length and changes between the time intervals are not incorporated with this method.

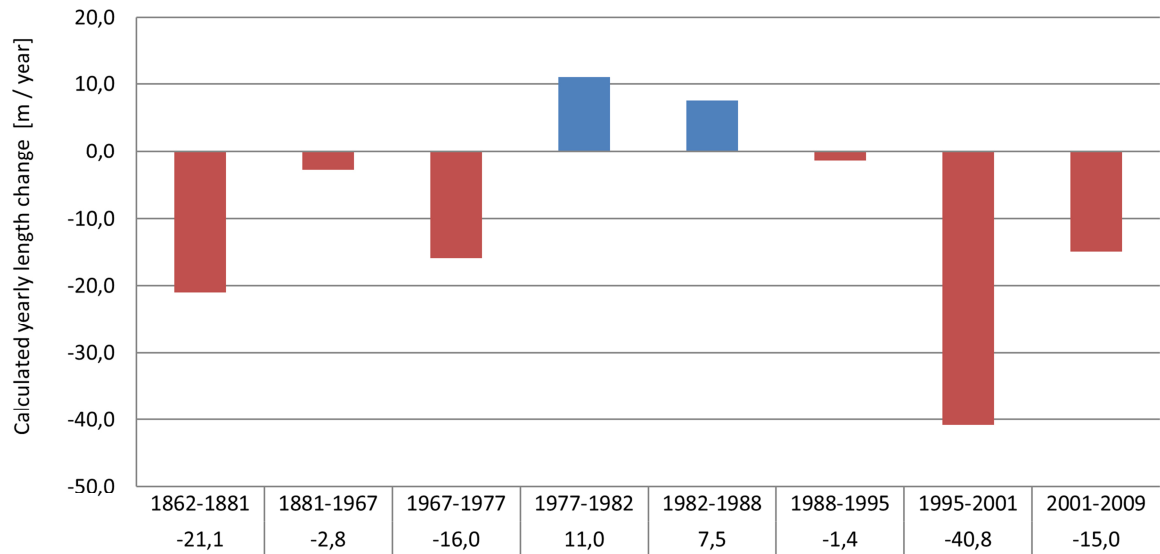


Figure 12: Calculated mean yearly length changes of Triftgletscher

The length changes between the time intervals were divided by the number of years of the corresponding time period for this figure. This compensates for the different length of the time intervals of figure 11. It is important to note that those values are only theoretical as the changes during one time interval are not observed and also advances could have happened during a retreat phase and vice versa.

3.2.3 Aerial Images Comparison

The orthogonal aerial image composite shows the same trend that could be observed with the pixel maps (see *Figure 14, next page*). From a technical perspective, it is important to note that in the accumulation area and especially on the steep slopes the aerial images do not always overlap very well due to the complex distortion of the original images and the difficulties to find common georeferencing points for all points in time.

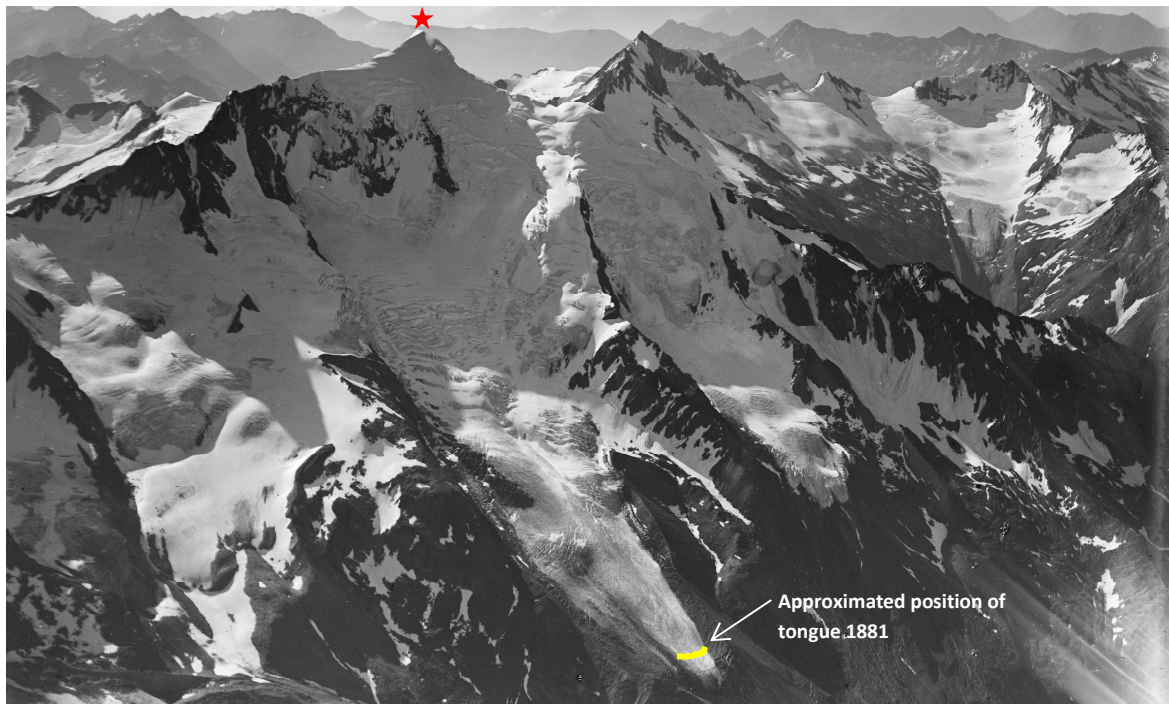


Figure 13: Oblique aerial photograph from 1919 and position of tongue 1881
 The background image (LBS_MH01-001036) is from 1919. The position of the tongue 1881 is marked with a yellow line. © ETHZ

The oblique image from 1919 provides evidence that Triftgletscher had advanced in 1919 compared to 1881 again because the position of the tongue is further downslope than in 1881 (see *Figure 13*). The other oblique images do not cover the tongue, but they show that Instabil 1 was supported from below 1919, 1949 and 1955 and no striking geometrical changes have happened. For further information about this see chapter 4 Short-term Evolution.

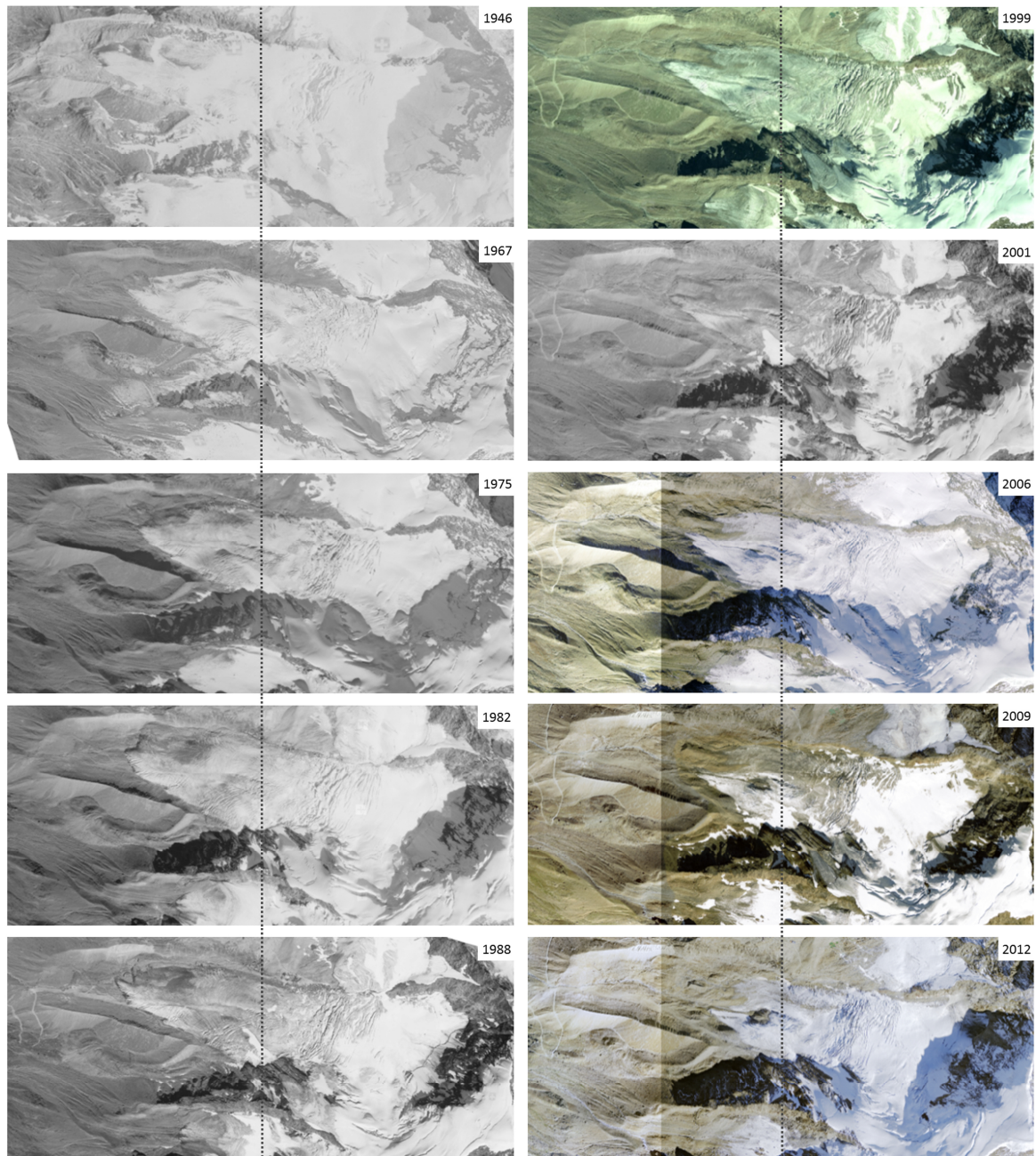


Figure 14: Orthogonal aerial image composite

On the right upper corner of each aerial photograph the year it was taken is highlighted. The black dotted line can be used as a reference for comparison. © swisstopo

3.2.4 Surface Change

First of all, the results of the comparison of the contour lines of the DEMs and the maps is discussed because this was the reason to produce another DEM to assess to long-term evolution better, especially on the plateau around 3200 m a.s.l.

For 1995 the contour lines of the map and the DHM25 overlap in the whole area of interest (*see Figure 15*). No deviations of the contour lines can be observed and even relatively small features and curves of the map are reproduced by the contour lines of the elevation model.

The results are different for 2009 as the contour lines of the map and the swissALTI^{3D} overlap below 3000 m a.s.l., but on the plateau around 3200 m a.s.l. as well as in the steep north-west slope of Weissmies the contour lines do not overlap in many parts (*see Figure 16, next page*). The height differences are in the range of 5 to 20 m whereas the map has higher elevation values than the swissALTI^{3D}.

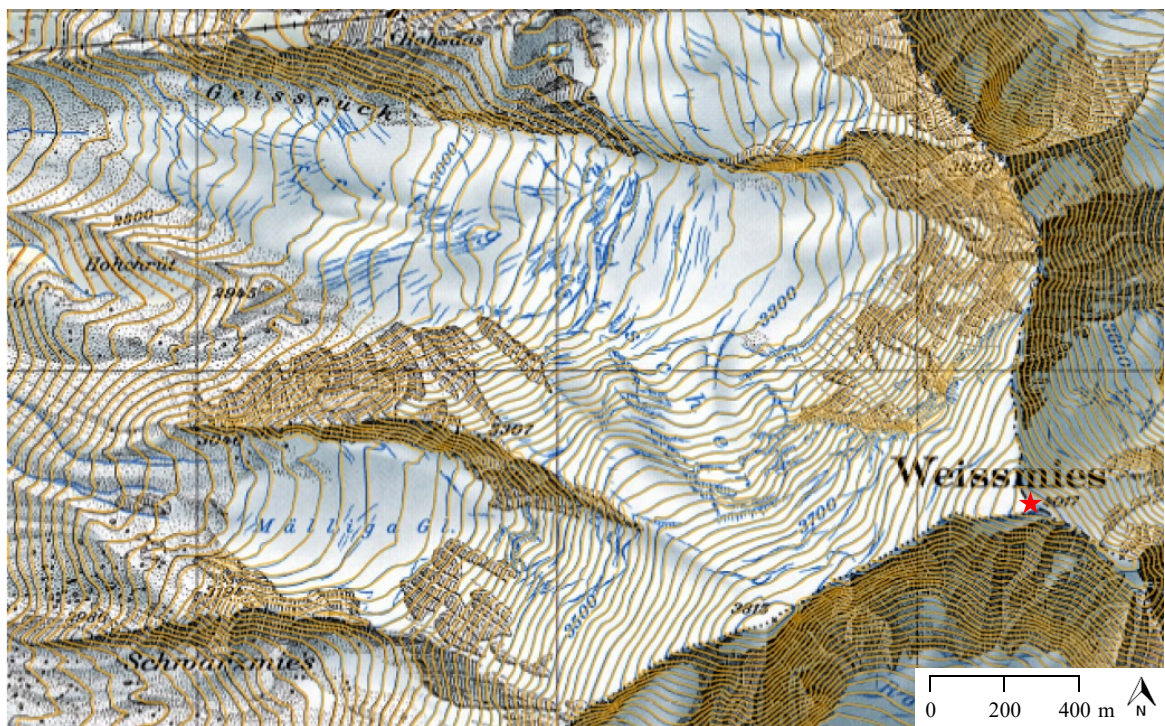


Figure 15: DHM25 (1995) compared to the pixel map 1:25'000 (1995)

The background map is the pixel map from 1995 and the calculated 20 m contour lines from the DHM25 are depicted with orange lines. © swisstopo

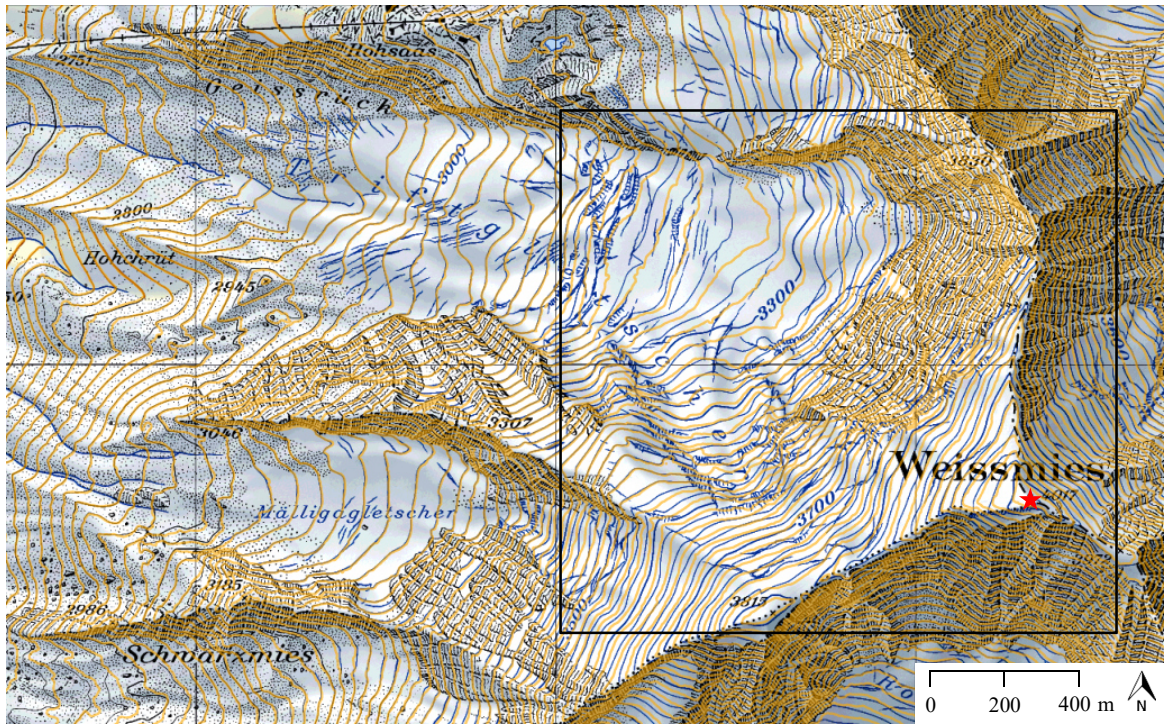


Figure 16: swissALTI^{3D} (2009) compared to pixel map 1:25'000 (2009)

The background map is the pixel map from 2009 and the calculated 20 m contour lines from the swissALTI^{3D} are depicted with orange lines. The area where the contour lines do not overlap well is indicated by a black rectangle. © swisstopo

The DEM1982, which was created because of these results, can be seen in a 3D visualization in *Figure 17* and in a textured version in *Figure 18* (for both see next page). From the solid model it becomes clear that towards the margins of the DEM1982 the accuracy decreases because the surface is represented by a wavy terrain (1) that is not observed in reality in these areas. On the other hand, the tongue (2) as well as the plateau and Instabil 1 (3) seem to be represented in an appropriate manner. It is even possible to detect the supporting structures below Instabil 1 in the DEM1982 and the large crevasses in downslope direction of the plateau.

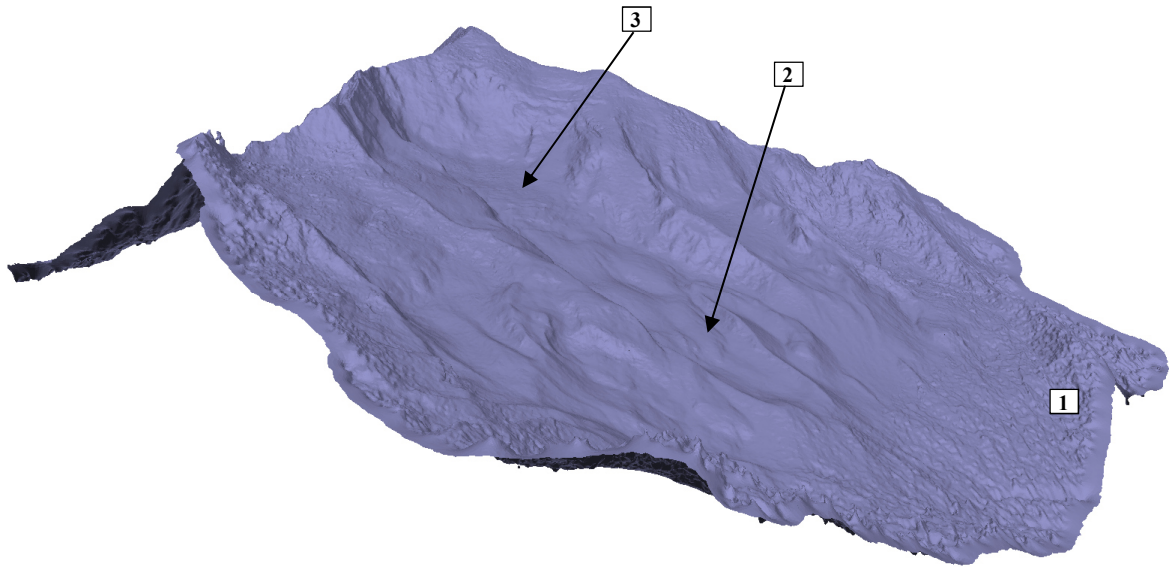


Figure 17: 3D visualization of the DEM1982 solid model

The numbers are references that are used in the text. The image is a perspective view from Agisoft PhotoScan. For an orthogonal image of the solid model, see *Figure 40 (Appendix)*.

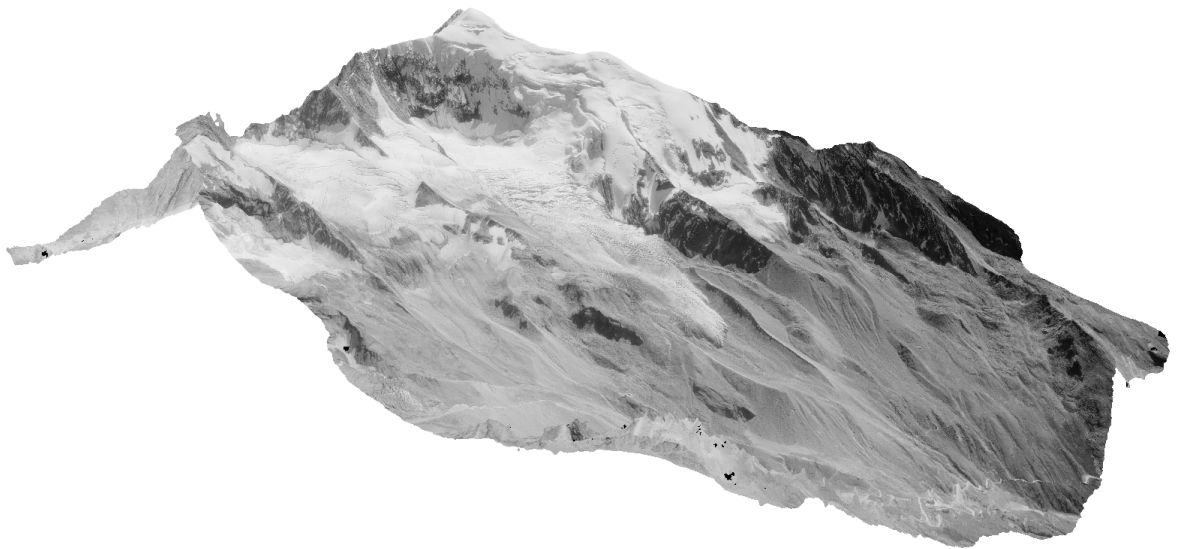


Figure 18: 3D visualization of the DEM1982 textured model

The image is a perspective view from Agisoft PhotoScan. An orthogonal image of the textured model is shown in *Figure 7*. The texture was calculated from the aerial images from 1982. © swisstopo

The analysis of the west-east longitudinal profiles shows a strong overall decrease of the surface at the tongue (1) from 1971 to 2014 with values in the range of 60 - 70 m (*see Figure 19, next page*). 1977 and 1982 the surface at the tongue increased first, but then the surface subsided constantly until 2014. The profile also shows that the map data on the plateau at around 3200-3300 m a.s.l. (2) for 2009 differs from swissALTI^{3D} values from 2009 as they are 10-15 m lower. All map elevation values on the plateau are pretty similar. The DEM1982 is around 25 m higher than the other data available in this area. On the tongue, the map data from 1982 and the DEM1982 overlap well.

The graph of the longitudinal profile II (*see Figure 20, next page*), which was only used for the DEMs, shows first of all a similar trend: a strong decrease of the surface at the tongue (1) from 1982 to 2014. Further, the subsidence of the plateau at 3200 m a.s.l. (2) can be observed with values around 20 to 25 m. The DEM1982 line fits well with the DEM2014 and the swissALTI^{3D} around the summit (3). Additionally the DEM1982 overlaps with the swissALTI^{3D} at around 2700 m a.s.l. where no glacier was present for both DEMs (4). The DEM2014 does not cover this area and therefore no comparison can be conducted. From 600 to 900 m horizontal distance (5) the subsidence of the tongue from 2009 to 2014 can be seen with values in the range of 10 to 15 m.

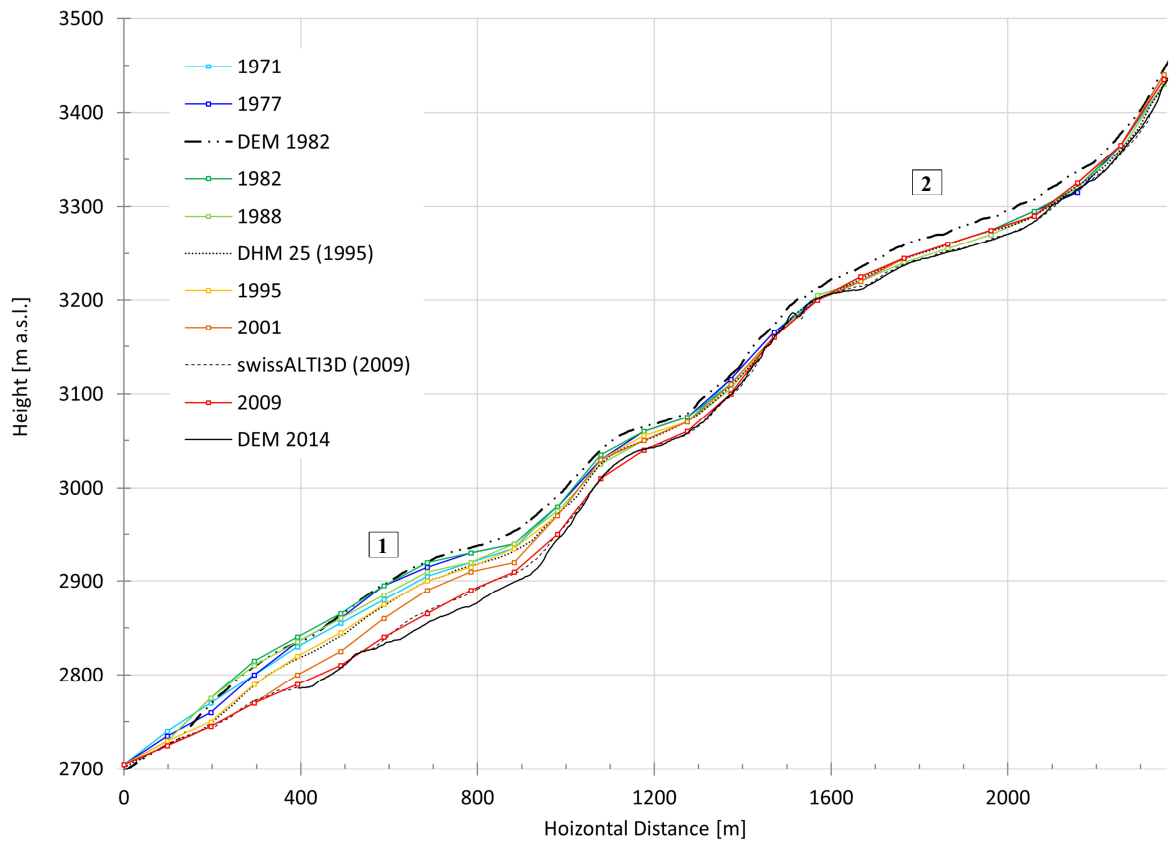


Figure 19: Results of the longitudinal profile in west-east direction
On the y-axis the surface heights of the different maps and DEMs are plotted along the horizontal distance of the profile. The numbers are references that are used in the text.

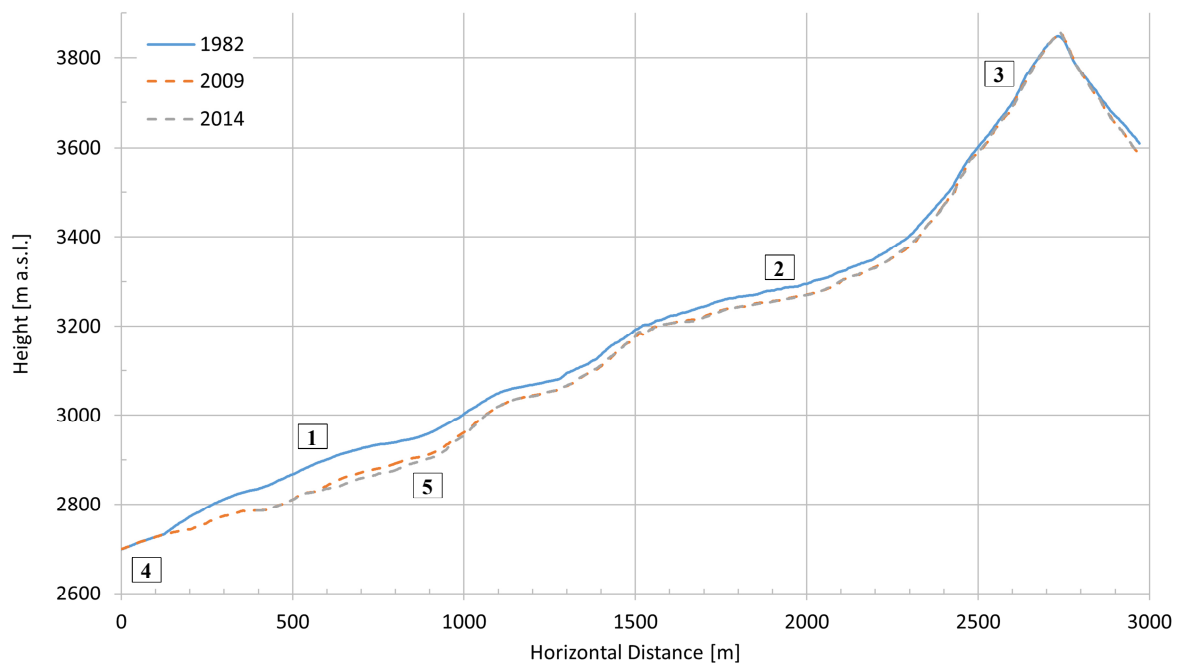


Figure 20: Results of the longitudinal profile II
On the y-axis the surface heights of the three different DEMs are plotted along the horizontal distance of the profile. The numbers are references that are used in the text.

The longitudinal profile in north-south direction of the steep part (*see Figure 21, below*) shows also the subsidence of the plateau (1). At 3350 m a.s.l. (2) the DEM2014 is higher than the swissALTI^{3D} from 2009. Further upslope at 3550 m a.s.l. (3) it looks like the surface has moved to the left on the graph. Towards the summit (4) the four elevation models overlap pretty much. Moreover, the DEM1982 and the DHM 25 are more or less overlapping on the steep part (5). The much lower surface values in this area from 2014 are an indication for larger changes.

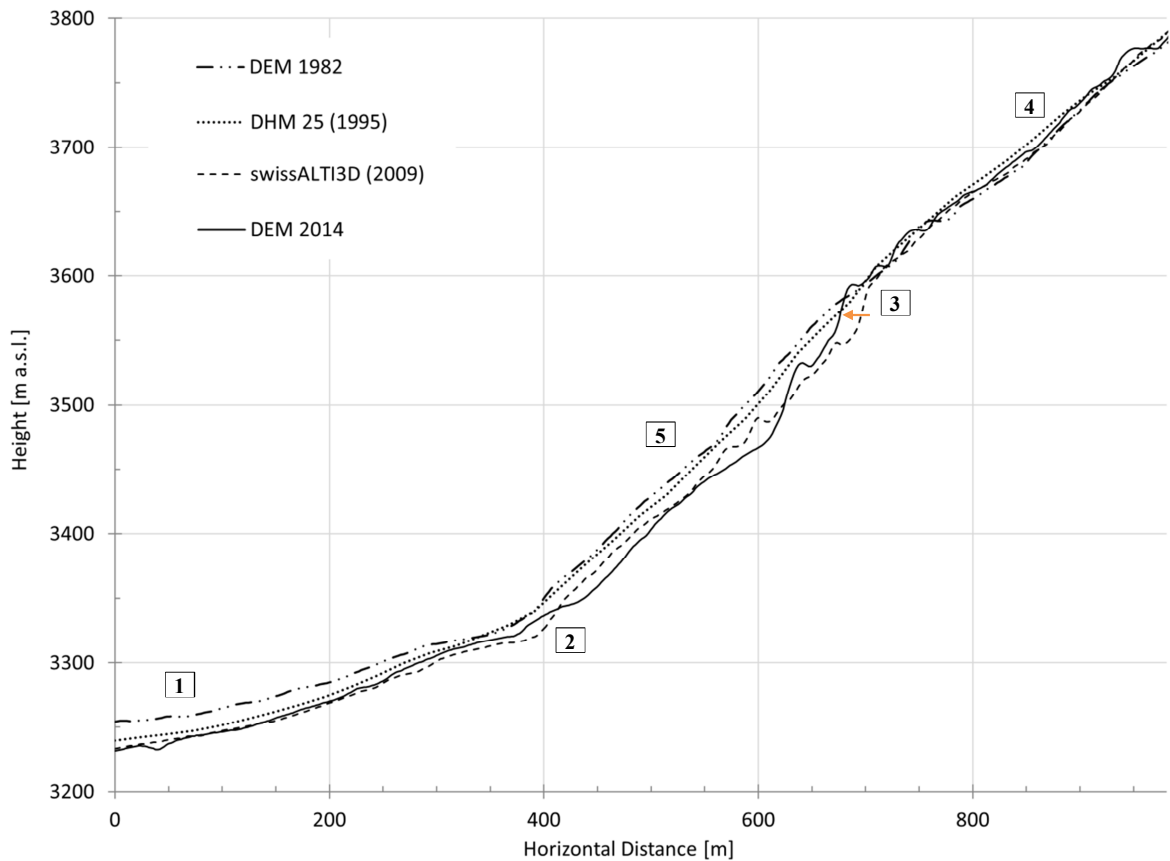


Figure 21: Results of the longitudinal profile in north-south direction

On the y-axis the surface heights of the four different DEMs are plotted along the horizontal distance of the profile. The numbers are references that are used in the text.

The profiles already allowed some statements about the long-term evolution. The difference images of the DEMs make studies for the whole area of interest possible.

First some general remarks to the presented difference images. The mean deviations for the swissALTI^{3D}, the DEM2014 and the DEM2015 were assumed to be in the range of 1-3 m as it was specified by swisstopo (*see Table 1*). Changes between -2.9 and 2.9 m over the time periods were labelled transparent. For the DEM1982 this range was set to -9.9 to 9.9 m after a visual analysis of some stable areas and the swissALTI^{3D} (2009) difference image where deviations in the range of 8-10 m were observed. Therefore the value range was adapted for the classification of the map using the DEM1982.

The surface change from 1982 to 2009 (*see Figure 22*) is characterised by a strong surface decrease. At the tongue of Triftgletscher (1) values up to 66 m decrease can be observed. The two smaller glaciers Mälligagletscher in the south and Hohlaubgletscher in the north of Triftgletscher (2) show a similar evolution. The surfaces decreased there mostly around 20 to 40 m. On the plateau (3) two distinct areas can be distinguished: the surface of the northern part of the plateau has decreased 20 to 30 meters whereas for the southern part values in the range of 15 m decrease can be observed. At the location of Instabil 1 (4) a strong decrease of the surface of 40 m and more is shown by the data at the spot where bedrock appeared 2004 and the following years (*for further information see chapter 4 Recent Evolution*). At the steep south facing walls of Weissmies (5) rather large surface changes can be detected as well as on steep ridges and moraines (6).

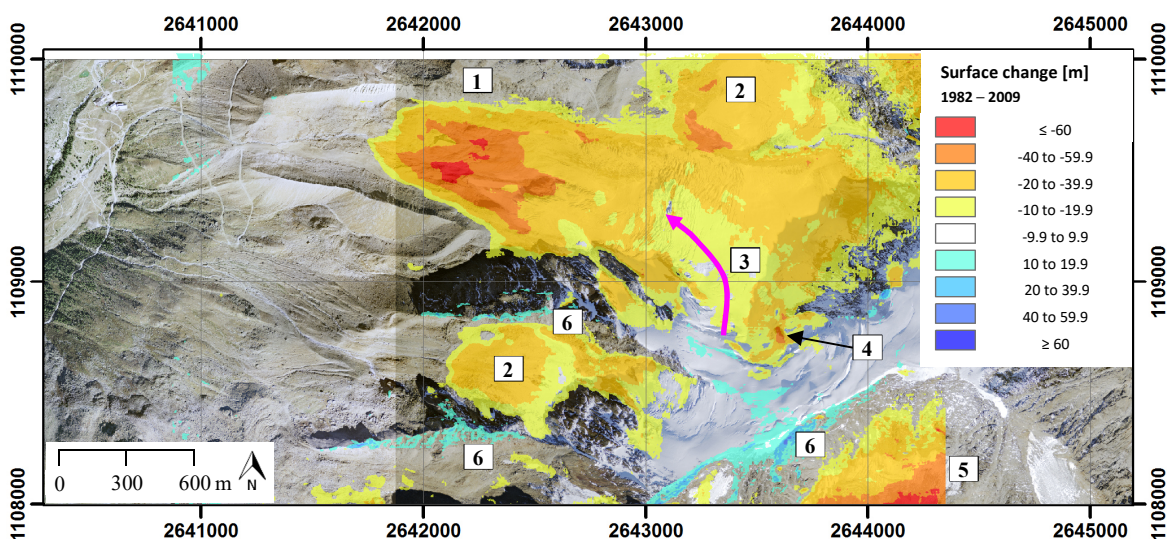


Figure 22: Surface change 1982 – 2009

For this difference image the DEM1982 was subtracted from the swissALTI^{3D} (2009). Values in the range -9.9 to 9.9 m are displayed transparent. The numbers are references that are used in the text. The background image is the SWISSIMAGE level 2 from 2012. The pink arrow is used for the discussion in chapter 3. © swisstopo

The surface change from 2009 to 2014 (*see Figure 23*) shows a continuing decrease at the tongue at Triftgletscher (1) in the range of 10 to 25 m and at the tongues of Mälligagletscher and Hohlaubgletscher in the range of 3 to 12 m (2). On the plateau (3) no bigger areas with changes larger than the mean deviations are observed. Towards the steeper part (4) areas with increased surface altitudes are shown by the data. Below the location of Instabil 1 the surface decreased up to 22 m (5). Relatively large surface changes can again be observed on the steep south facing walls of Weissmies and on the ridges and moraines (6).

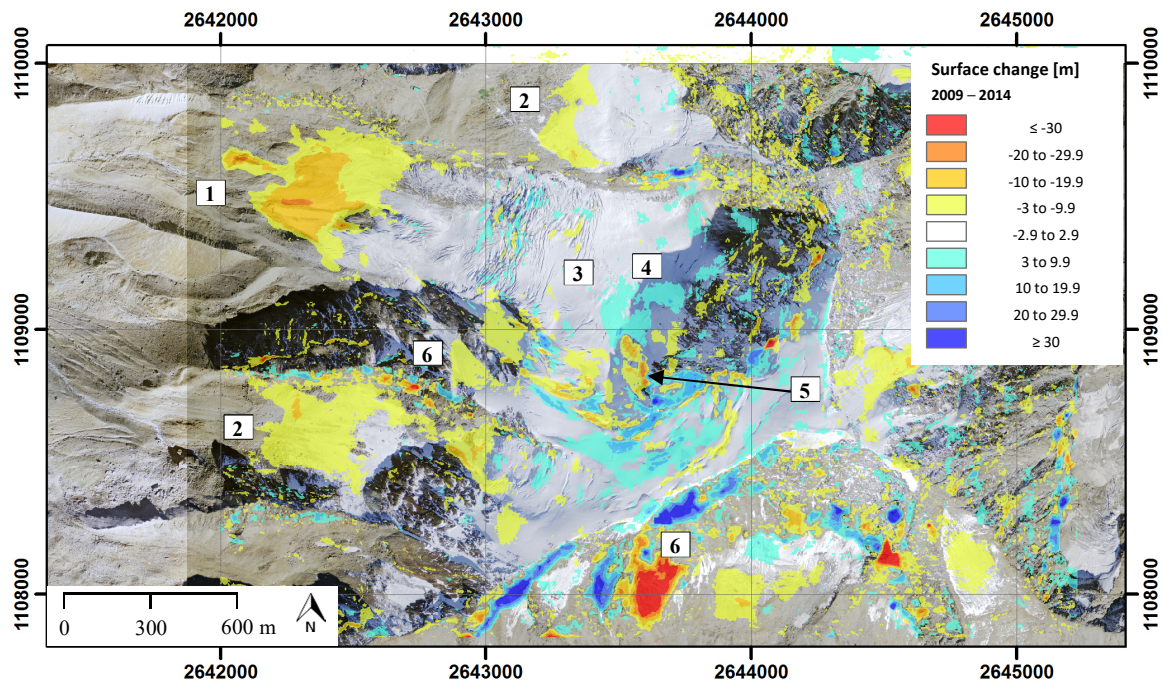


Figure 23: Surface change 2009 – 2014

For this difference image the swissALTI^{3D} (2009) was subtracted from the DEM2014. Values in the range of -2.9 to 2.9 m are displayed transparent. The numbers are references that are used in the text. The background image is the SWISSIMAGE level 2 from 2012. © swisstopo

Between 2014 and 2015 the surface changes are smaller in general (*see Figure 24*). At the tongue of Triftgletscher (1) the surface subsided around 5 m. Mälligagletscher and Hohlaubgletscher (2) do not show a decrease of surface in this time interval. On the plateau (3) large changes cannot be observed. The area with increase towards the steeper part observed 2009 to 2014 (4) is now characterized by a surface decrease in the same value range. Alternate bands of decreasing and increasing surfaces are observed in the steep part (5). The relatively large surface changes on the steep south facing rockwall, the moraines and the steep ridges are still present (6).

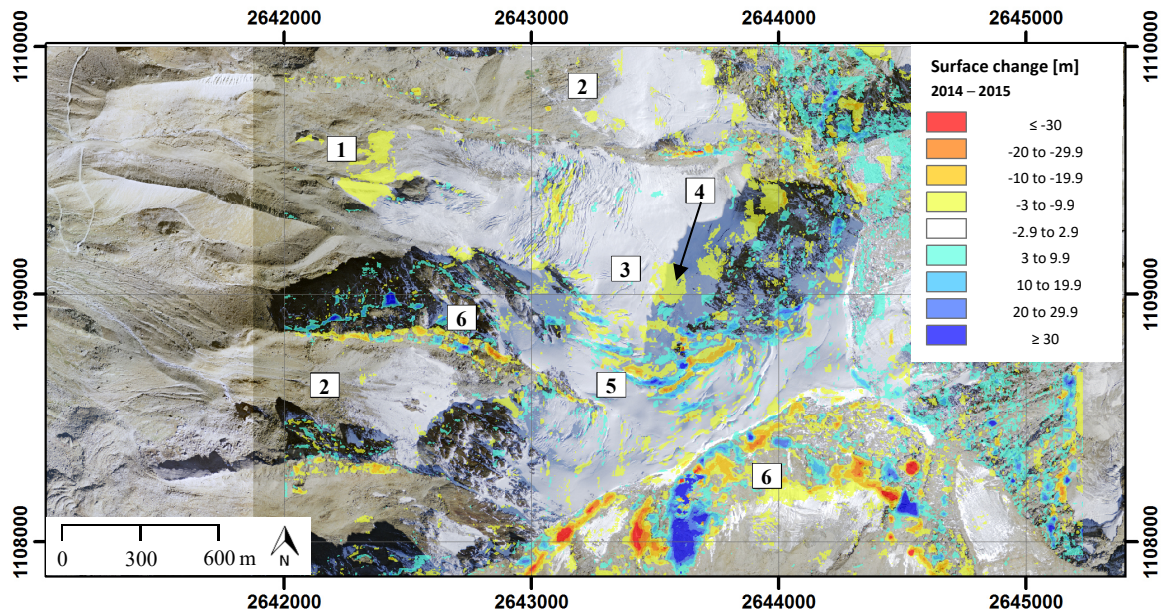


Figure 24: Surface change 2014 – 2015

For this difference image the DEM2014 was subtracted from the DEM2015. Values in the range of -2.9 to 2.9 m are displayed transparent. The numbers are references that are used in the text. The background image is the SWISSIMAGE level 2 from 2012. © swisstopo

3.3 Discussion

The general longterm trend of melting and subsequent retreating of the tongue of Triftgletscher fits well with further observations from other alpine glaciers, see for example the *Swiss Glacier Monitoring Network (GLAMOS)* [2016] or *Pellicciotti et al.* [2014]. Also the advance of the Triftgletscher from 1982 to 1988 corresponds with the advance of many Swiss glaciers in the 1980s [GLAMOS, 2016]. The broad tongue from 1988 can be related to observations from other advancing glaciers that often show a paw like form of the tongue [Müller, 1987]. This is therefore also a clear sign for an advance. The advance around 1919 detected with the oblique aerial image is also reported from other Swiss glaciers of the Swiss Glacier Monitoring Network (see Figure 25, next page). If we compare the evolution of Triftgletscher with the Allalingletscher that is located around 10 km southwest in the same main valley, similar patterns can be detected; the length increased 1910 to 1920 and between 1970 and 1985 (see Figure 41, Appendix). The evolution of Triftgletscher is therefore nothing unusual: it follows the general trend of glacier melting in the alps.

1978 the cable car to Kreuzboden was built which was then followed by the second section of the mountain railways to Hohsaas in 1982/1983 [hohsaas.info, 2016]. This section was replaced 2005 by a more modern cable car. That these changes are all visible

on the maps shows that update status on the maps in this perimeter is good. The same accounts for the glacier tongue and the ablation area. The results of chapter 3.2.4 Surface Change shows that in the accumulation area the update status and / or the accuracy of the maps have to be questioned. It is not surprising that the map from 1995 and the DHM25 overlap perfectly in the whole study area because the DHM25 is based on the height information from the pixel maps 1:25'000 [swisstopo DHM25, 2005]. What we can learn from these results is that we still can use pixel maps for surface analyses in ablation areas, where the update status is good. But we should be careful with such comparisons in the accumulation area. The comparison of the pixel map from 2009 and the swissALTI^{3D} (2009) shows exactly this as in the ablation area the contour lines of the more precise DEM and the map overlap. For future map comparisons the height information in the accumulation area will be better, as the new Swiss national map 1:25'000 will be based on the information from the swissALTI^{3D} and not from the DHM25 anymore [swisstopo.ch, 2016].

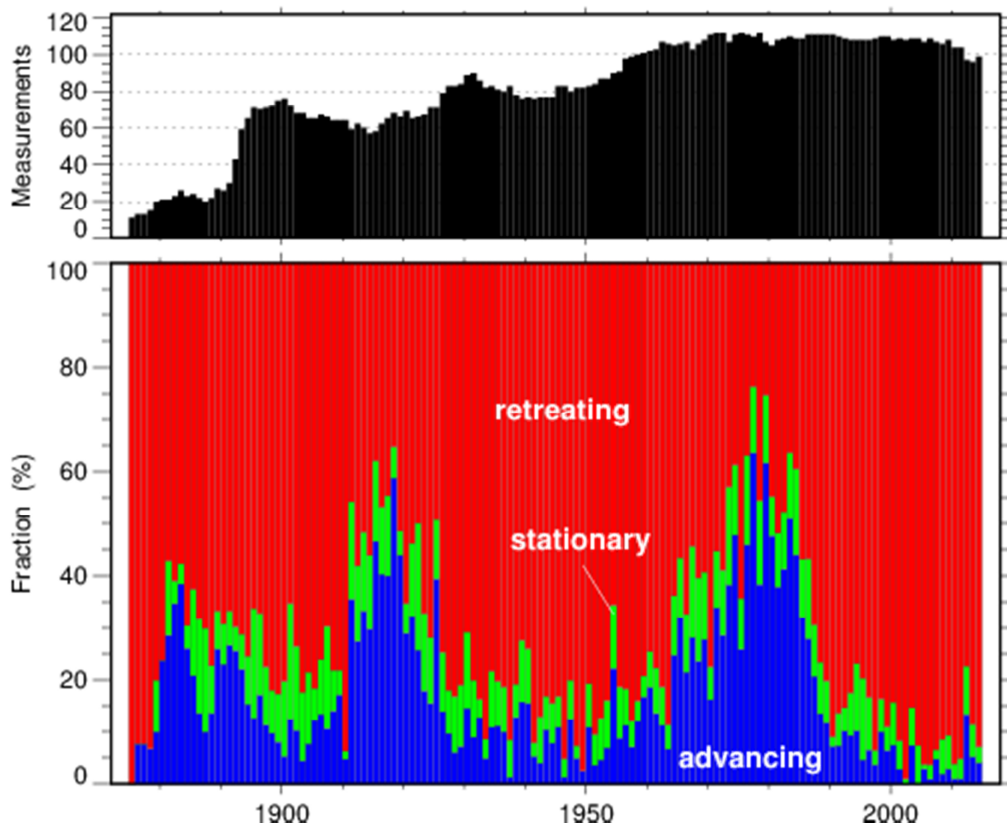


Figure 25: Swiss alpine glacier observations over time [GLAMOS, 2016]

The upper graph shows the number of glacier measured over time. In the graph below the yearly fraction of the measured glaciers **retreating**, **stationary** and **advancing** are plotted over time. © GLAMOS

The DEM1982 created with Agisoft Photoscan fills the information gap in the accumulation area and it allows to confirm the thesis of *Preiswerk et al.* [2016] that the surface of the glacier has subsided on the plateau. The decreasing accuracy at the margins of the DEM1982 can be explained with the stereo correlation method used; In these areas the overlap of the pictures is smaller or even only one image is available as the area of overlap was set mainly on the area of the glacier. But how can we explain the relatively large area with less surface decrease in the southern part of the plateau? One explanation could be that - through the glacier flow from the Triftgletscher above - this part has been supplied by ice that compensated partly for the increased melt at these altitudes. In *Figure 22* this flow line is indicated with a pink arrow. Higher temperatures led eventually also to an increased ice flow to this part of the plateau: Due to more melt water, the increased water pressure enhanced basal sliding and so more ice supply was possible from above.

A strong surface decrease can be observed in the west of Instabil 1 where bedrock appeared the first time in 2004. With the data used in this analysis, the evolution of this decrease is hard to reconstruct due to the larger scale applied. How this decrease has developed will be discussed further in chapter 4 Recent Evolution.

The DEM2014 was produced with data from 02.09.2014. The increase of the surface near the steep parts could be explained with ice avalanches from which visual records are available from the 27.08.2014 (*see Figure 26, next page*). The increase towards the steep part is also visible in the north-south profile (*see Figure 21*). The following decrease from 2014 to 2015 at the same location could then be a consequence of the lower icefall activity and surface melt in 2015. The DEM2015 is from 21.9.2015, therefore enough time for melt would have been available during the melting season. But if melt has occurred at the location of the ice avalanches the question arises why no melt in the northern part of the plateau was detected between 2014 to 2015. So another explanation could be that the ice and snow of the avalanches compacted and therefore the surface decreased again.

The observation of presumably moving parts (indicated with an orange arrow) made in *Figure 21* can be transferred to the difference image from 2014 to 2015 where alternating surface changes were observed in the steep part. This moving parts could be crevasses moving in flow direction and therefore leading to a strong change in surface height (the crevasses are relatively deep compared to surrounding surface). Similar patterns can be detected in the difference image from 2009 to 2014.

All three difference images are characterized by strong surface changes in steep terrain (steep ridges, moraines and steep rock walls) that is assumed to be more or less stable or that the values are out of a realistic range (*see for example Figure 24*; more than 30 m surface change in a large area over one year on the steep south facing rockwall of Weissmies). Therefore the data in very steep terrain has to be regarded with suspicion for all DEMs. But for the studies conducted the author considers the accuracy of the DEMs as sufficient because the plateau is a rather flat area compared to the steep parts with larger errors.



Figure 26: Ice avalanche recorded on the 27.08.2014

The **red** line highlights the outline of the ice avalanches, the **green** line shows the normal route of the mountaineers taken after the ice falls. The photographer already did the labelling. © Peter Albert

For the DEM1982 also further limitations have to be taken into account. For the creation of this DEM only nine aerial images were used which were all oriented more or less orthogonal. Two of the pictures had been even taken three days earlier than the other ones, which means different illumination and shadowing for the two time steps. The few pictures are technically a drawback because in the manual of the software one of the guidelines for capturing scenarios says it is recommended to use as many photos as

possible with good overlap (60% side, 80 % forward) [*Agisoft Photoscan Manual*, 2016]. Further shiny or transparent objects should be avoided or at least been shot under a cloudy sky. With glacier ice and snow characterized by high albedo, the conditions found at the study site are for sure not optimal. Also because aerial pictures are flown when there are preferably no clouds at all. In the author's opinion, the original georeferenced aerial images from swisstopo could have probably even given a better DEM result. But the questions addressed in this thesis with the DEM1982 are rather large-scale, therefore there was no need to use and buy those pictures. This relatively simple approach could also be applied for other glaciers with enough aerial pictures available for one point in time and could help to reconstruct the long-term evolution or older glacier surfaces.

3.4 Summary of Results

This section shortly summarizes the results and discussions of this chapter:

- A general trend of melting of the tongue and subsequent retreating of Triftgletscher is observed. Two confirmed advances occurred around 1919 and in the 1980s. These results correspond well with other observations from alpine glaciers.
- Mälligagletscher and Hohlaubgletscher near Triftgletscher and Allalngletscher around 10 km in the southwest show a similar evolution.
- Approximately 1080 m upslope retreat of the tongue occurred between 1862 to 2009.
- The surface decrease at the tongue of Triftgletscher is of over 60 m between 1971 and 2015.
- The hypothesis of the subsiding plateau around 3200 m a.s.l from *Preiswerk et al.* [2016] is supported by the analysis of the DEM1982. The decrease of the surface in this area is in the range of 15 to 30 m. Ice flow from the Triftgletscher above could have reduced the decrease in the southern part of the plateau.
- The Swiss national maps 1:25'000 can be used for comparison in the ablation area, for the accumulation area the data has to be questioned.
- The approach of creating a DEM from aerial photographs with Agisoft Photoscan can also be used for other glaciers to reconstruct past surface geometries – given that there are enough aerial photographs from the same point in time available.

4 Recent Evolution

The study of the recent evolution of Instabil 1 allows a more detailed analysis of the long-term indications gathered in chapter 3. Especially the summer of 2015 and the hydrological system are analyzed with new approaches and data availability to assess the instability better.

4.1 Material and Methods

4.1.1 Data

For the reconstruction of the recent evolution of the unstable part, a comparison of images, weather data and velocity measurements was conducted. Due to contractual reasons, the author of this thesis had not access to all the data described in 1.1 Background, in particular the radar velocity measurements. The data specifications and their sources are presented in the table below.

Table 2: Data overview for the assessment of the recent evolution

Abbreviations: AGS = actual glacier status in the dataset, Perma = PermaSense Project (<http://www.permasense.ch>) and Meteo = Federal Office of Meteorology and Climatology of Switzerland (MeteoSwiss, <http://www.meteoswiss.admin.ch>)

	Description of dataset	AGS	Source
Images			
<i>Webcam</i>	Nikon D300 S, PermaSense project The camera was installed in late summer 2014 at the top station Hohsaas of the mountain railways Hohsaas [approximate coordinates: 2'642'683 E 1'109'955 N] with 15 min time interval between the pictures taken. They are available from the 16.10.2014 on.	2014 - 2016	Perma
<i>hikr.org</i>	This non-profit website for reports from hikers and mountaineers features many images of the Weissmies from different years. The photographers were contacted to clear the usage rights and then the images were downloaded or received by email.	Year of pictures	Various
Weather data			
<i>MeteoSwiss</i>	Temperature and precipitation measurements from the Federal Office of Meteorology and Climatology of Switzerland (MeteoSwiss). Data access was secured through the University license of CLIMAP from MeteoSwiss. The following data was used for this thesis: Station Grächen and Gornergrat: <ul style="list-style-type: none"> • Daily maximum temperatures [°C] • Hourly mean temperatures [°C] 	Date of data	Meteo

	Station Grächen: <ul style="list-style-type: none"> Daily precipitation [mm] No precipitation measurements were available for the Gornergrat weather station.		
Velocity data			
GPS	Two low-cost GPS sensors (only L1 frequency) were installed by the VAW on 11.06.2015 on Instabil 1. Starting coordinates of the two sensors: WM01: 2643767.015 E / 1108779.428 N WM02: 2643674.077 E / 1108802.800 N Standard deviation of the 3D velocity (24 hours): in most of the measurements < 1 cm	Date of data	Perma

4.1.2 Geometric Changes of Instabil 1

The comparison of the DEMs in chapter 3 Long-term Evolution showed large surface changes in the area of Instabil 1. To assess this changes better, pictures from hikr.org [2016] were used for a qualitative analysis. On this non-profit website hikers and mountaineers regularly publish reports and photos of their mountain-tours. To clear the usage rights of the pictures, the photographers were contacted by e-mail. In addition, other similar websites were searched for suitable images and the usage rights were also requested. The period of time covered is from 1985 to 2014. The images were used to produce a compiled figure that highlights the geometrical changes, for chapter 4.1.3 Hydrology and as historical record for the appendix. The oblique aerial images from chapter 3 Long-term Evolution were also used for comparison.

4.1.3 Hydrology

The images of the webcam installed at the Hohsaas mountain station were analyzed for any signs of water and water flow during summer 2015. For 2014 such an analysis was not possible, as the webcam images are only available from the 16.10.2014.

A semi-qualitative classification (*see Table 3, next page*) was used to describe the observed water flow. The classification combines the amount of water as well as the subglacial hydrological system in a Drainage Efficiency Water Flow (DEWF) index. The higher the value of the index, the more water is visible and also the more efficient is the drainage system. A channeled drainage system is seen as the most efficient hydrological system in this classification.

The observation period was set from 01.04.2015 to 30.09.2015. This time period was chosen after a coarse overview of the webcam data to reduce analysis of time periods without water flow visible. As the webcam takes every 15 minutes an image, also a reference time had to be chosen to reduce the data amount, which had to be analyzed. Images in the morning showed often a very low contrast because of the weaker illumination and shadows in the area of interest. A good illumination as well as good contrast were observed at 15:30 Central European Time (CET). If the weather conditions did not allow an observation at this time, the picture at 0800 in the morning was also taken into account. *See the Table 9 (Appendix) for the observation protocol.*

Table 3: DEWF Index

DEWF Index	Hydrological System
− 1	No data (fog, clouds, camera system down)
0	No water flow visible
10	Sheet flow, relatively small amounts of water
20	Sheet flow, strong
30	Sheet flow combined with frontal channel or single low to medium frontal channel
40	Mainly strong frontal channel

The webcam data does not allow statements about the hydrological system in the past. Therefore also the pictures from 4.1.2 Geometric changes of Instabil 1 were used and searched for the evidence of water flow.

4.1.4 Weather Data

Temperature and precipitation measurements from weather stations next to the study area can give information about how water could have influenced the glacier bed through melt or even rain. There are no MeteoSwiss stations in very close proximity to the Weissmies summit, but this is not unusual for mountainous areas because the distribution of weather stations in such areas is often sparse [Rolland, 2003]. The two weather stations of Grächen (1605 m a.s.l.) and Gornergrat (3129 m a.s.l.) are the closest available weather stations, which were accessed with the University licence of CLIMAP (version: 8.4) from the Federal Office of Meteorology and Climatology (MeteoSwiss). The coordinates of the weather stations are the following (*see also Figure 27, next page*):

Gornergrat: 2°626'900 E / 1°092'512 N (3129 m a.s.l.)

Grächen: 2°630'738 E / 1°116'062 N (1605 m a.s.l.)

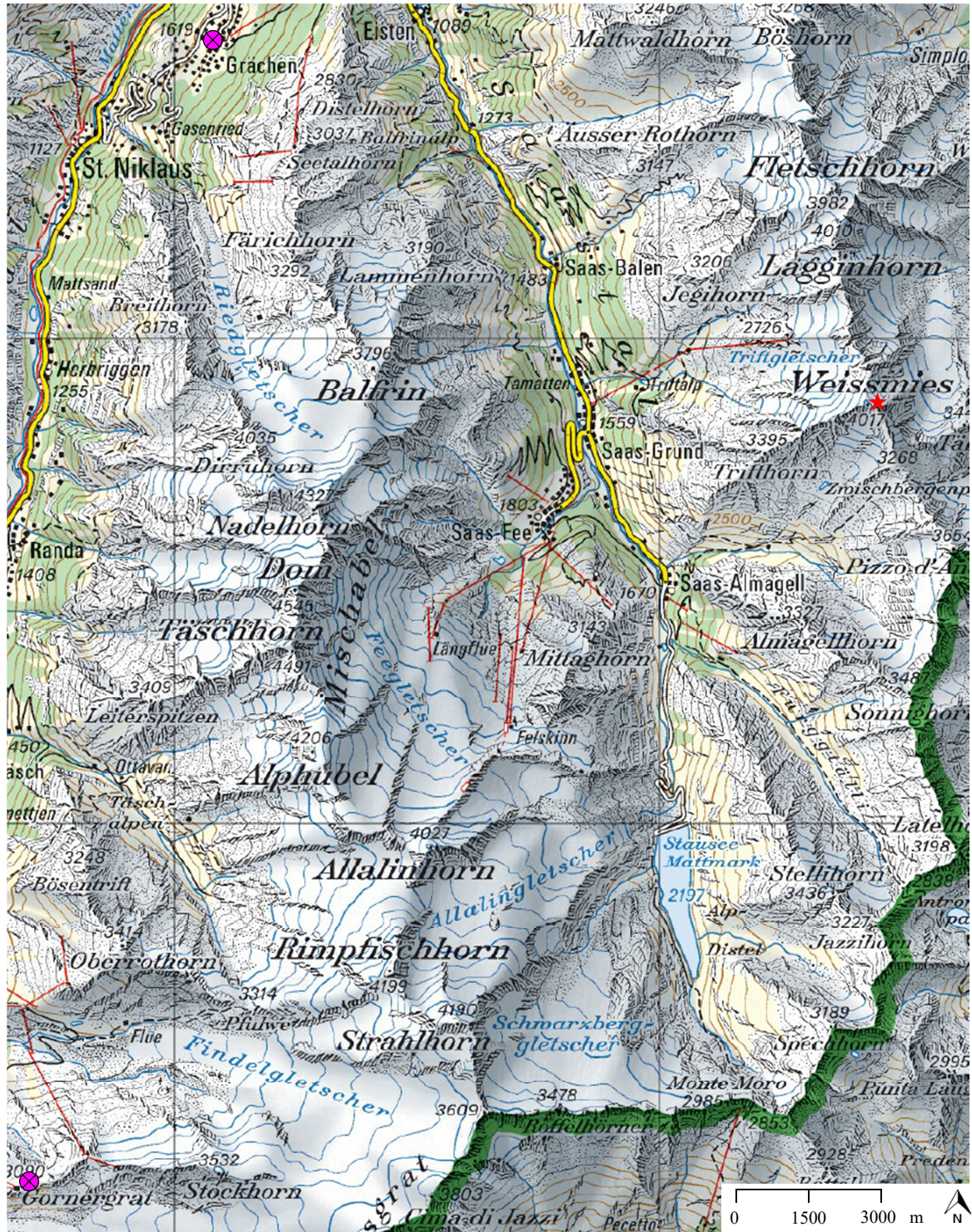


Figure 27: Locations of the weather stations Grächen and Gornergrat

The two weather stations are shown with pink circles. The cross within the circle marks the precise spot of the weather station. The background map is the Swiss national map 1:200'000 from 2014. © swisstopo

The altitude of the two weather stations is lower than the altitude of Instabil 1. But to investigate melting processes the temperatures are of high importance in this study. With increasing elevation, temperatures decrease typically, although certain atmospheric conditions can lead to temperature inversions, which are frequently observed in valleys, especially in winter [Kirchner *et al.*, 2013]. An approach to scale the temperature measurements is the use of lapse rates that display the empirical relationship between air temperature and altitude [Gao *et al.*, 2012]. The altitudinal lapse rate of temperature (ALRT) is defined as the normalized temperature difference between a lower and a higher site and is measured in $^{\circ}\text{C} / 100 \text{ m}$ altitude difference [Fang and Yoda, 1988 in Kirchner *et al.*, 2013]. The ALRT is usually negative, inversions are defined as a positive ALRT. For dry air the ALRT is $-0.98 \text{ }^{\circ}\text{C} / 100 \text{ m}$, this is also called the dry-adiabatic ALRT [Kirchner *et al.*, 2013]. The condensation process of water vapour in the atmosphere leads to the moist-adiabatic ALRT that is lower than the dry-adiabatic ALRT due to the latent heat release. Richard and Tonnel [1985 in Rolland, 2003] have observed a mean yearly temperature decrease of $-0.56 \text{ }^{\circ}\text{C} / 100 \text{ m}$ in the Valais. After an analysis of Gao *et al.* [2012] the most common methods typically assume lapse rates in the range of $-0.6 \text{ }^{\circ}\text{C} / 100 \text{ m}$ to $-0.65 \text{ }^{\circ}\text{C} / 100 \text{ m}$. With measurements they could show that warmer months in the alpine region were characterized by lapse rates in the range of $-0.6 \text{ }^{\circ}\text{C} / 100 \text{ m}$ to $-0.7 \text{ }^{\circ}\text{C} / 100 \text{ m}$. The variability of the lapse rate from April to August was low.

From weather stations different temperature measurements are available: for example daily mean, minimum and maximum temperatures. After Rolland [2003] the highest interpolation reliability was found for maximum temperatures. For this reason daily maximum temperatures were used from the two stations to calculate the temperatures at 3500 m a.s.l. where water flow could be observed at Instabil 1 in 2014 and 2015 [Preiswerk *et al.* 2016]. A stable lapse rate of $-0.65 \text{ }^{\circ}\text{C} / 100 \text{ m}$ was assumed for the calculations because it is often used as a standard in literature. The main analysis is conducted for the melting period of summer 2015. Therefore, a stable lapse rate can be used due to the observed low variability of the lapse rate in the melting period in another study (*see above*). To the daily maximum temperature values of the two stations a correction factor was added. In both cases the correction factor is negative due to the lower altitude of the weather stations (*see Table 4, next page*).

Table 4: Correction factors for the weather stations Grächen and Gornergrat

Station	Altitude [m a.s.l.]	Δ Altitude [m] (to 3500 m a.s.l.)	Correction factor [°C] (lapse rate: -0.65 °C / 100 m)
Grächen	1605	1895	-12,32
Gornergrat	3129	371	-2,41

In addition, from the hourly mean temperatures the positive degree-days, respectively the positive degree-hours per day were calculated. The standard definition for degree-days varies around the world, but often degree-days are calculated by using daily mean temperature values [Day *et al.*, 2006]. The author therefore also used mean temperature values. The base temperature was set to 0 °C because this is the melting point of water. For the thesis it is assumed that temperatures greater than 0° C lead to melt of glacier ice and / or the snow lying on the ice. Positive temperature differences were summed over the day and divided by the number of readings (24). Negative hourly mean temperatures were set to zero. This approach is the most precise way to calculate positive degree-days and positive degree hours [Day *et al.*, 2006].

4.1.5 Velocities

On the 11.06.2015 two low priced GPS sensors were installed on Instabil 1 by the Laboratory of Hydraulics, Hydrology and Glaciology (VAW) of ETH to measure the surface velocities (*see Figure 28, next page*). The GPS sensors work only with the L1 frequency. Despite this disadvantage, the accuracy of the measurements is in the cm range due to the use of differential processing [Preiswerk *et al.* 2016]. For this report the daily (temporal resolution 24 hours) mean 3D velocities of the sensors were used. Also measurements with 4 hours temporal resolution would have been available. Due to the higher measurement uncertainty and outliers of this data, the 24 hours data was preferred.

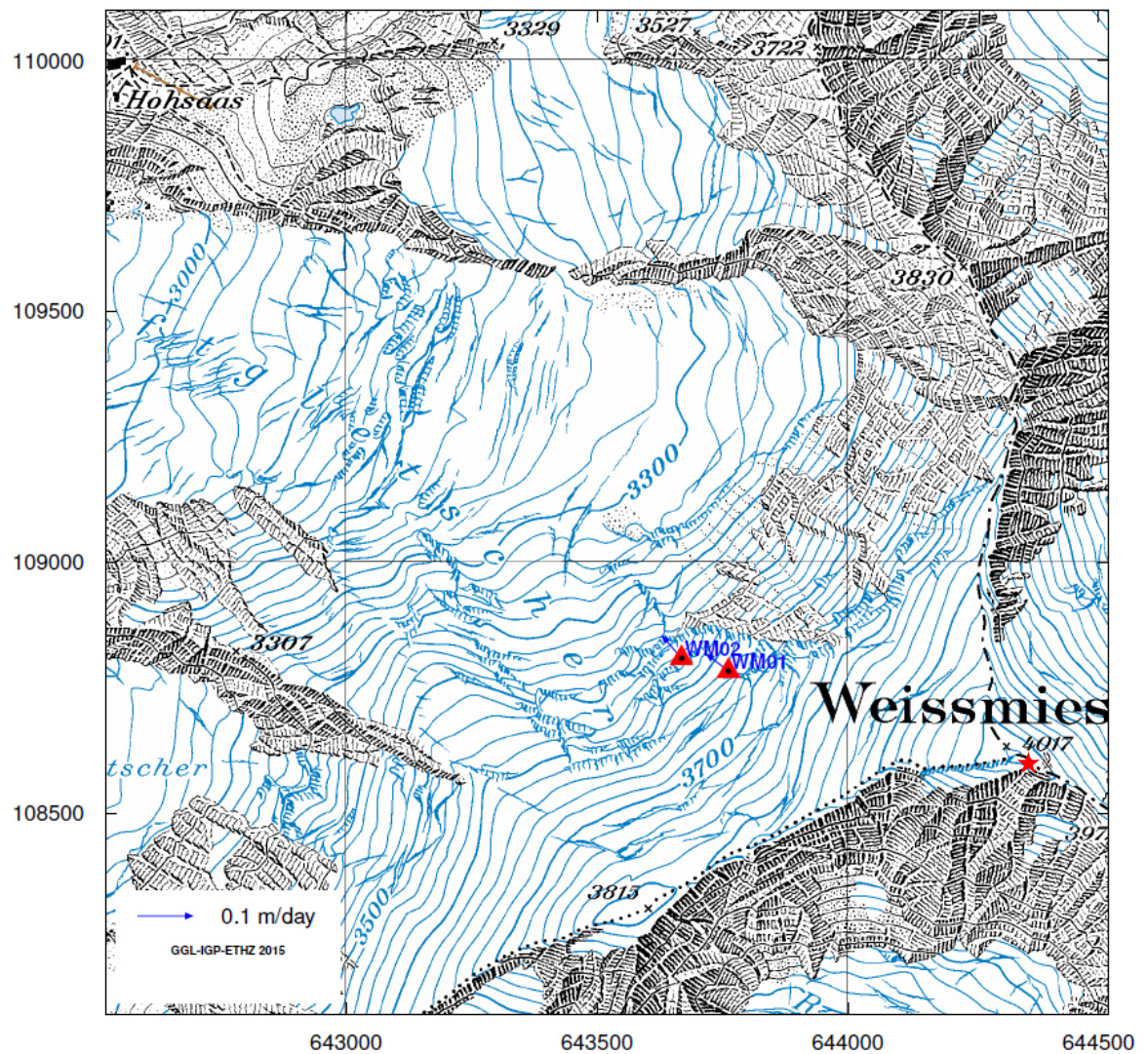


Figure 28: Position of the GPS sensors WM01 and WM02

Overview of the positions of the GPS sensors WM01 and WM02. The background map is the Swiss map raster from 2009. © ETHZ, swisstopo

4.2 Results

4.2.1 Geometric Changes of Instabil 1

1985 Instabil 1 was still connected with the surrounding ice of Triftgletscher (*see Figure 29, next page*). The surface at the transition zone (1) looks ragged at this point in time. Compared to 1955 the situation 1985 looks pretty similar; the nowadays unstable ice masses were supported by ice from below and from the side. Also the depression in the ice surface on the right of Instabil 1 (2) is observable like in 1955. 1992 the situation did not change much regarding the ice connection. But it seems that larger crevasses had developed in the transition zone (1). The ice masses of Instabil 1 were still supported by ice from below (3), but the amount of ice seems to have decreased.

From the pictures of 2003 (*see Figures 50 and 51, Appendix*) it becomes clear that at this point in time the ice connection at the transition zone was still intact. But one year later in 2004 the first time bedrock is visible (1) on the right side of Instabil 1 (*see Figure 30, page 50*). Further the surface in this transition zone between Instabil 1 and rest of Triftgletscher has subsided massively (1). The triangular contours of Instabil 1 are now better visible. From 2004 to 2015 an enlargement of the area where bedrock has appeared can be observed. On the image from 2011 a small ice fall can be observed on the left of the front of Instabil 1. 2012 the support from below has been reduced to a minimum (*see Figures 76 and 78, Appendix*).

The changes in the transition zone are characterized more detailed in *Figure 31* (*see page 51*). The surface has decreased massively from 1985 to 2015. From the DEM analyses, we know that this decrease is around 40 m. The bedrock appearance started with relatively small spots that then extended and connected. The largest area of bedrock can be observed from 2011 and the following years. To have a closer look at this evolution, see also the historical archive collected for this thesis in the appendix.

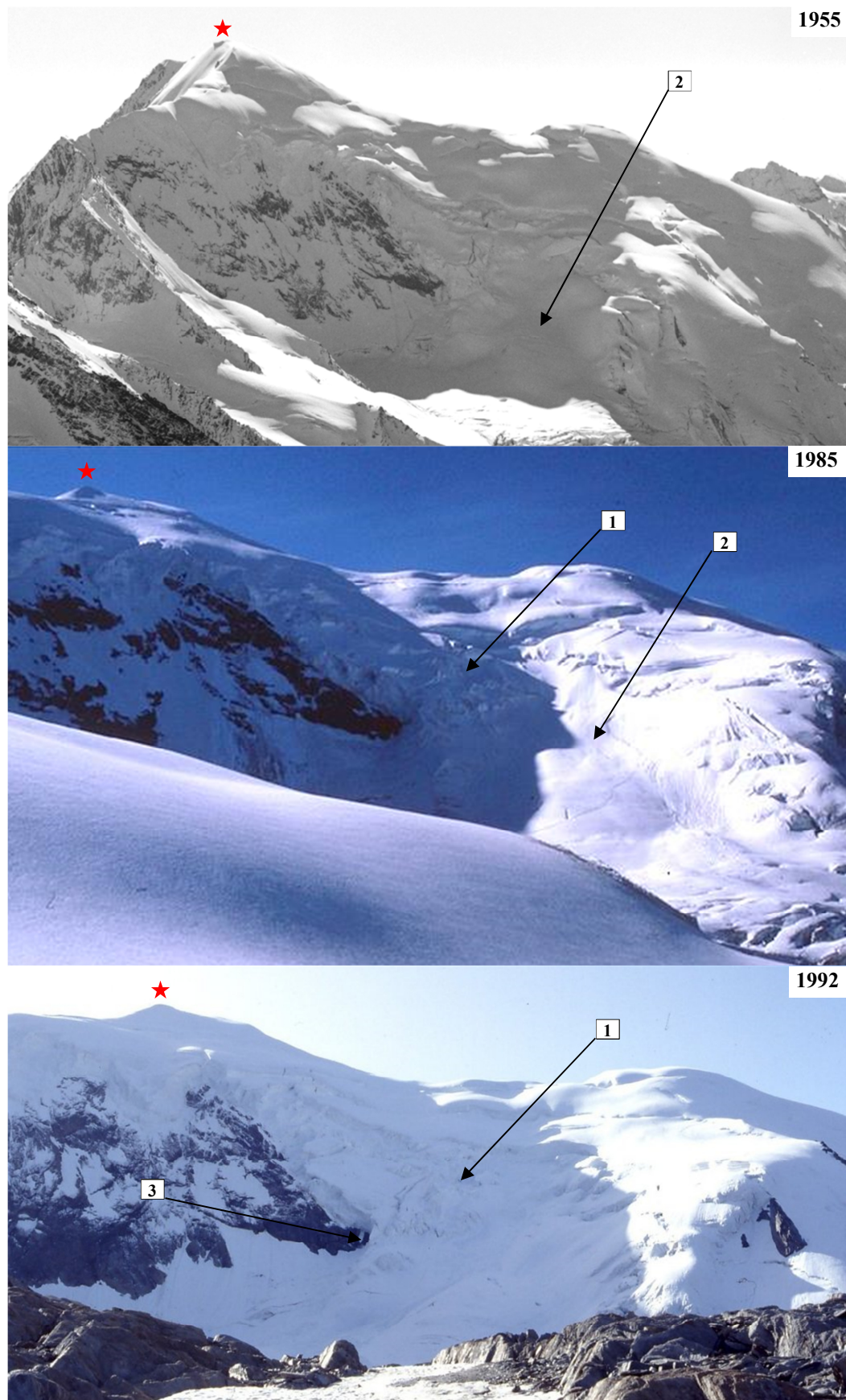


Figure 29: Instabil 1 1955, 1985 and 1992

The evolution of Instabil 1 is shown with 3 pictures for the time period 1955 to 1992. The numbers with arrows are references that are used in the text.

© ETHZ, Johannes Erlbruch and Emil Abadoglu (chronological order)

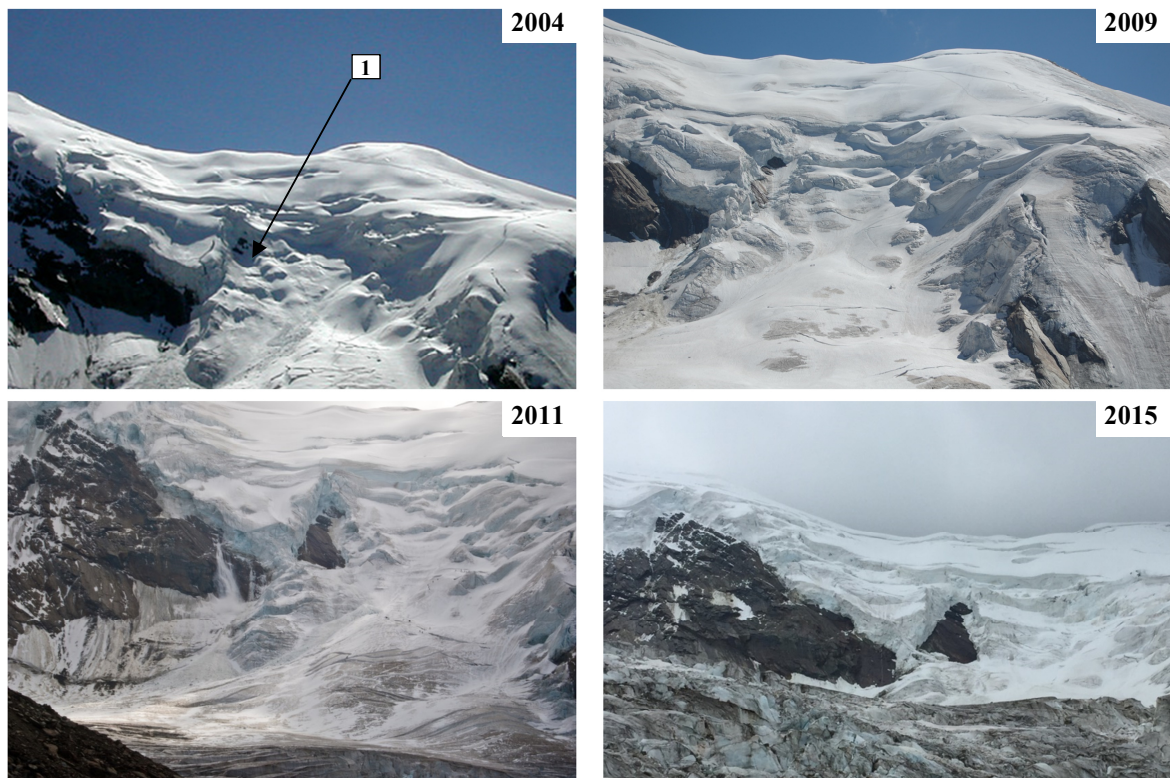


Figure 30: Instabil 1 2003, 2009, 2011 and 2015

The evolution of Instabil 1 is shown with 4 pictures for the time period of 2003 to 2015. The number with the arrow is a reference that is used in the text.

© Marco (2004, anonymous), Alexander Müdespacher (2009 and 2015) and Vivian Boyer (2011)

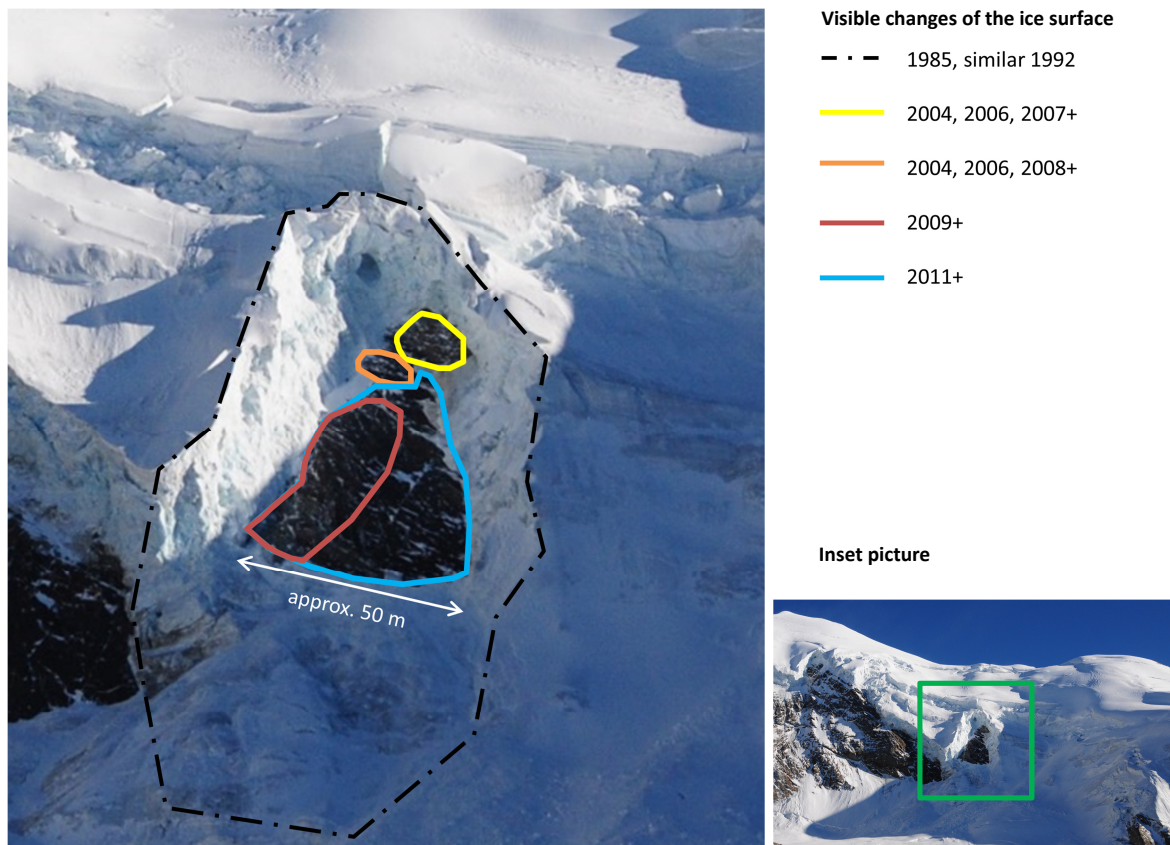


Figure 31: Visible changes of the ice surface at Instabil 1 between 1985 and 2015

For 1985 to 2015 the bedrock appearance and the ice surface changes are highlighted. The black point line shows the extent of the ice 1985. The colored lines show when bedrock could be observed at these locations. The + stands for the corresponding year and the following years until 2015 (e.g. 2007+). The background image is from 2014. © PermaSense Project

4.2.2 Hydrology, Weather Data and Velocities

Due to the theoretical entanglement discussed in chapter 2 (the subglacial drainage system has an influence on the velocities and is influenced by the temperatures), the results of the hydrological observations as well as the weather and velocity measurements are presented together in this chapter.

The comparison of the DEWF index with the lapsed maximum temperatures shows that the drainage system was 2015 strongly connected with the temperatures above 0 °C (*see Figure 32, page 53*). Water was only observed when the temperatures allowed melting. The temperature peaks correlate well with peaks of the subglacial drainage system. A similar result was achieved with the positive degree hours and the DEWF index (*see Figure 42, Appendix*). The DEWF index increases with increasing time. From a DEWF index of 20 to a DEWF index of 40 two months elapsed. At the beginning of the melting season in May (1), relatively strong precipitation peaks (up to nearly 40 mm day) were

measured in Grächen, but they seem not to have had an influence on the DEWF index – at least not the following days when the webcam data was available again. Around end of June and begin of July a period with the highest maximum temperatures and the most positive degree hours a day of the melting period 2015 can be observed (2). But during this time the DEWF index did not reach its maximum value. This value was reached one month later together with a temperature peak in early August for the first time (3).

Regarding the evaluation of the drainage system from the webcam images it is important to note the shadows in the scenery, changing contrast, new snow and fog made the assessment challenging.

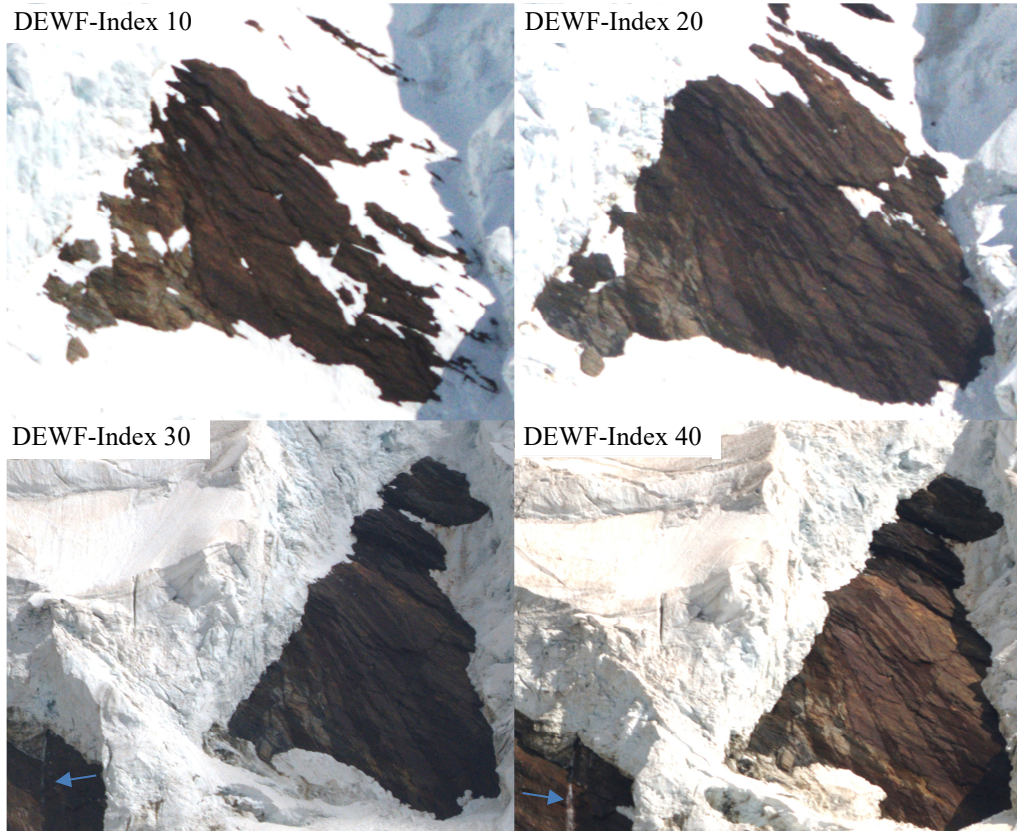
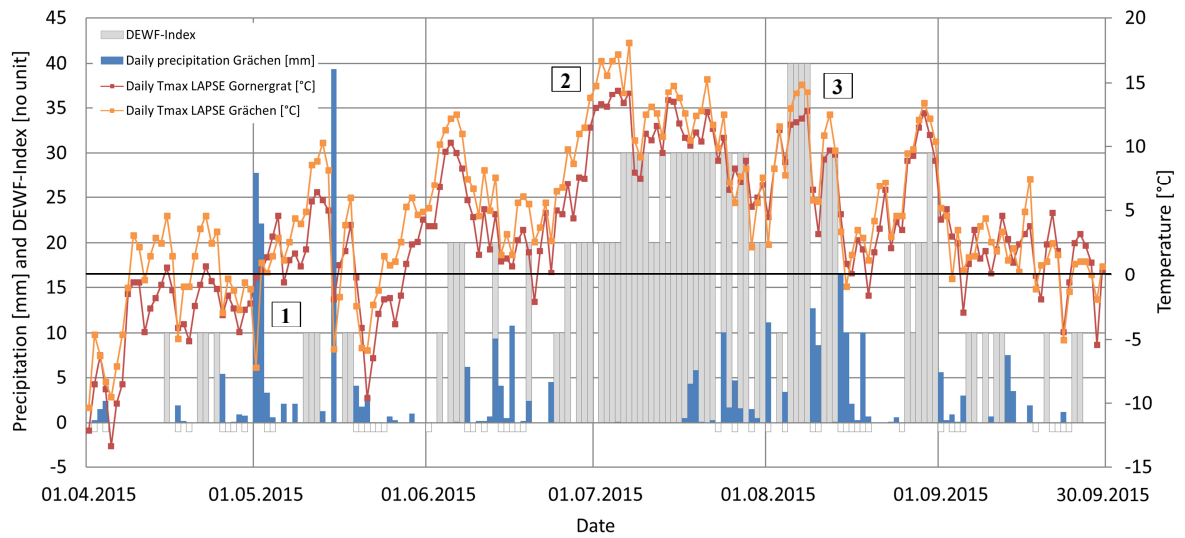


Figure 32: Drainage system of Instabil 1 in summer 2015 compared to weather data

The upper graph shows the evolution of the DEWF index together with temperature and precipitation measurements. For the temperatures a lapse rate of $-0.65\text{ }^{\circ}\text{C} / 100\text{ m}$ was used. A negative DEWF index means no data. The 4 images below are examples for the corresponding DEWF values. The numbers are references that are used in the text. The blue arrows show the channels. © PermaSense Project

When the DEWF index and cumulative degree hours for 2015 are plotted together (*see Figure 33*), a kind of hysteresis curve is visible, which is indicated with a gray arrow for the two weather stations in the figure: With increasing cumulative positive degree hours (lapsed temperatures) the DEWF index increases. To reach a DEWF index of 40 from the start of the melting season around 7000 cumulative degree hours are needed according to the figure. After reaching this state, the DEWF index decreases towards the end of the melting season (which is the maximum value of the cumulative degree hours) again to 0.

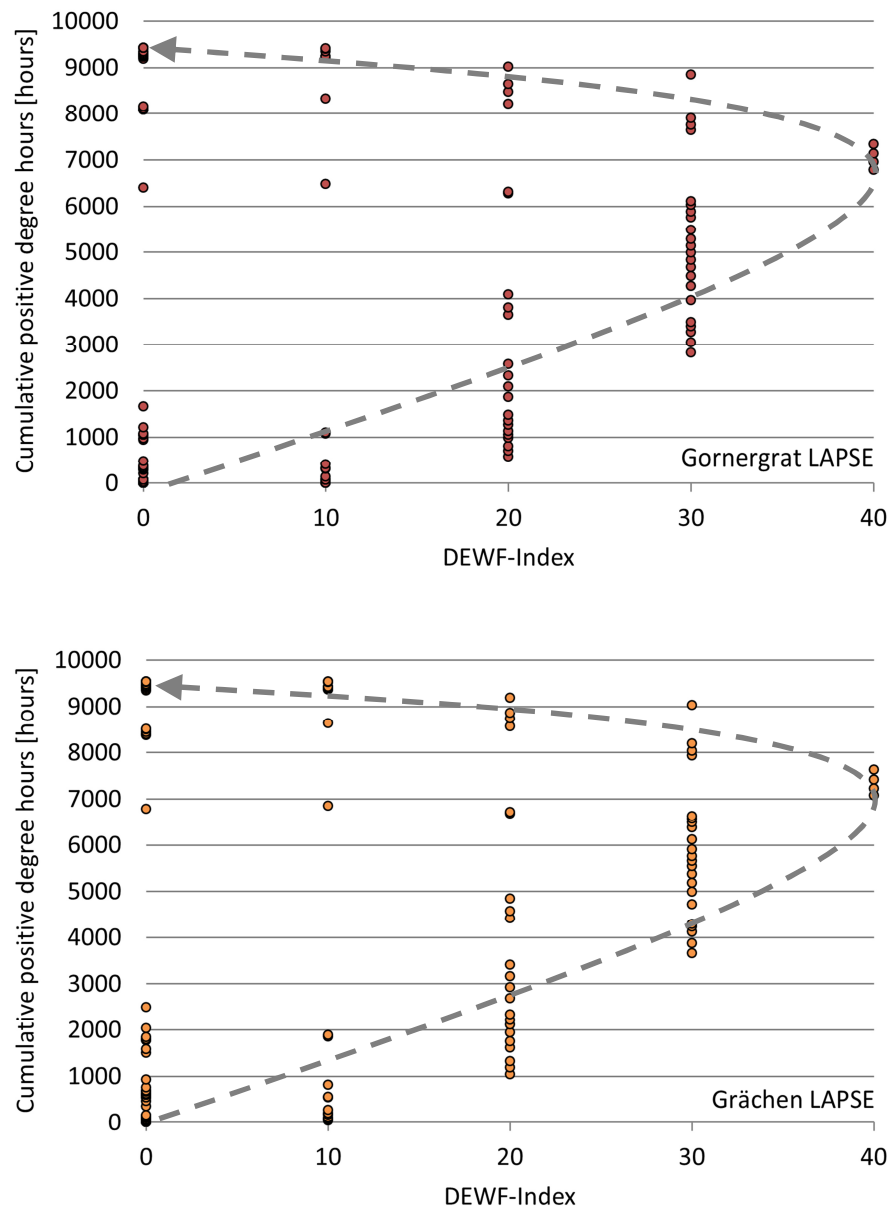


Figure 33: Cumulative degree hours and DEWF index for summer 2015

The upper graph shows the cumulative degree hours and corresponding DEWF index values for the Gornergrat weather station, the graph below shows the same for the Grächen weather station. The gray arrows indicate the evolution during the melting period.

The dynamic behavior of Instabil 1 was measured with two GPS sensors and is plotted in *Figure 34* to compare it with the DEWF index and the temperatures. At the beginning of July (1), the temperatures drop and so do the velocities. Prior to this drop, the velocities were more or less stable between 5 and 10 cm / d. Then the temperatures increase and decrease again and the velocities follow this trend (especially WM01). The temperature peak at the begin of August (2) is also followed by a velocity peak. But this peak is not so big as the velocities measured at the begin of July. Then around end of August / begin of September, we can see a similar behaviour of the velocities (3) with a small delay. During the melting period, the overall velocity increases are only a few cm per day.

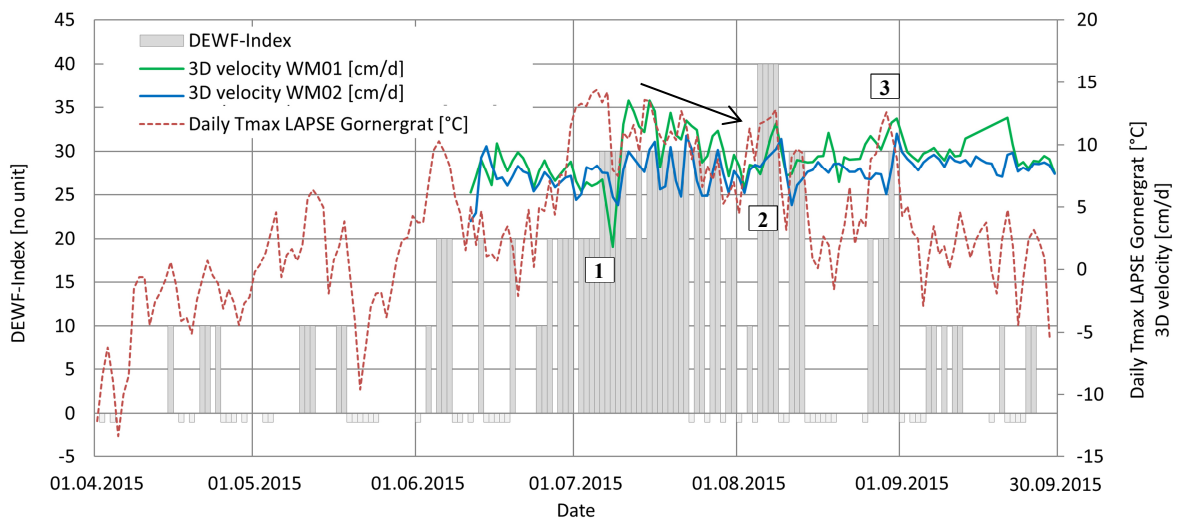


Figure 34: GPS measurements, DEWF index and temperatures for summer 2015

The graph shows the GPS velocities of WM01 and WM02 together with the evolution of the DEWF index and temperature data. For the temperatures a lapse rate of $-0.65\text{ }^{\circ}\text{C} / 100\text{ m}$ was used. A negative DEWF index means no data. The numbers are references that are used in the text. The black arrow is used in the discussion of the results.

The full dataset of the GPS measurements (*see Figures 43 and 44, Appendix*) shows that in winter 2015 / 2016 the velocities were mostly in the range of 5 to 8 cm per day, while WM02 shows generally a bit lower velocities than WM01. The standard deviation for the velocities is for most of the measurement points smaller than 1 cm / d.

To compare the summer of 2015 with the summer of 2014, the precipitation values and the maximum temperature values lapsed at Instabil 1 are plotted in *Figure 34* (*see next page*). Especially in July and August the maximum temperatures in 2015 are most of the time clearly warmer than in summer 2014. During end of July and in August much more precipitation was measured in 2014; one peak can be observed at the beginning of August

and another peak at the end of August together with an increase in the maximum temperatures.

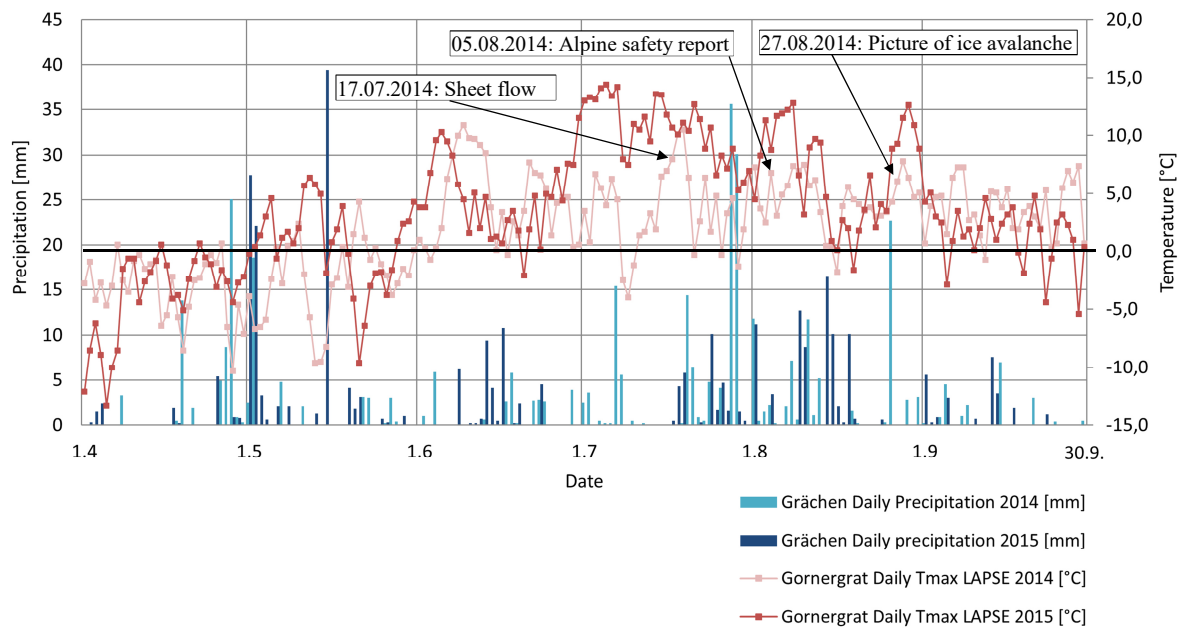


Figure 35: Weather of summer 2014 compared to summer 2015

The maximum lapsed temperatures from Gornergrat and the precipitation values from Grächen are shown for May to September 2014 and 2015. The additional date information is used in the discussion of these results.

About the subglacial drainage system evolution in summer 2014 not so much data is available, as the webcam was installed just on the 16.10.2014. The few available pictures allow the following statements: On the 17.07.2014 ice can be observed on the bedrock beside Instabil 1 (see Figure 36, next page). A picture from the beginning of August with less contrast on the side leads to the assumption that a small frontal channel was active on the 05.08.2014 (see Figure 37, next page). Due to the low contrast it is not possible to say if sheet flow occurred at this point in time. The picture shown in Preiswerk et al. [2016] from the 30.09.2014 indicates sheet flow at the end of September.



Figure 36: Ice on the bedrock besides Instabil 1 on the 17.07.2014
The image shows ice in the transition zone of Instabil 1. © Clemens Walter

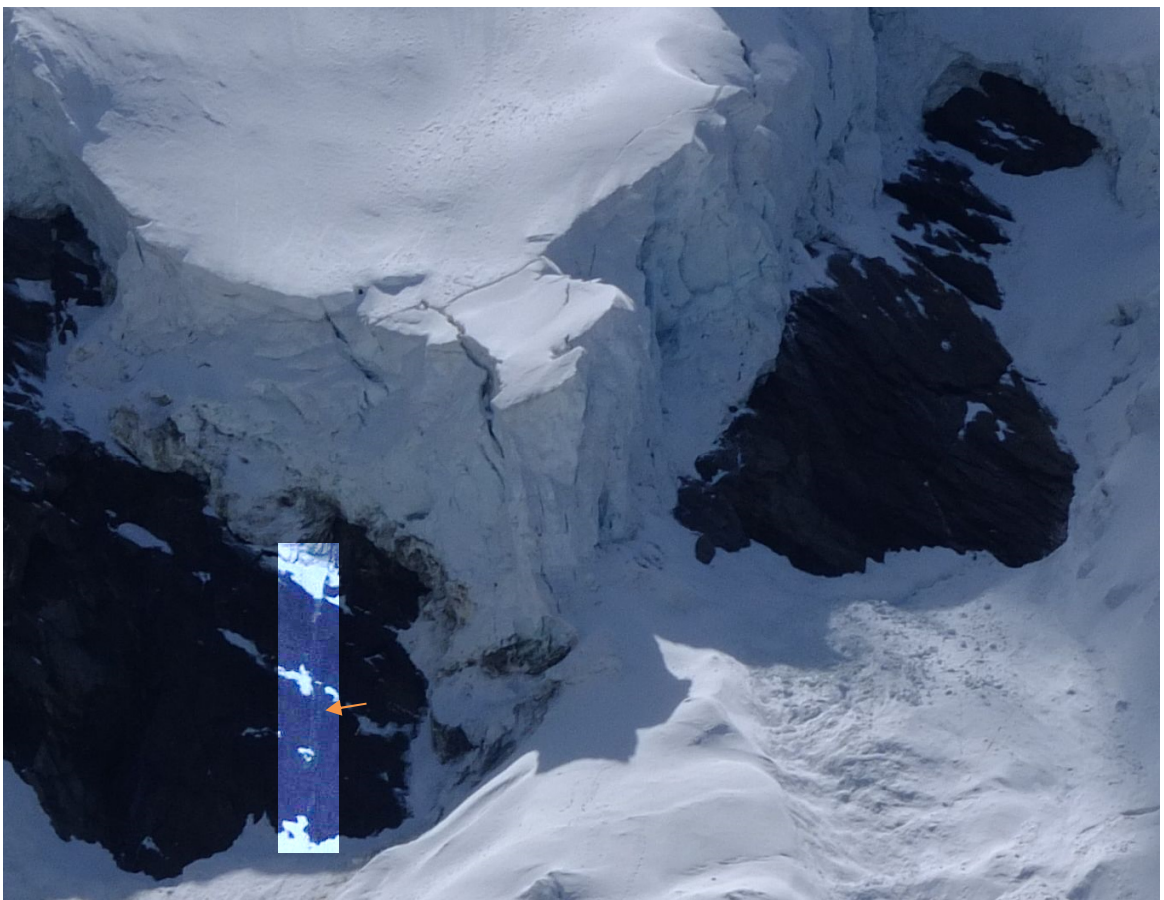


Figure 37: Assumed small channel below Instabil 1 on the 05.08.2014
In the area where the channel is assumed the brightness was increased to make the channel better visible.
The orange arrow points to the channel. © Alexandra Bürge

From these observations, the question also arises how the hydrological system was in the past. *Figure 38* on the next page shows observable subglacial drainage systems from 2003 to 2013. Most of the pictures were taken in August during the high season of mountaineering and hiking at the Weissmies. In 2003 and 2004 a distinct frontal channeled stream can be detected. In 2009 sheet flow on the side can be confirmed. In addition to that the frozen water in the front provides evidence of two more or less channeled frontal streams in the same year. The picture of 2010 only gives evidence of a strong frontal stream. From 2011 to 2013 frontal channeled streams with sheet flow on the side can be observed, whereas the sheet flow in 2011 cannot really be confirmed due to the low contrast in the image. According to the images, the location of the frontal stream can vary between the years.

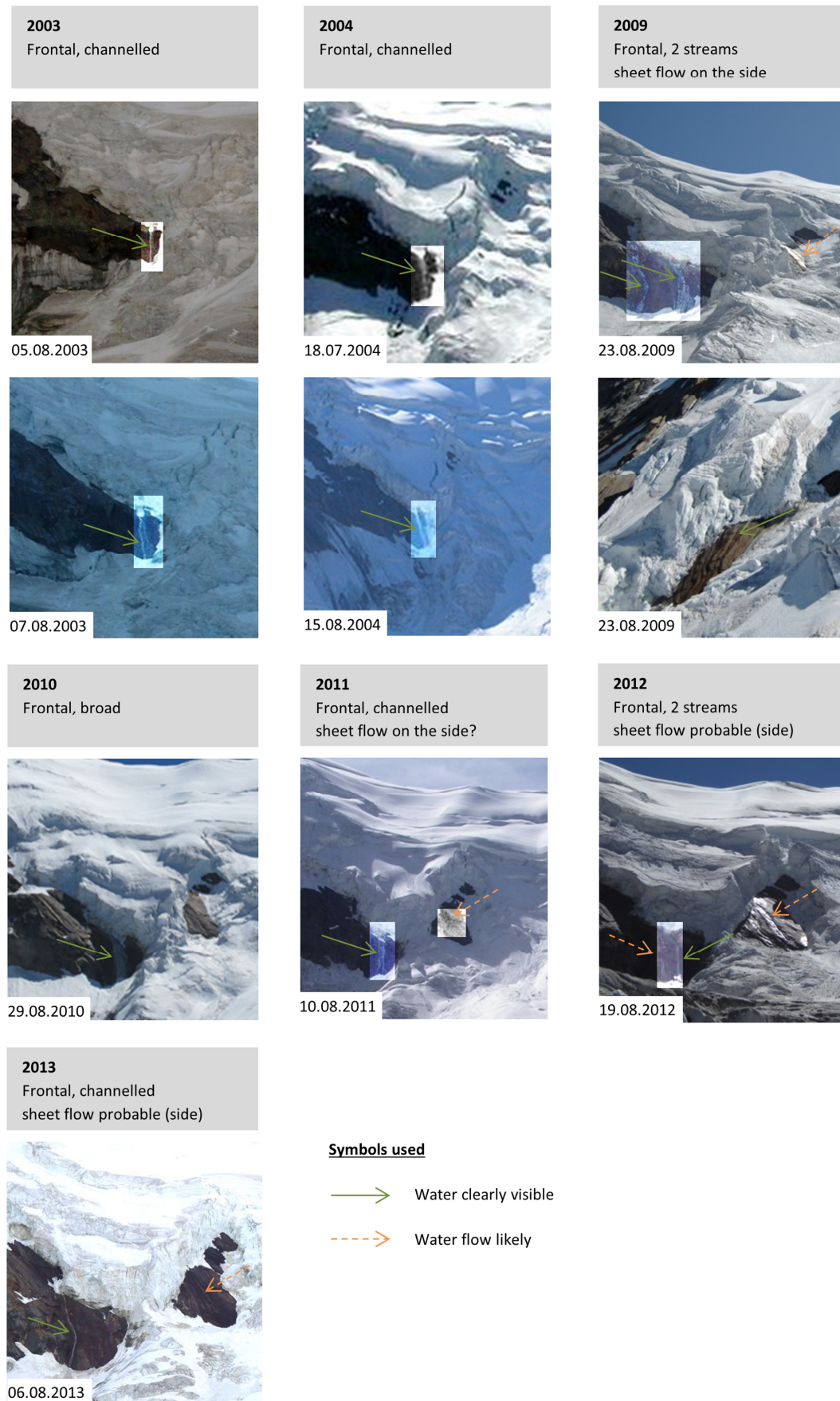


Figure 38: Observable subglacial drainage systems before 2014

For each available year the observed drainage system is shown with an image. In some areas the brightness was increased to improve the visibility. The green arrows indicate clear water flow, the orange arrows likely water flow. 2011 the indications for sheet flow are not so clear compared to 2009, 2012 and 2013. © Jürgen Wißkirchen, Georg Rothe, Marco (anonymous), Cyrill Rüegger, Alexander Müdspacher, Marcel Fuchs, Michael Thut, Oliver Schmid and Dennis Henß

4.3 Discussion

The surface decrease of Triftgletscher near Instabil 1 was already discussed in chapter 3 long-term Evolution. The results of the recent evolution back these results as the support from below has also decreased in the pictures from hikr.org and other sources. The increasing amount of crevasses in the transition zone during this evolution, where later bedrock appeared, could already be a sign of destabilization processes in this area. The most striking changes were observed after the summer of 2003. An explanation for the appearance of bedrock in 2004 and the massive decrease of the surface in the transition zone could be the summer heat wave that affected Europe in 2003. In Switzerland, the summer average was 4 to 5.5 °C higher than the 1961-1990 reference period [García-Herrera *et al.*, 2010]. Two periods of exceptional heating can be distinguished for the summer 2003: first in June and second in the first half of August in which the temperatures were significantly higher than in June at a daily and weekly scale.

Moreover, the effects of the heat wave were amplified by a lack of precipitation which led to reduced soil moisture, surface evaporation and evapotranspiration and therefore to a positive feedback effect [Beniston and Diaz, 2004]. Dramatic consequences of the heat wave like droughts and an increase in mortality were observed. Regarding the case study of this report, the consequences of the heat wave for alpine glaciers are of interest. Various studies estimated to total mass loss of alpine glaciers in the range of 5–10 % [García-Herrera *et al.*, 2010]. The freezing limit rose above 4500 m a.s.l. for 10 days, which led to anomalous thawing, also of permafrost. Other results from field measurements indicate an average loss in thickness of glaciers in the European Alps of about 3 m water equivalent which corresponds to approximately five times more than the average loss during the exceptionally warm period 1980-2000 [De Bono *et al.*, 2004].

Zappa and Kan [2007] showed that the reduced discharge during the heat wave 2003 in 15 % glaciated alpine basins was strongly compensated by ice melt so that the discharge during summer 2003 for these basins was very close to the historical annual and summer averages. The study showed that ice melt is directly correlated to anomalies in the aridity index which means that when the aridity index is low (very dry conditions), glacier melt is high. This result is another indication that the summer heat wave 2003 has influenced Triftgletscher a lot. Together with the information that the freezing limit rose above 4500 m a.s.l. it becomes clear that Instabil 1 was also very likely affected by the heat wave.

Once the surface and the support from below has decreased in the transition zone, the steep ice walls of Instabil 1 were probably also subject of an increased icefall activity which then further increased the disintegration of Instabil 1. Once bedrock appears, the albedo of these spots decreases in comparison to the surrounding ice and snow [Coakley, 2003 and Dobos, 2006]. Heating of this spots lead to an enlargement over time, which makes this areas again subject to more heating and so a feedback loop could develop.

Apart from the geometrical changes, the evolution of the subglacial drainage system is of high importance to assess the instability better. We could see that in summer 2015 the drainage system was very dependent on the temperature as well as the time it has to develop. Although very high maximum temperatures were measured at the beginning of July, the drainage system still was not efficient enough to form strong a strong frontal channel. We can see a similar development of the drainage system as theoretically described in 2.3 Subglacial Drainage Systems: The melting season starts with relatively little amounts of water draining on the side of Instabil 1 which then gradually increases. Over time - given that the temperatures are high enough to allow melt - the drainage system develops further into a faster and more efficient drainage system which finally consists of a strong frontal stream. Towards the end of the melting season the melt of ice is smaller, less water is evacuated and therefore the channels then gradually close and the drainage systems become inefficient again.

The figure comparing the cumulative degree hours with the DEWF index shows that some heating in the system is needed until it can evolve further. Higher temperatures lead to more melt and therefore probably to a faster development of a channelled drainage system. The GPS velocity measurements seem to follow the temperature values with a small delay, but it is important to note that the changes are relatively small. During the temperature peak at the beginning of August, the velocities are lower than during the temperature peak in mid of July. An explanation could be the observed transition to a more efficient drainage system that leads to a decrease of the velocities. But because the temperatures had decreased before this temperature peak, it would also be possible that only the temperature decrease had influenced the basal motion by less meltwater. This is the reason why further measurements would be needed to confirm if the change in the subglacial drainage system really has such an influence. As already highlighted before, the observed changes are relatively small and do not reach the values of the summer 2014. Taking the velocity measurements during winter 2015 / 2016 into account, the difference of the

velocities between winter and summer provides further evidence that the drainage system and / or the temperatures influence the dynamic of Instabil 1 as the velocities in winter are clearly lower.

For 2014 no velocity measurements are available and the subglacial drainage system cannot be reconstructed for the whole melting season. But with the weather data from 2014 and the observations from 2015 some conclusions can be drawn.

Figure 36 shows ice on the side of Instabil 1 on the 17.07.2014, which could be due to an ice avalanche. But because of the temperature increase measured during this period of time and also the location of the ice it seems more likely that it is frozen sheet flow. *Figure 37* from the 05.08.2014 suggests that a small frontal channel existed at that time. In 2015 already in mid of July such a small frontal channel was observed. This means that the subglacial drainage system was 2014 not equally developed. This is not surprising as the temperatures at the beginning of July were clearly lower in 2014. The alpine safety report from the 04.08.2014 [*alpinesicherheit.ch*, 2016], indicating increased ice fall activity at Instabil 1, as well as the picture of the larger ice avalanche from the 27.08.2014 (see *Figure 26, page 39*) lie both in a phase of increasing temperatures in 2014. The increased meltwater and the subsequent water pressure at the bed together with the less efficient drainage system could therefore have led to higher velocities and the observed ice fall activity. These results back the hypothesis of *Preiswerk et al.* [2016]. Interesting in this context is that in Grächen high precipitation values were measured prior to the safety report as well as the observed large ice avalanche. This means there could also be an influence of rain. As the precipitation measurements were not conducted exactly at the study site, this effect cannot be confirmed for sure.

Because the unstable part has slowed down after 2014, it would also be possible that in 2014 a change from polythermal to fully temperate conditions at the bed has occurred. As *Preiswerk et al.* [2016] have highlighted the glacier is likely in a transition from cold to temperate as meltwater warms the previously cold bedrock. Subglacial water systems could also be observed in the years before, so eventually the transition is more advanced than previously assumed and the change in bedrock conditions has occurred without a large break off.

To conclude, the evolution of the instability is connected to geometrical changes (lack of support) as well a change in the thermal conditions at the glacier bed. The destabilization

process in the Weissmies case took relatively long from 1985 to the increased icefall activity in 2014.

The slowdown of Instabil 1 arises the question if the monitoring is still necessary. In the view of the author, the GPS measurements can be used to control the glacier dynamics and they would help to detect future changes. They are cheaper than the radar measurements with the disadvantage that they are only point measurements. Also in winter, for cold instability conditions (*see chapter 5 Synthesis*), the GPS measurements would help to assess the time of break off.

4.4 Summary of Results

This section shortly summarizes the results and discussions of this chapter:

- The decreasing support from below and the disintegration of the transition zone is clearly visible since 1992 and the following years. Larger crevasses developed in the area of the transition zone, which could already be signs for the disintegration before the surface decreased and bedrock appeared in 2004.
- The area with bedrock visible in the transition zone extended from 2004 to 2015 massively.
- An explanation for the strong changes in 2004 could be the summer heat wave 2003, which led to 5-10 % total mass loss of alpine glaciers and a rise of the freezing limit above 4500 m a.s.l. for 10 days.
- The drainage system during summer 2015 was strongly connected to positive temperatures. Peaks in the DEWF index occurred simultaneously with temperature and daily positive degree hours peaks. But besides temperatures, time is another important parameter influencing the DEWF index because the drainage system needed 2 months to develop and reach the maximum value of the DEWF index of 40.
- The GPS velocities followed the temperatures most of the time in summer 2015. From the data it is not clear if the type of drainage system has influenced the velocities. The velocities in winter 2015 / 2016 were clearly lower than in summer with values in the range of 5 to 8 cm per day (in summer the velocities were twice as high).

- From 2014 we know that in early August a small frontal channel existed. In 2015 already mid of July such a small frontal channel was observed. This means that the subglacial drainage system was 2014 not equally developed. This is not surprising as the temperatures at the beginning of July were clearly lower in 2014. These results support the hypothesis of *Preiswerk et al.* [2016] that assumed a change in the subglacial drainage system.
- Increased ice fall activity at Instabil 1 in 2014 (alpine safety report, picture of larger ice avalanche) occurred during a phase of increased temperatures. Prior to these events, high precipitation values were measured in Grächen. This additional water could have influenced the velocities. Due to the location of the weather station, this result cannot be confirmed for sure.
- Data from subglacial drainage systems are available from the years 2003, 2004 and from 2009 to 2013, often indicating a frontal channel and from 2009 on also sheet flow on the side. Therefore the thermal transition at the glacier bed is eventually more advanced than previously assumed.

5

Synthesis

This chapter merges the results from chapter 3 and 4 and discusses future implications of the instability at the Weissmies.

5.1 Conclusion

With this thesis a detailed long-term reconstruction of the evolution of Triftgletscher was conducted that has not existed before. These insights allowed a better understanding of why Instabil 1 has become unstable over the course of time, especially it was proven with DEMs that the relatively flat surface below the instability has decreased.

Further, it was possible due to the large amount of pictures collected to connect the disintegration and the surface decrease in the transition zone of Instabil 1 with the summer heat wave 2003. The introduced DEWF index is a simple but still very useful approach when it comes to study a drainage system where no other measurements are available or possible. The connection of the DEWF index with temperature and velocity measurements allowed more precise statements about the drainage system in summer 2015 and gave some further insights about the drainage system in 2014. The analysis for 2015 demonstrated that the subglacial drainage system at Instabil 1 is a dynamic system that changes over time and also during the melting season.

This thesis showed that the evolution of the instability at the Weissmies hanging glacier is a combination of geometrical changes as well as thermal changes at the glacier bed – both emerging from climate warming. Last but not least the thesis also revealed the need for accurate and local data to assess hanging glacier stabilities better.

5.2 Future Evolution and Hazard Assessment

This thesis has set its focus on the past evolution of the instability. But for the hazard potential, it is also of high importance how Instabil 1 will evolve in the next years and decades.

As already discussed, Instabil 1 is very likely in a transition from cold to temperate conditions at the glacier bed. This means in the long run the ice-bedrock interface will be temperate - if it is not already. As we have seen in chapter 2.2 Types of Instabilities the

thermal nature at the glacier bed plays a very important role regarding the type of instability and the possibilities of the break off assessment and prediction. A temperate state at the bed could be better assessed as break offs are coupled with rapid changes of the subglacial water runoff. Temperature and precipitation measurements could help to detect such phases and could then together with velocity measurements be used for an early warning system.

The summer heat wave 2003 showed that such periods with high temperatures and corresponding melt above 3000 m a.s.l. can lead to a strong disintegration of ice masses. It is expected that similar events will occur in the second half of this century as a result of global climate warming and increased variability in temperature and precipitation [Zappa and Kan, 2007]. In addition, it is assumed that such events will occur with much greater frequency in future [Beniston and Diaz, 2004]. For future scenarios in alpine regions above 1500 m a.s.l. temperature increases of up to 4.2 °C until the end of the 21st century were modelled [EEA, 2009].

For Instabil 1 this could mean that the area with visible bedrock on the side will expand further and that Instabil 1 will be more and more disintegrated through melt and ice falls or ice avalanches. The disintegration can happen in small chunks or at once, which would be very dangerous. The warmer summers would promote through more melt rather an efficient subglacial drainage system, especially in July and August. This has also the implication that larger break offs would probably more likely occur in spring or towards the end of the melting season when the drainage system is not efficient enough and a pulse of subglacial water flow could trigger a rupture event. Signs that help to estimate the time for such a pulse of subglacial water flow can be a sudden temperature increase and / or strong precipitation in the study area.

In winter, the cold glacier instability principles can be applied to Instabil 1 because no water is visible. The GPS measurements are in this case very useful for the prediction of the time of break off. These calculations cannot be conducted in summer due to the influence of meltwater.

5.3 Open Questions and Limitations

Data availability is one of the main limitations when it comes to assess the instabilities at the Weissmies in more detail. About the conditions at the bed only indirect information (for example water flow or surface velocities) can be used at the moment to evaluate the

situation. Moreover, it is not known how the bedrock beneath Instabil 1 is structured. Temperature measurements at the bed and ground penetrating radar (GPR) measurements would for sure improve the knowledge about the processes at the ice-bedrock interface, but due to the steep, heavily crevassed and icefall endangered terrain it is not surprising that such measurements have not yet been conducted. Also *Preiswerk et al.* [2016] suggest such analyses.

Another possibility to gain even more information about the subglacial drainage system would be discharge measurements and / or dye tracer experiments. But for these measurements it would be necessary to work on the unstable part of the glacier. The dye tracer measurements could be shifted to the tongue (insertion of the tracer still on Instabil 1 for example by helicopter), but would they would there be influenced too much by the melt of the much bigger rest of Triftgletscher.

This thesis characterized the drainage system for summer 2015 in a detailed manner. But for the summer of 2014 such an approach is not possible due to image availability. It could be possibility a for future research to study the drainage system for summer 2016 or even 2017 (if the webcam is then still installed at that point in time) with the same approach. Due to the low contrast on some of the webcam images, an infrared camera could probably also help to observe the drainage system better.

Acknowledgement

Foremost I would like to express my gratitude to my supervisor Dr. Jérôme Faillettaz for his support and the engaging discussions that made this master thesis possible. He supported me with his in-depth knowledge and I could ask him for advice whenever I needed it. Further, I would like to thank Prof. Dr. Andreas Vieli as head of the Unit Glaciology and Geomorphodynamics Group 3G for his helpful comments and the participation in many discussions with Dr. Jérôme Faillettaz. I would like to thank Johann Müller (PhD student 3G) for his help with the Agisoft PhotoScan software and Dr. Frank Paul (Senior researcher 3G) for his provided information about the DHM25.

My thanks go also to the group Glaciology of the Laboratory of Hydraulics, Hydrology and Glaciology (VAW) of the ETH headed by Prof. Dr. Martin Funk, which supported me with data and background information of the Weissmies case. Especially the discussions with Lukas Preiswerk (PhD student VAW) bore fruit and gave new insights. In addition, I would like to thank Dr. Jan Beutel (ETH, Computer Engineering and Networks Lab) for his help and the data from the PermaSense network, especially the GPS data.

Last but not least I would like to thank my family and friends who motivated and encouraged me during the whole writing process of the master thesis.

† In memories of Tanja & Cyrill Rüeegger-Buhr and Daniel Hohl

During the process of clarification of the usage rights of the Weissmies pictures from hikr.org I was shocked to read that one of the photographers, his wife and a friend of them died due to an avalanche at Piz Palü on the 13.06.2009.

References

- Alean, J. (1985), Ice avalanches: some empirical information about their formation and reach, *Journal of Glaciology*, 31(109), 324–333.
- Beniston, M., and H. F. Diaz (2004), The 2003 heat wave as an example of summers in a greenhouse climate?: Observations and climate model simulations for Basel, Switzerland, *Global and Planetary Change*, 44(1-4), 73–81, doi:10.1016/j.gloplacha.2004.06.006.
- Coakley, J.A. (2003), Reflectance and albedo, surface, *Encyclopedia of Atmospheric Sciences*, 1st edition, Holton, J.R., J. Pyle and J.A. Curry (Editors), Academic Press, 1914–1923.
- Day, T., B. Franklin, M. Fry, M. Holmes, T. Johnston, J. Mansfield, D. Wood, and H. Davies (2006), Degree-Days - Theory and Application, *TM41: 2006*, CIBSE, London. Online available: <http://www.cibse.org/Knowledge/knowledge-items/detail?id=a0q20000008I73TAAS> (last access : 22.09.2016)
- De Bono, A., P. Peduzzi, S. Kluser, and G. Giuliani (2004), Impacts of Summer 2003 Heat Wave in Europe, *United Nations Environment Programme - Environment Alert Bulletin*(2), 1–4. Online available: <http://archive-ouverte.unige.ch/unige:32255> (last access: 05.09.2016)
- Dobos, E. (2006): Albedo, *Encyclopedia of Soil Science*, 2nd edition, Lal, R. (Editor), Taylor & Francis, New York, Abingdon, Oxon, 64–66.
- EEA (2009), Regional climate change and adaptation. *The Alps facing the challenge of changing water resources*. Office for Official Publications of the European Communities, Luxemburg, doi:10.2800/12552.
- Faillietaz, J., M. Funk, and C. Vincent (2015), Avalanching glacier instabilities: Review on processes and early warning perspectives, *Reviews of Geophysics*, 53(2), 203–224, doi:10.1002/2014RG000466.
- Fang, J.Y., and K. Yoda (1988), Climate and vegetation in China: changes in the altitudinal lapse rate of temperature and distribution of sea level temperature, *Ecological Research*, 3, 37–51, doi:10.1007/BF02348693.
- Flowers, G. E. (2015), Modelling water flow under glaciers and ice sheets, *Proceedings of the Royal Society A: Mathematical, Physical and Engineering Sciences*, 471(2176), doi:10.1098/rspa.2014.0907.
- Fountain, A. G., and J. S. Walder (1998), Water Flow Through Temperate Glaciers, *Reviews of Geophysics*, 36(3), 299–328, doi:10.1029/97RG03579.
- Gao, L., M. Bernhardt, and K. Schulz (2012), Elevation correction of ERA-Interim temperature data in complex terrain, *Hydrology and Earth System Sciences*, 16(12), 4661–4673, doi:10.5194/hess-16-4661-2012.
- García-Herrera, R., J. Díaz, R. M. Trigo, J. Luterbacher, and E. M. Fischer (2010), A Review of the European Summer Heat Wave of 2003, *Critical Reviews in Environmental Science and Technology*, 40(4), 267–306, doi:10.1080/10643380802238137.
- Gilbert, A., C. Vincent, O. Gagliardini, J. Krug, and E. Berthier (2015), Assessment of thermal change in cold avalanching glaciers in relation to climate warming, *Geophysical Research Letters*, 42(15), 6382–6390, doi:10.1002/2015GL064838.
- GLAMOS (2016): Glaciological reports (1881-2016). "The Swiss Glaciers", *Yearbooks of the Cryospheric Commission of the Swiss Academy of Sciences* (SCNAT) published since 1964 by

- the Laboratory of Hydraulics, Hydrology and Glaciology (VAW) of ETH Zürich. No. 1-134. Online available: <http://glaciology.ethz.ch/swiss-glaciers/> (last accessed: 05.09.2016)
- Haeberli, W., C. Hugel, A. Käb, S. Zraggen-Oswald, A. Polkvoj, I. Galushkin, I. Zotikov, and N. Osokin (2004), The Kolka-Karmadon rock/ice slide of 20 September 2002: An extraordinary event of historical dimensions in North Ossetia, Russian Caucasus, *Journal of Glaciology*, 50(171), 533–546, doi:10.3189/172756504781829710.
- Hubbard, B., and P. Nienow (1997), Alpine subglacial hydrology, *Quaternary Science Reviews*, 16(9), 939–955, doi:10.1016/S0277-3791(97)00031-0.
- Kirchner, M., T. Faus-Kessler, G. Jakobi, M. Leuchner, L. Ries, H.-E. Scheel, and P. Suppan (2013), Altitudinal temperature lapse rates in an Alpine valley: Trends and the influence of season and weather patterns, *International Journal of Climatology*, 33(3), 539–555, doi:10.1002/joc.3444.
- Margreth, S., J. Faillettaz, M. Funk, M. Vagliasindi, F. Diotri, and M. Broccolato (2011), Safety concept for hazards caused by ice avalanches from the Whymper hanging glacier in the Mont Blanc Massif, *Cold Regions Science and Technology*, 69(2-3), 194–201, doi:10.1016/j.coldregions.2011.03.006.
- Müller, P. (1987), Parametrisierung der Gletscher-Klima-Beziehung für die Praxis: Grundlagen und Beispiele, *Dissertation at ETH* (Swiss Federal Institute of Technology in Zurich), ETH dissertation number: 8335.
- Nuth, C., and A. Käb (2011), Co-registration and bias corrections of satellite elevation data sets for quantifying glacier thickness change, *The Cryosphere*, 5(1), 271–290, doi:10.5194/tc-5-271-2011.
- Nye, J. (1976), Water flow in glaciers: jökulhlaups, tunnels and veins. *Journal of Glaciology*, 17 (76), 181–287, doi: 10.3198/1976JoG17-76-181-207.
- Pellicciotti, F., M. Carenzo, R. Bordoy, and M. Stoffel (2014), Changes in glaciers in the Swiss Alps and impact on basin hydrology: current state of the art and future research, *The Science of the Total Environment*, 493, 1152–1170, doi:10.1016/j.scitotenv.2014.04.022.
- Pralong, A., and M. Funk (2006), On the instability of avalanching glaciers, *Journal of Glaciology*, 52(176), 31–48, doi:10.3189/172756506781828980.
- Preiswerk, L. E., F. Walter, S. Anandakrishnan, G. Barfucci, J. Beutel, P. G. Burkett, P. Canassy, M. Funk, P. Limpach, E. Marchetti, L. Meier, and F. Neyer (2016), Monitoring unstable parts in the ice-covered Weissmies northwest face, *13th Congress INTERPRAEVENT*, 434–443. Online available: http://interpraevent2016.ch/assets/editor/files/IP16_CP_digital.pdf (last access: 05.09.2016)
- Richard, L., and A. Tonnel (1985), Contribution à l'étude bioclimatique de l'arc alpin, *Documents de Cartographie Ecologique*, 28, 33–64.
- Rolland, C. (2003), Spatial and Seasonal Variations of Air Temperature Lapse Rates in Alpine Regions, *Journal of Climate*, 16(7), 1032–1046, doi:10.1175/1520-0442(2003)016<1032:SASVOA>2.0.CO;2.
- Röthlisberger, H. (1972). Water pressure in subglacial channels, *Journal of Glaciology*, 11 (62), 177–203.
- Röthlisberger, H. (1981), Eislawinen und Ausbrüche von Gletscherseen, in Gletscher und Klima - glaciers et climat, *Jahrbuch der Schweizerischen Naturforschenden Gesellschaft*,

- wissenschaftlicher Teil 1978, Kasser, P. (Editor), Birkhäuser Verlag Basel, Boston, Stuttgart, 170–212.
- swisstopo DHM25 (2005): DHM25 Das digitale Höhenmodell der Schweiz, *Produktinformation*, Juni 2005. Online available: https://www.swisstopo.admin.ch/content/swisstopo-internet/de/home/products/height/dhm25/_jcr_content/contentPar/tabs/items/dokumente/tabPar/downloadadlist/downloadItems/868_1464696772548.download/dhm25infode.pdf
- Zappa, M., and C. Kan (2007), Extreme heat and runoff extremes in the Swiss Alps, *Natural Hazards and Earth System Sciences*, 7(3), 375–389, doi:10.5194/nhess-7-375-2007.

| Online sources |

- Agisoft PhotoScan Manual (2016):
http://www.agisoft.com/pdf/photoscan-pro_1_2_en.pdf (last access: 27.05.2016)
- alpinesicherheit.ch (2016):
<http://www.alpinesicherheit.ch/safety/detail/id/379> (last access: 19.09.2016)
- ArcGIS.com (2016)
<https://desktop.arcgis.com/de/desktop/latest/manage-data/raster-and-images/fundamentals-for-georeferencing-a-raster-dataset.htm> (last access: 14.01.2016)
- Earth Sciences Spektrum (2016)
<http://www.spektrum.de/lexikon/geowissenschaften/> (last access: 27.05.2016)
- geopraevent.ch (2015)
<http://www.geopraevent.ch/> (last access: 30.07.2015)
- hikr.org (2015)
<http://www.hikr.org/> (last access: 10.09.2016)
- hohsass.info (2016)
<http://www.hohsaas.info/index.php/geschichte> (last access: 27.05.2016)
- swisstopo.ch (2016)
http://www.swisstopo.admin.ch/internet/swisstopo/de/home/topics/nlk/nlk_facts.html (last access: 27.05.2016)
- USGS (2016)
<http://pubs.usgs.gov/of/2004/1216/glaciertypes/glaciertypes.html> (last access: 27.05.2016)

6 Appendix

The supplementary digital results described in *Table 5* can be found on the provided CD in the folder DIGITAL RESULTS.

Table 5: Overview of the supplementary digital results on DVD

Name	Short description of the data set	Chapter Reference
Triftgletscher_PM_1967_2009.gif	Animation of pixel maps	3.1.2
Tongue_Triftgletscher_PM_1862_2009.gif	Animation of position of tongue	3.1.3
Longitudinal_Profile_1971_2014.gif	Animation of the changes of the glacier surface using map information and DEMs	3.1.5
DEM1982_Weissmies.tif	DEM of the study area created with aerial images from 1982	3.1.5

Table 6: Software configuration of Agisoft PhotoScan
If not indicated differently, the default values are used.

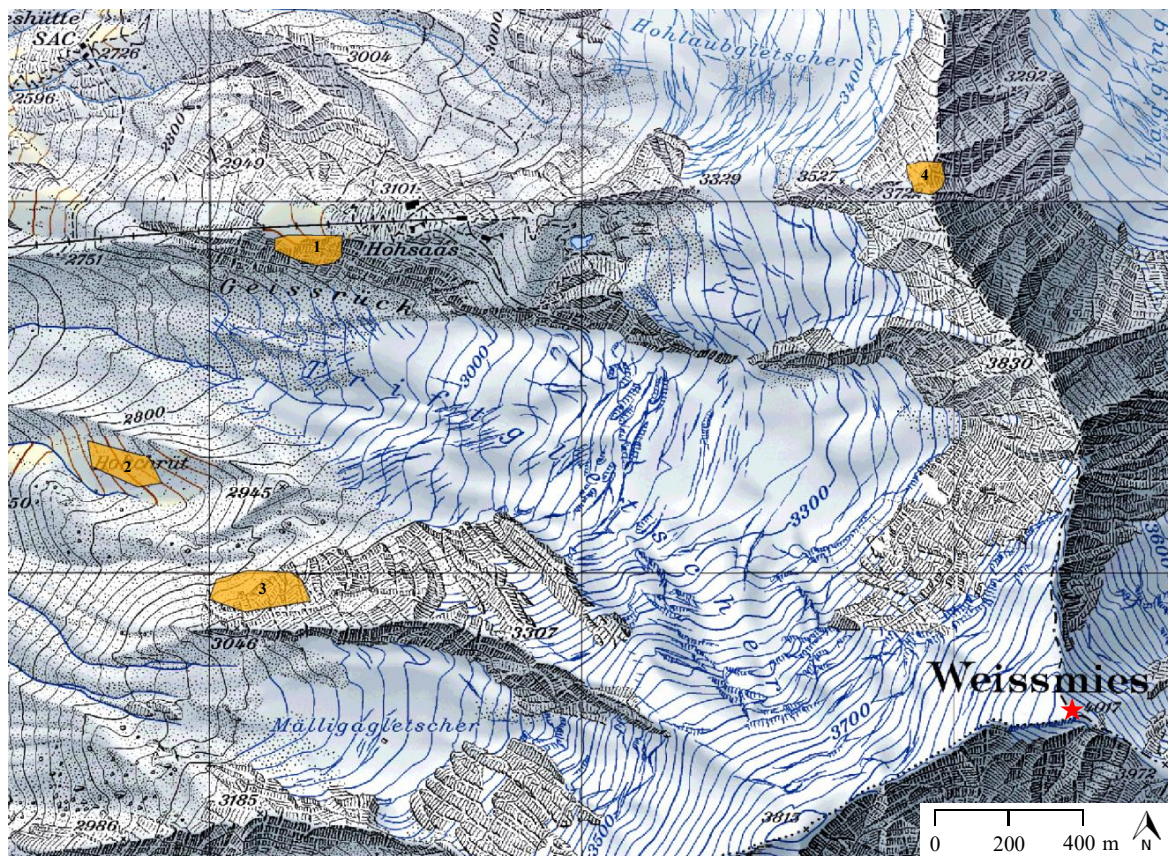
Step	Settings
Align Photos	Accuracy: Medium Pair selection: Generic Key point limit: 40'000 Tie point limit: 0
Build Dense Cloud	Quality: High Depth Filtering: Aggressive
Build Mesh	Surface Type: Arbitrary Source Data: Dense Cloud Face Count: High (898'376)

Table 7: Georeferencing points for the DEM1982

Point Nr	Easting [m]	Northing [m]	Altitude [m]
1	2642542.02	1109939.33	3105.7
5	2641331.99	1108794.32	2696.5
9	2642149.75	1108358.94	3173.8
15	2644304.53	1109092.81	3857.3
18	2641673.02	1110415.96	2725.8
19	2643921.53	1110060.07	3714.2
20	2642139.51	1109255.82	2911.4

Table 8: Description and area of the Co-registration polygons

Polygon	Description of the Underground	Area [m ²]
1	Mostly steep rock walls near the mountain railways.	11997.55372
2	Lateral moraine of the Triftgletscher. It is assumed that this moraine is stable enough for the calculations needed further in this study.	13618.490411
3	Mostly steep rock walls.	22302.208856
4	Not glaciated alpine summit area. The peak was used as a reference point.	7188.566923
Sum =		55106.81991

**Figure 39:** Polygons of the stable areas for the Co-registration

The yellow polygons were used as stable areas for the Co-registration process. The numbers indicate the reference for table 8. The background map is the swiss map raster 1:25'000 from 2009. © swisstopo

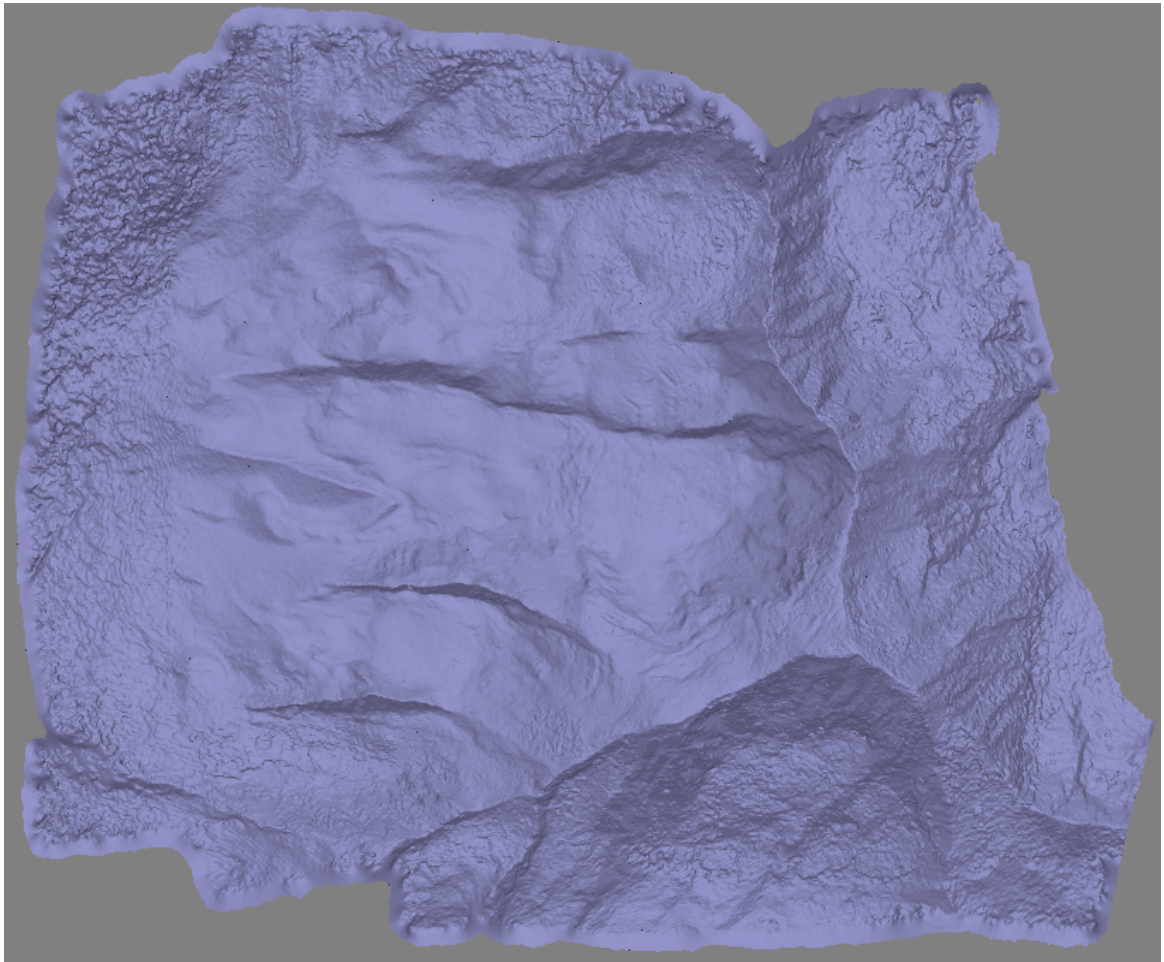


Figure 40: Orthogonal view of the DEM1982 solid model
The model was created in Agisoft Photoscan from aerial photographs from 1982.

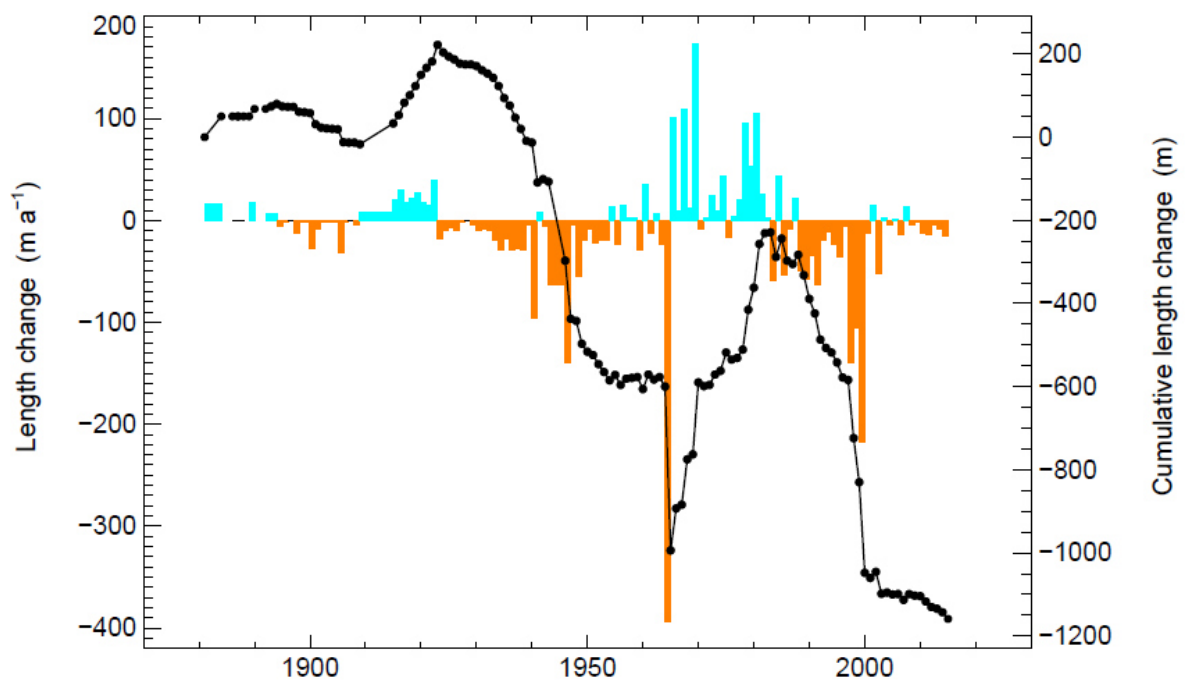


Figure 41: Length changes of Allalngletscher between 1881 and 2015 [GLAMOS, 2016]
The blue bars indicate a glacier increase and the orange bars a glacier decrease. The black dotted line represents the cumulative length change. © GLAMOS

Table 9: Observation protocol for the DEWF index

Date	DEWF Index	Comments
01.04.2015	0	
02.04.2015	-1	
03.04.2015	0	
04.04.2015	-1	
05.04.2015	0	
06.04.2015	0	
07.04.2015	0	
08.04.2015	0	
09.04.2015	0	
10.04.2015	0	
11.04.2015	0	
12.04.2015	0	
13.04.2015	0	
14.04.2015	0	
15.04.2015	10	small stream, not really sheet flow
16.04.2015	0	
17.04.2015	-1	
18.04.2015	0	new snow
19.04.2015	-1	
20.04.2015	0	
21.04.2015	10	small stream, not really sheet flow
22.04.2015	10	larger than the day before
23.04.2015	0	
24.04.2015	10	small stream, not really sheet flow
25.04.2015	-1	
26.04.2015	-1	
27.04.2015	-1	
28.04.2015	0	new snow
29.04.2015	-1	
30.04.2015	0	
01.05.2015	0	
02.05.2015	0	
03.05.2015	-1	
04.05.2015	-1	
05.05.2015	0	
06.05.2015	0	
07.05.2015	0	
08.05.2015	0	
09.05.2015	0	
10.05.2015	10	small stream, not really sheet flow
11.05.2015	10	
12.05.2015	10	
13.05.2015	0	

14.05.2015	0	
15.05.2015	0	
16.05.2015	0	
17.05.2015	10	small stream, not really sheet flow, new snow
18.05.2015	10	
19.05.2015	-1	
20.05.2015	-1	
21.05.2015	-1	
22.05.2015	-1	
23.05.2015	-1	
24.05.2015	-1	
25.05.2015	0	
26.05.2015	0	
27.05.2015	0	
28.05.2015	0	
29.05.2015	0	
30.05.2015	0	
31.05.2015	0	
01.06.2015	-1	
02.06.2015	0	
03.06.2015	10	
04.06.2015	0	
05.06.2015	20	more than the events before
06.06.2015	20	
07.06.2015	20	
08.06.2015	-1	
09.06.2015	-1	
10.06.2015	0	
11.06.2015	-1	
12.06.2015	0	
13.06.2015	20	new snow
14.06.2015	-1	
15.06.2015	-1	
16.06.2015	-1	
17.06.2015	-1	
18.06.2015	-1	
19.06.2015	20	
20.06.2015	0	
21.06.2015	0	
22.06.2015	0	
23.06.2015	0	
24.06.2015	0	
25.06.2015	0	
26.06.2015	30	frontal flow is not very clear
27.06.2015	0	

28.06.2015	30	
29.06.2015	20	
30.06.2015	20	
01.07.2015	0	
02.07.2015	20	
03.07.2015	20	
04.07.2015	20	
05.07.2015	20	
06.07.2015	20	
07.07.2015	20	contrast on the right side not very good
08.07.2015	20	contrast on the right side not very good
09.07.2015	30	
10.07.2015	30	
11.07.2015	30	
12.07.2015	30	
13.07.2015	30	
14.07.2015	30	
15.07.2015	30	
16.07.2015	30	
17.07.2015	20	sheet flow not clear due to contrast
18.07.2015	30	
19.07.2015	20	sheet flow not clear due to contrast
20.07.2015	20	sheet flow not clear due to contrast
21.07.2015	20	sheet flow not clear due to contrast
22.07.2015	20	sheet flow not clear due to contrast
23.07.2015	-1	
24.07.2015	30	
25.07.2015	20	sheet flow not clear due to fog
26.07.2015	20	sheet flow not clear due to contrast
27.07.2015	30	
28.07.2015	30	
29.07.2015	-1	
30.07.2015	20	
31.07.2015	20	sheet flow not clear due to contrast
01.08.2015	-1	
02.08.2015	0	
03.08.2015	10	
04.08.2015	-1	
05.08.2015	40	strong frontal stream
06.08.2015	40	sheet flow not clear due to contrast, strong frontal stream
07.08.2015	40	strong frontal stream
08.08.2015	40	sheet flow not clear due to contrast, strong frontal stream
09.08.2015	-1	
10.08.2015	-1	

11.08.2015	30	new snow
12.08.2015	20	sheet flow not clear due to contrast
13.08.2015	20	sheet flow not clear due to contrast
14.08.2015	-1	
15.08.2015	-1	
16.08.2015	-1	
17.08.2015	-1	
18.08.2015	-1	
19.08.2015	-1	
20.08.2015	0	new snow
21.08.2015	0	
22.08.2015	0	
23.08.2015	0	low contrast due to fog
24.08.2015	0	low contrast due to fog
25.08.2015	-1	
26.08.2015	20	frontal stream no very clear
27.08.2015	10	not much water
28.08.2015	20	
29.08.2015	20	
30.08.2015	30	left frontal channel is active too
31.08.2015	20	sheet flow on the right is not good visible due to low contrast
01.09.2015	-1	
02.09.2015	0	bad contrast due to fog
03.09.2015	-1	
04.09.2015	20	bad contrast due to fog
05.09.2015	-1	new snow
06.09.2015	10	not clear if frontal stream or ice
07.09.2015	10	not clear if frontal stream or ice
08.09.2015	0	not clear if frontal stream or ice, sheet flow not clear due to bad contrast
09.09.2015	10	not much water on the right side, not clear if frontal stream or ice
10.09.2015	0	not clear if frontal stream or ice
11.09.2015	10	
12.09.2015	0	not much water on the right side, not clear if frontal stream or ice
13.09.2015	0	new snow
14.09.2015	0	
15.09.2015	0	
16.09.2015	0	
17.09.2015	0	
18.09.2015	-1	
19.09.2015	0	
20.09.2015	10	not much water on the right side
21.09.2015	-1	
22.09.2015	-1	

23.09.2015	-1	
24.09.2015	-1	
25.09.2015	10	very small
26.09.2015	10	very small
27.09.2015	0	
28.09.2015	0	sheet flow on the right is not good visible due to low contrast
29.09.2015	0	new snow
30.09.2015	0	

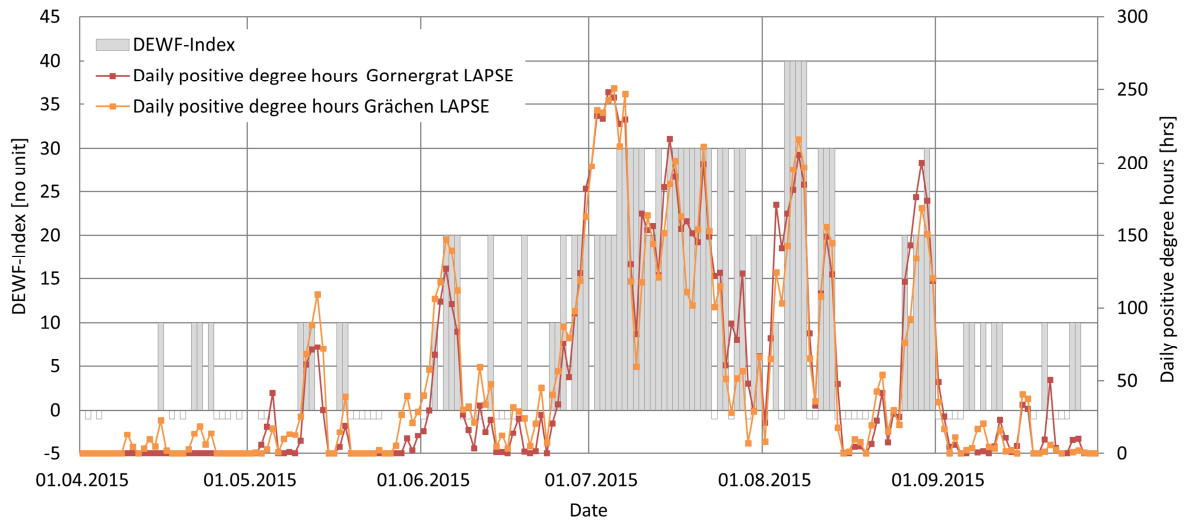


Figure 42: DEWF index and positive degree hours for summer 2015

The graph shows the evolution of the daily positive degree hours together with the evolution of the DEWF index. For the temperatures a lapse rate of $-0.65\text{ }^{\circ}\text{C} / 100\text{ m}$ was used. A negative DEWF index means no data.

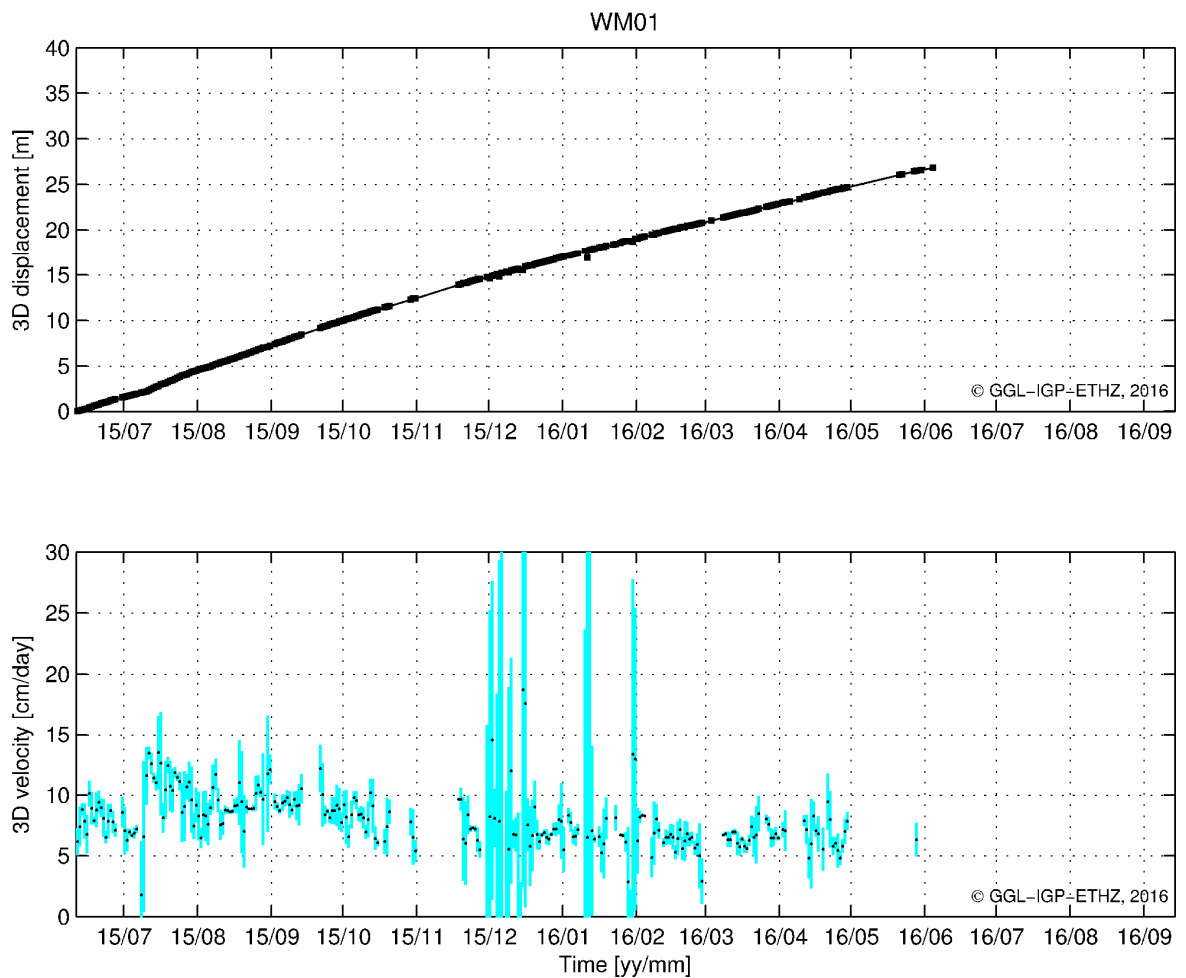


Figure 43: GPS 3D velocities of WM01 June 2015 to September 2016

The blue vertical bars are error bars with 99 % probability. The sensor respectively the signal was down for several points in time, which is indicated by blank spaces. © ETHZ

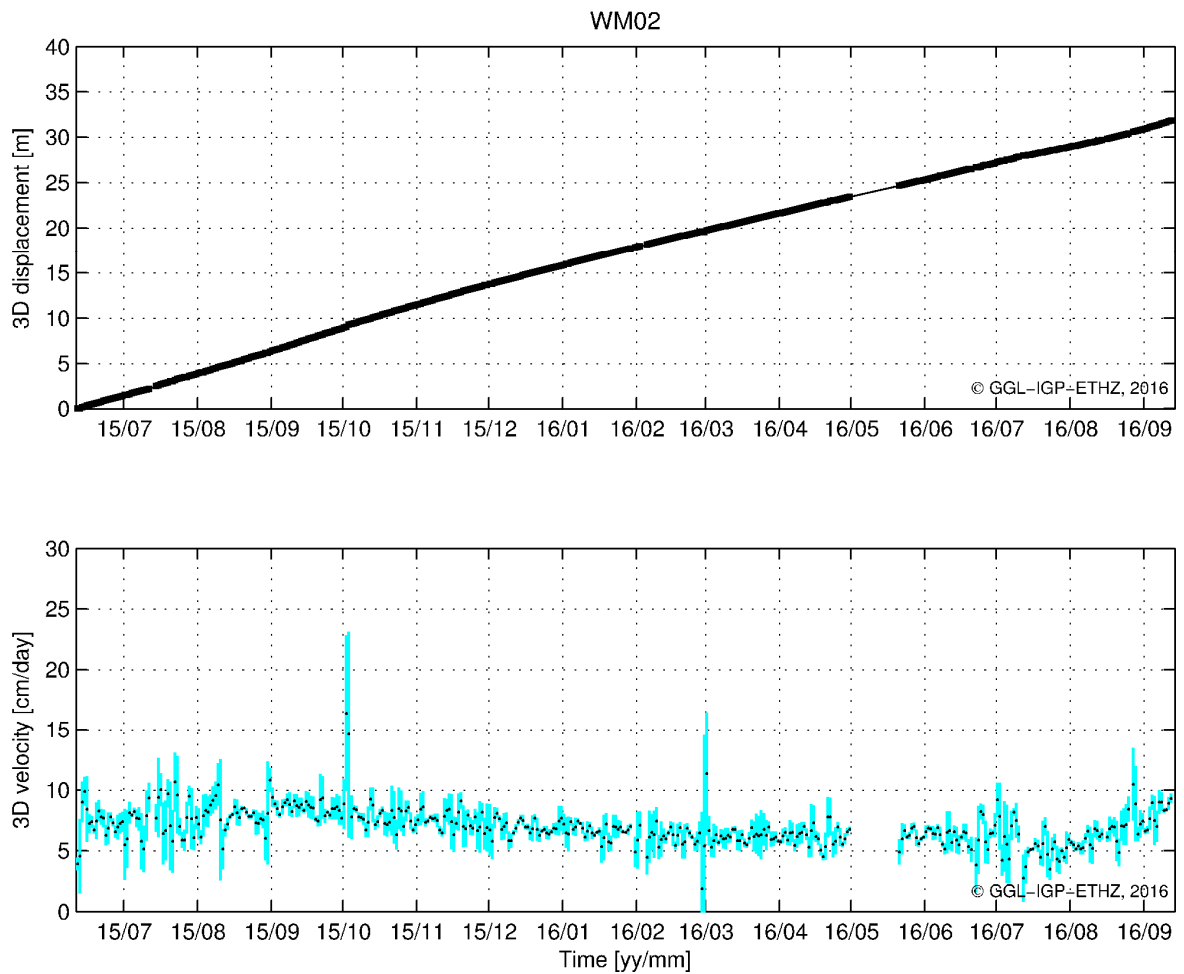


Figure 44: GPS 3D velocities of WM02 June 2015 to September 2016

The blue vertical bars are error bars with 99 % probability. The sensor respectively the signal was down for several points in time, which is indicated by blank spaces. © ETHZ

On the following pages a selection of the collected images of Instabil 1 is shown with the intention to serve as a historical record of its evolution. For some pictures from hikir.org no answer was received from the photographers. Therefore, only for time steps in between those pictures are used with the corresponding reference to the not cleared usage rights. For further pictures (for example from different angels) and contact information, the author of this thesis can be contacted.

Figure 45: 1919, Walter Mittelholzer, © ETHZ

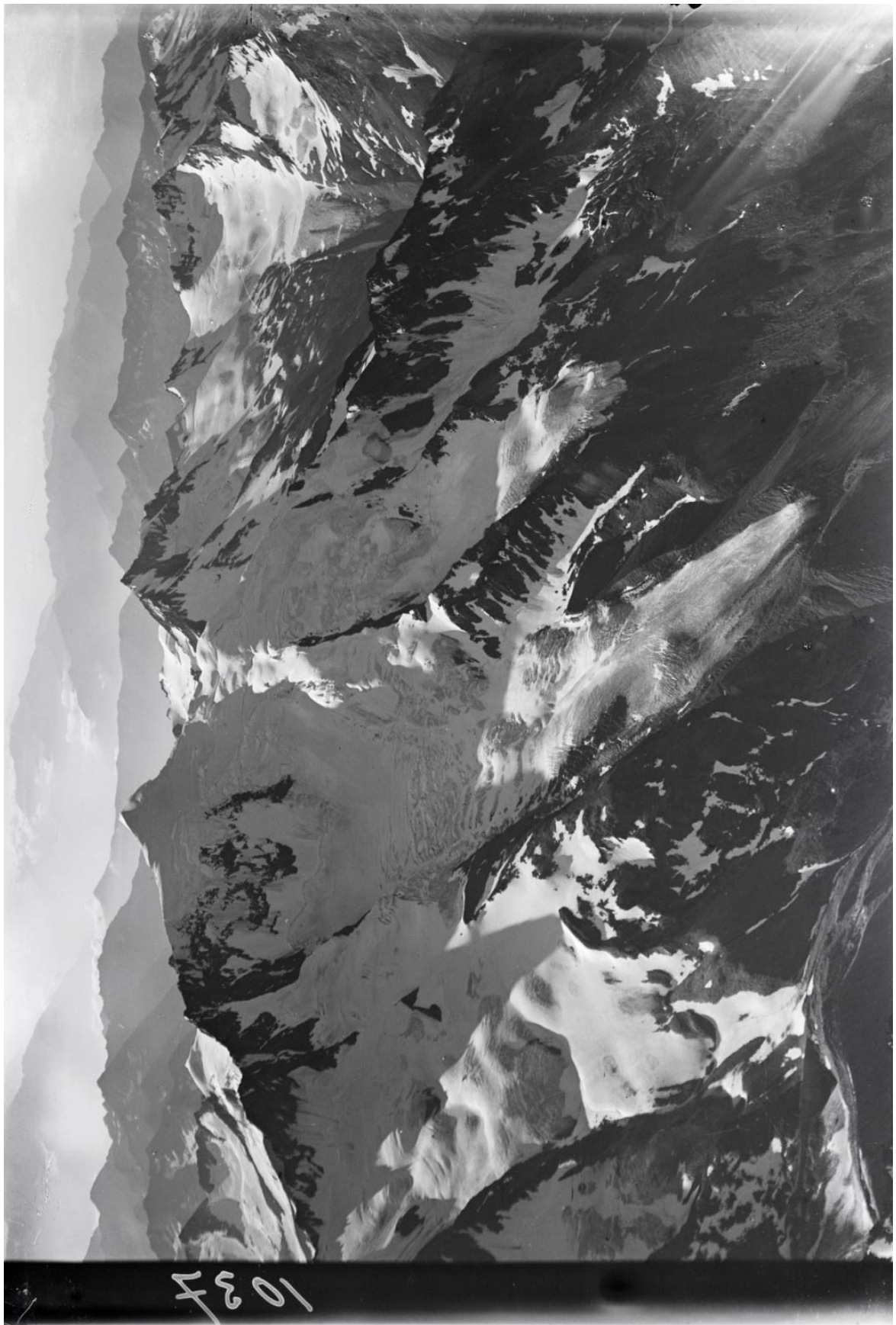


Figure 46: 1949, Werner Friedli, © ETHZ

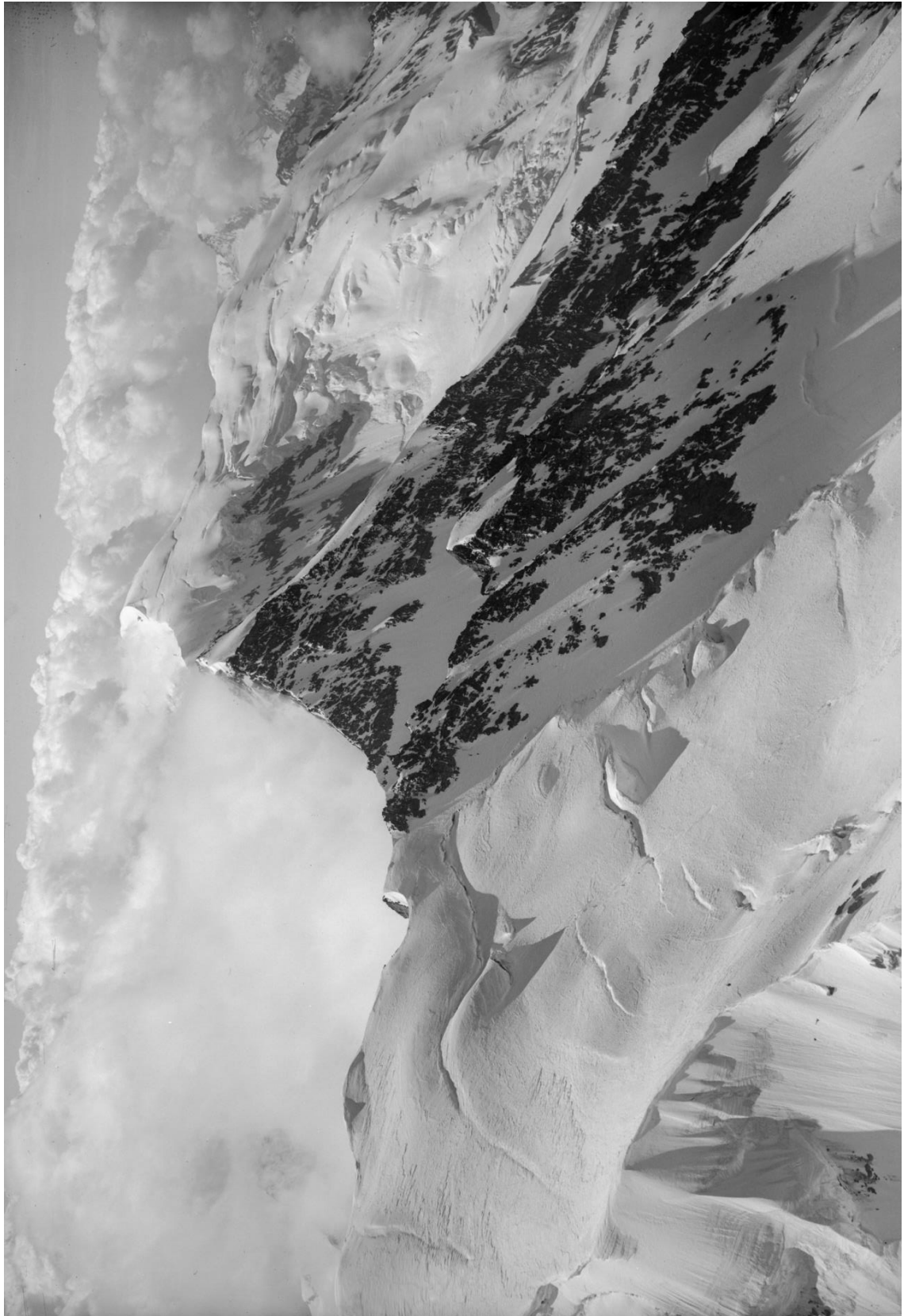


Figure 47: 16.07.1985, © Johannes Erlbruch



Figure 48: 16.07.1985, © Johannes Erlbruch



Figure 49: 11.08.1992, © Emil Abadoglu



Figure 50: 05.08.2003, © Jürgen Wißkirchen



Figure 51: 07.08.2003, © Georg Rothe



Figure 52: 18.07.2004, © Marco (from Florence, he would like to stay anonymous)



Figure 53: 15.08.2004, © Cyrill Rüegger



Figure 54: 17.07.2005, <http://www.hikr.org/tour/post40089.html>, no answer received, picture use rights pending



Figure 55: 17.07.2006, <http://www.hikr.org/tour/post2381.html>, no answer received, picture use rights pending



Figure 56: 07.07.2007, © Michael Thut



Figure 57: 04.08.2007, © Matthias Pilz



Figure 58: 29.06.2008, © Angelo Baldo



Figure 59: 09.07.2008, © Ole Konnerth



Figure 60: 04.07.2009, © Georg Rothe



Figure 61: 07.08.2009, © Katja (she would like to stay anonymous.)



Figure 62: 23.08.2009, © Alexander Müdespacher

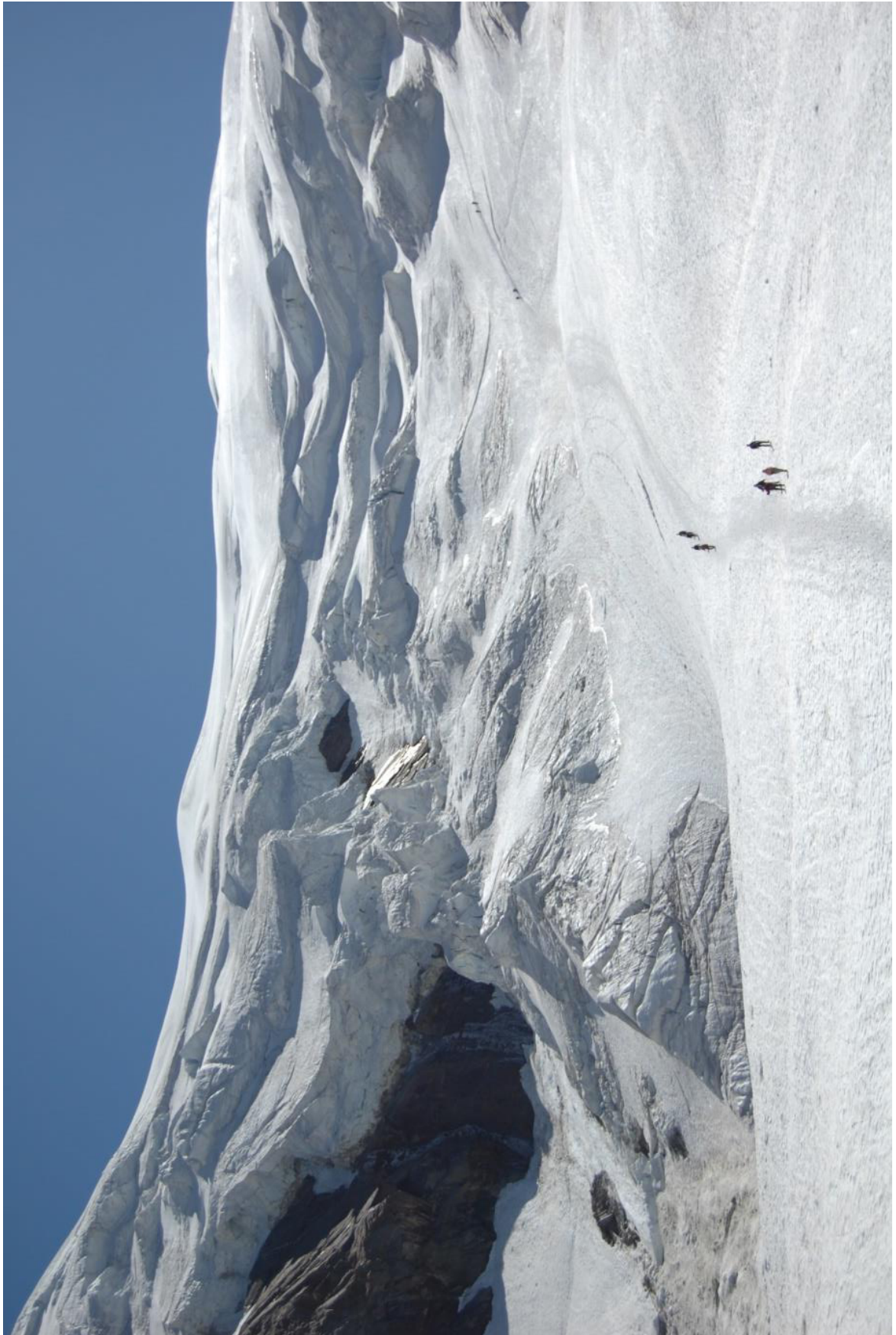


Figure 63: 23.08.2009, © Alexander Müdespacher



Figure 64: 23.08.2009, © Alexander Müdspacher



Figure 65: 30.07.2010, <http://www.hikr.org/tour/post26203.html>, no answer received, picture use rights pending



Figure 66: 29.08.2010, © Marcel Fuchs



Figure 67: 10.08.2011, © Michael Thut



Figure 68: 10.08.2011, © Michael Thut



Figure 69: 25.10.2011, © Vivian Boyer

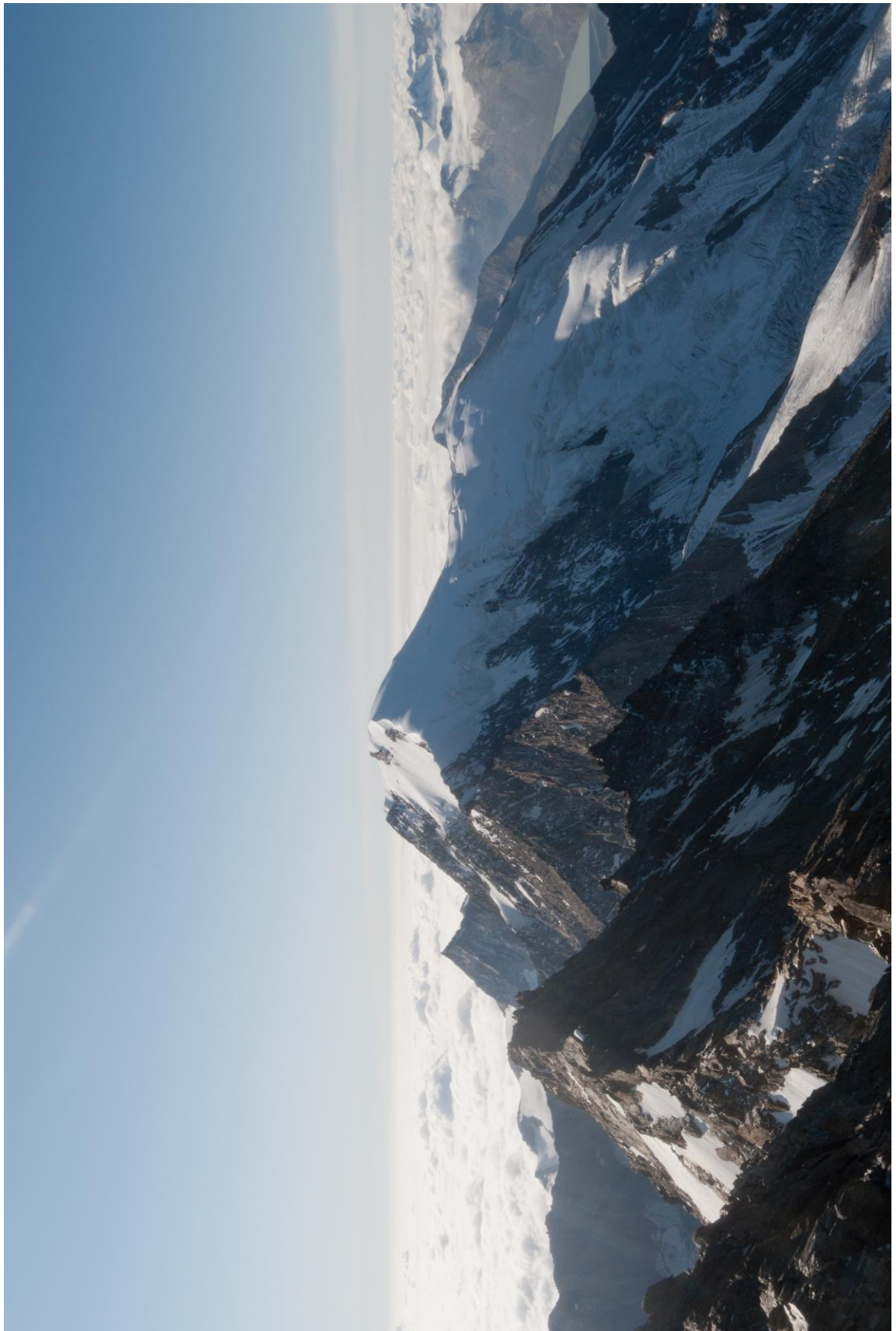


Figure 70: 26.10.2011, © Vivian Boyer



Figure 71: 26.10.2011, © Vivian Boyer



Figure 72: 26.10.2011, © Vivian Boyer

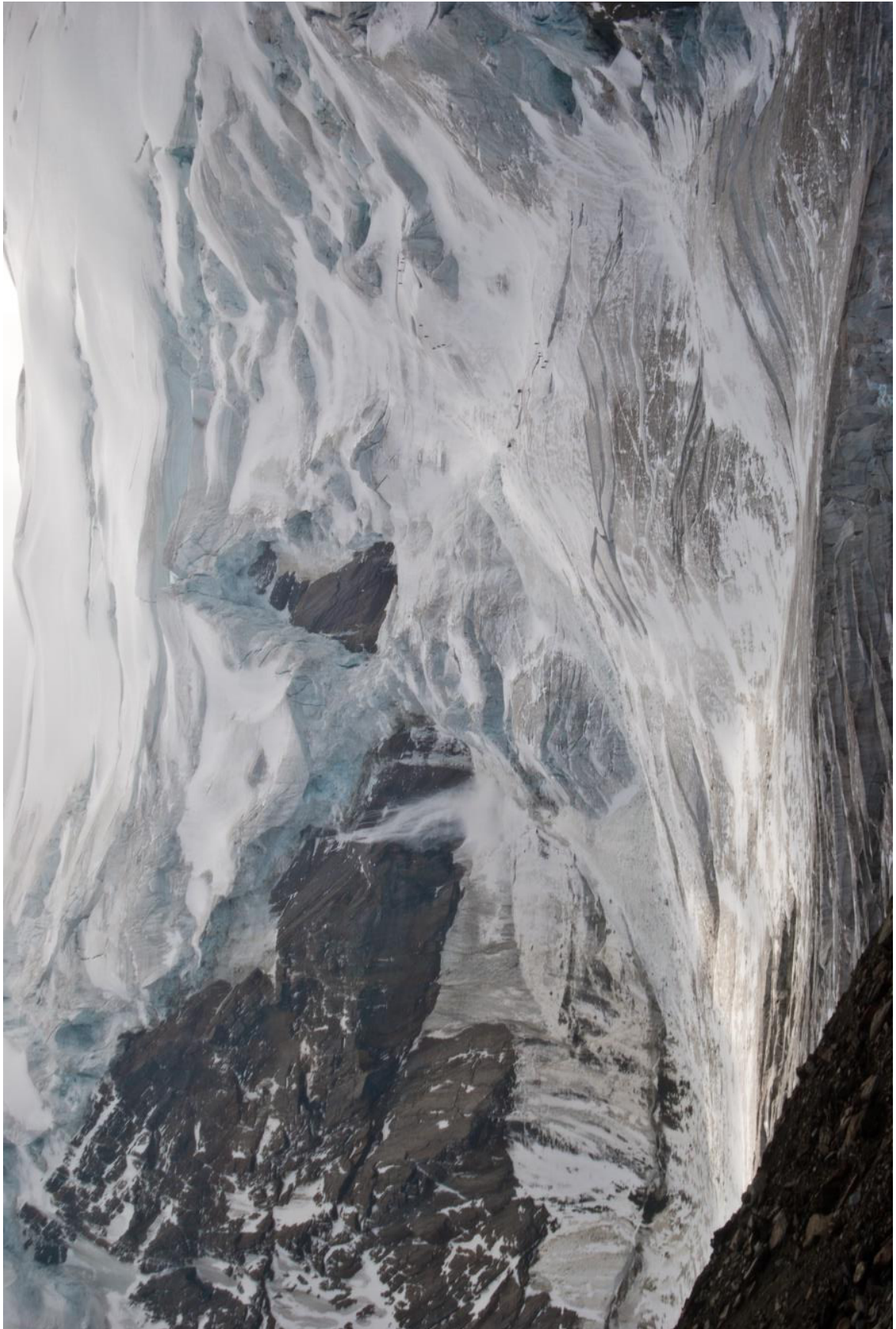


Figure 73: 23.07.2012, © Dimitri Enzler



Figure 74: 23.07.2012, © Dimitri Enzler

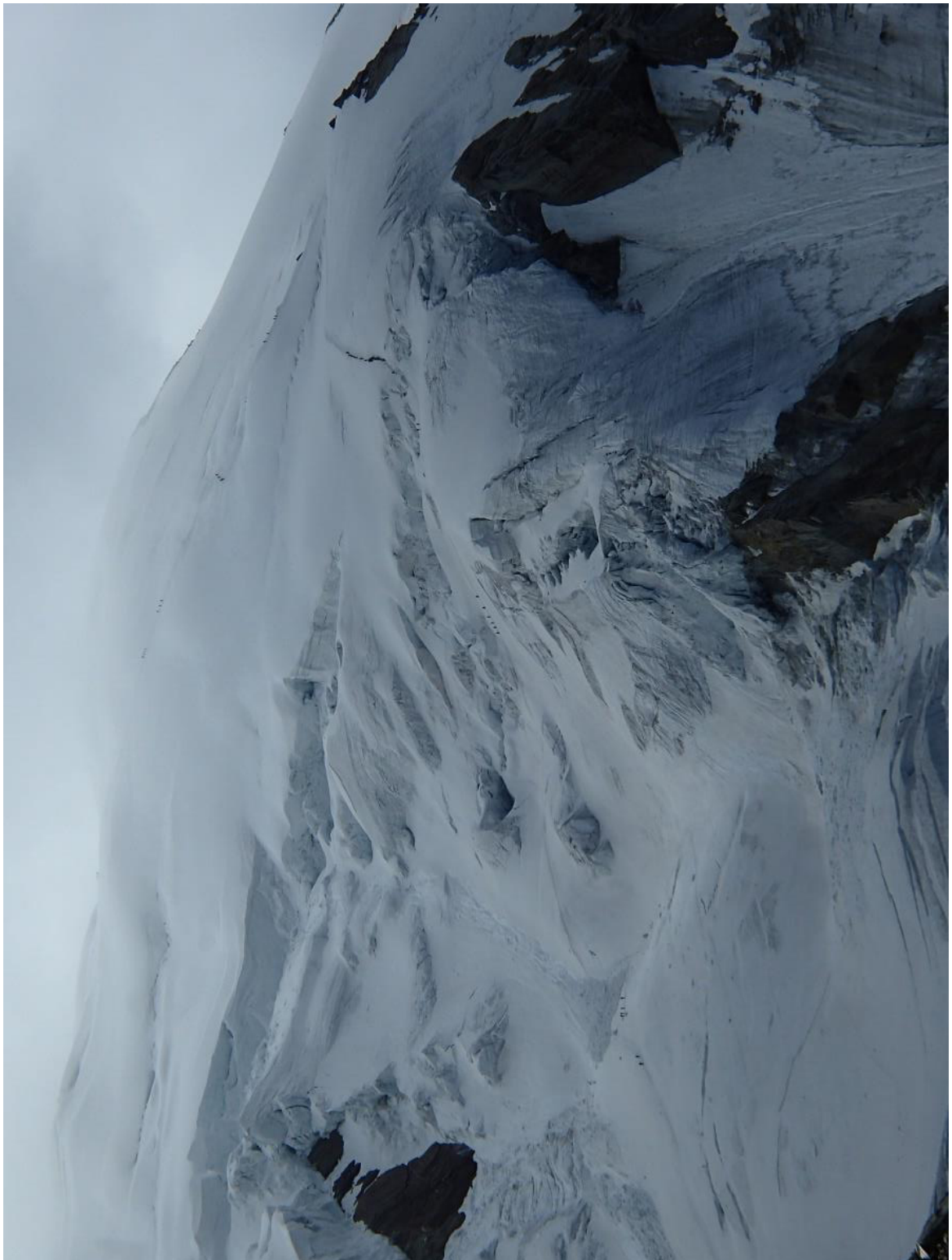


Figure 75: 19.08.2012, © Oliver Schmid

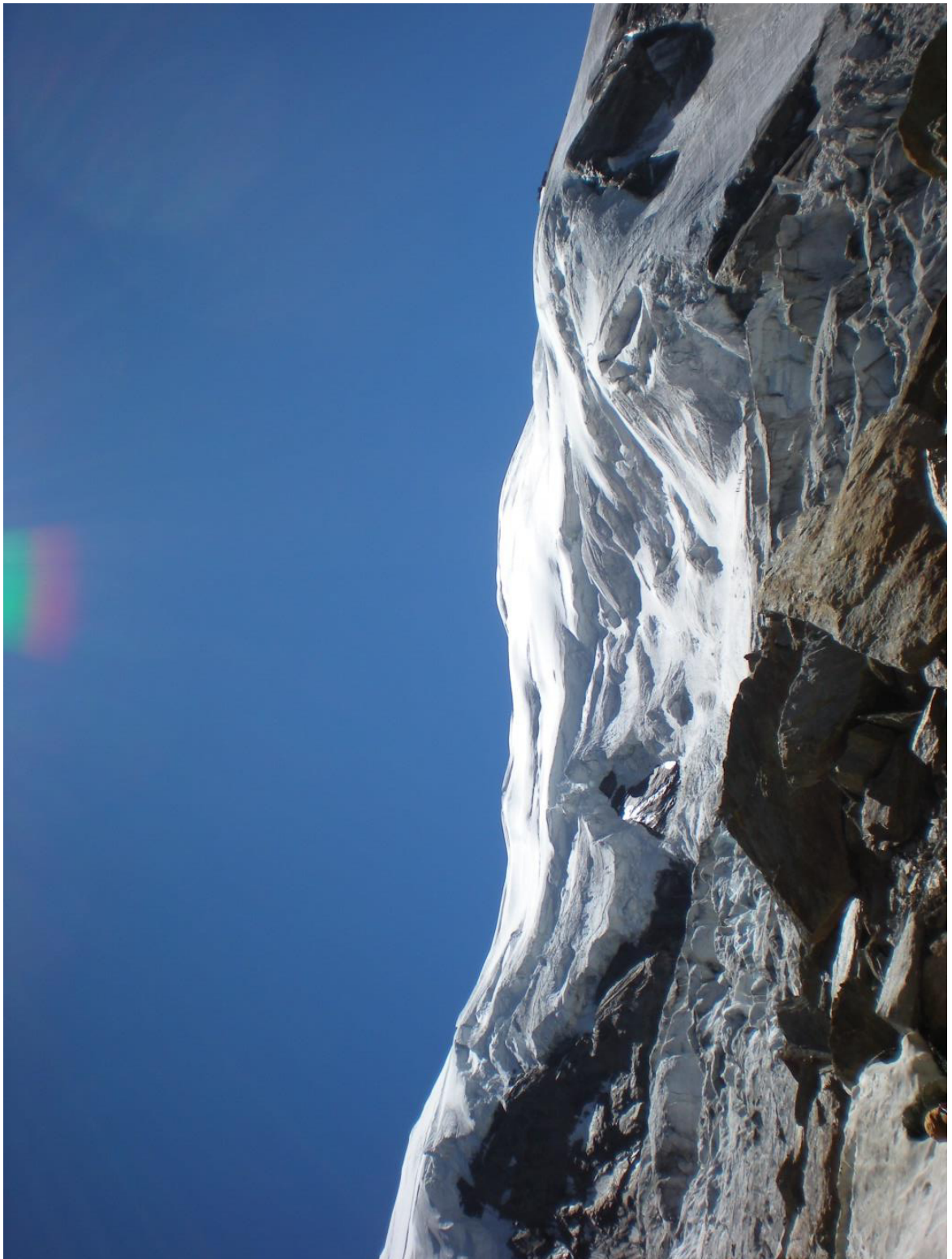


Figure 76: 19.08.2012, © Oliver Schmid



Figure 77: 27.08.2012, © Nicolas Merky



Figure 78: 27.08.2012, © Nicolas Merky



Figure 79: 22.07.2013, © Nicole Ochsner



Figure 80: 30.08.2013, © Fabian Duss

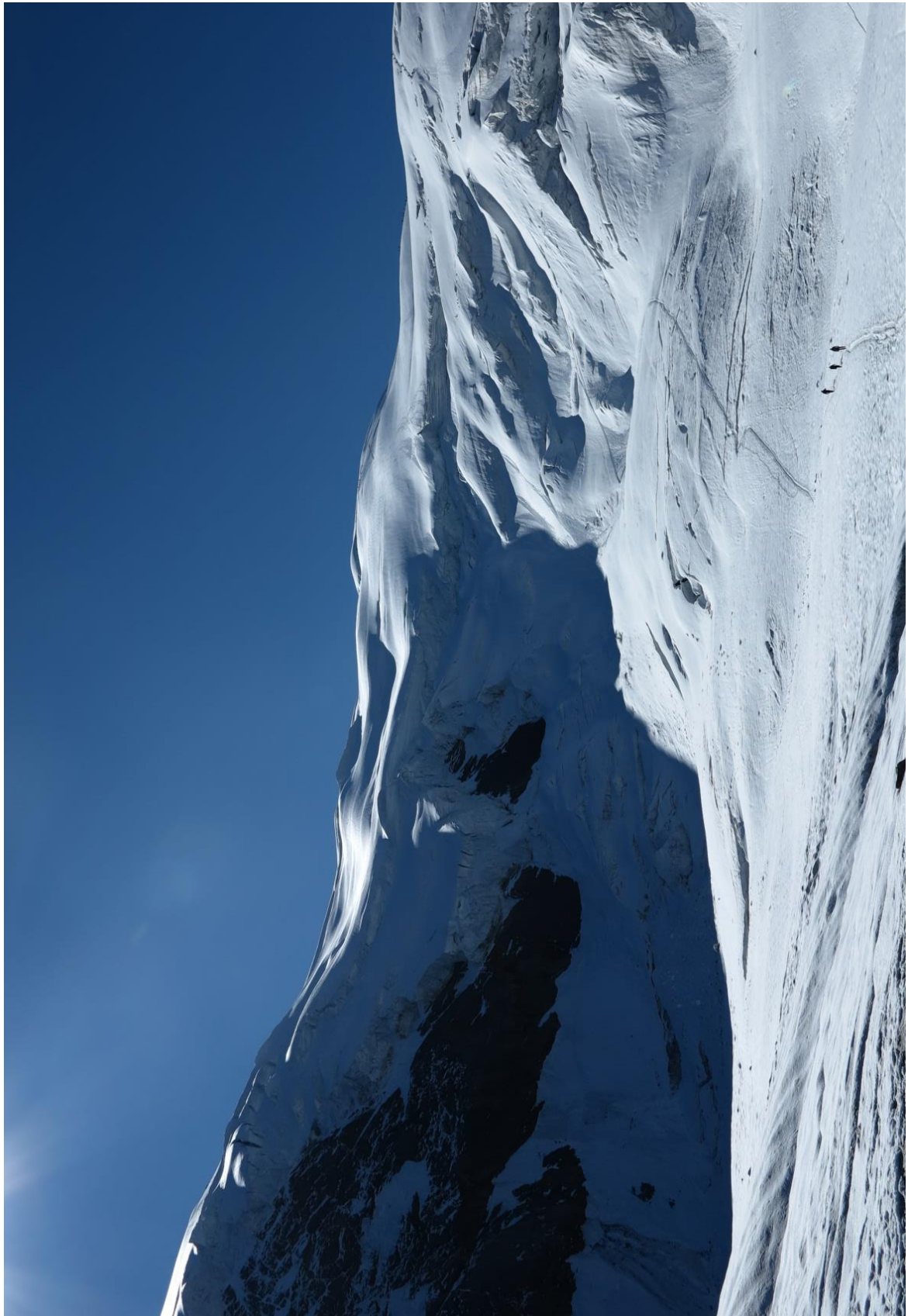


Figure 81: 06.08.2013, © Denis Henß



Figure 82: 15.07.2014, © Alexander Müdespacher

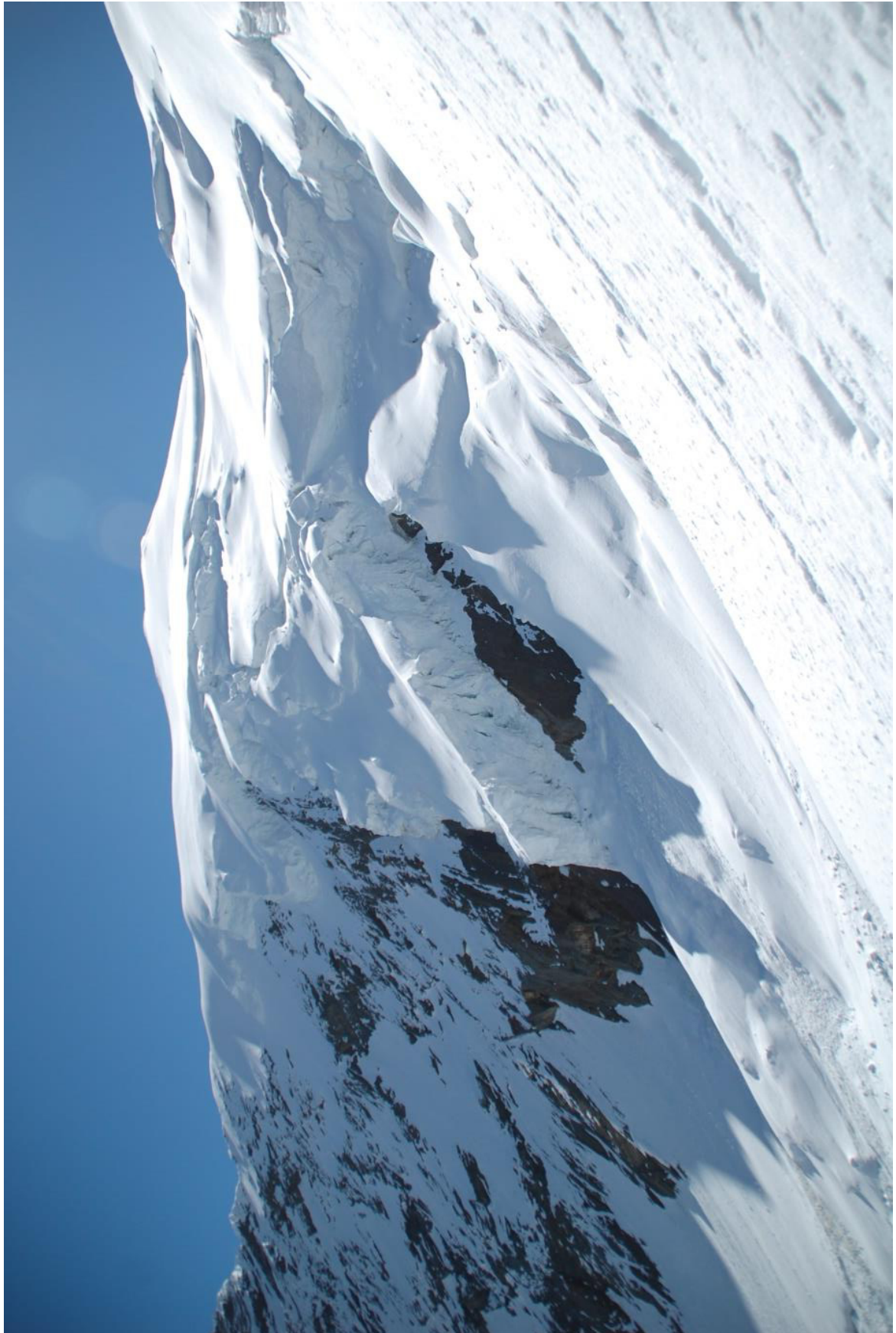


Figure 83: 15.07.2014, © Alexander Müdespacher

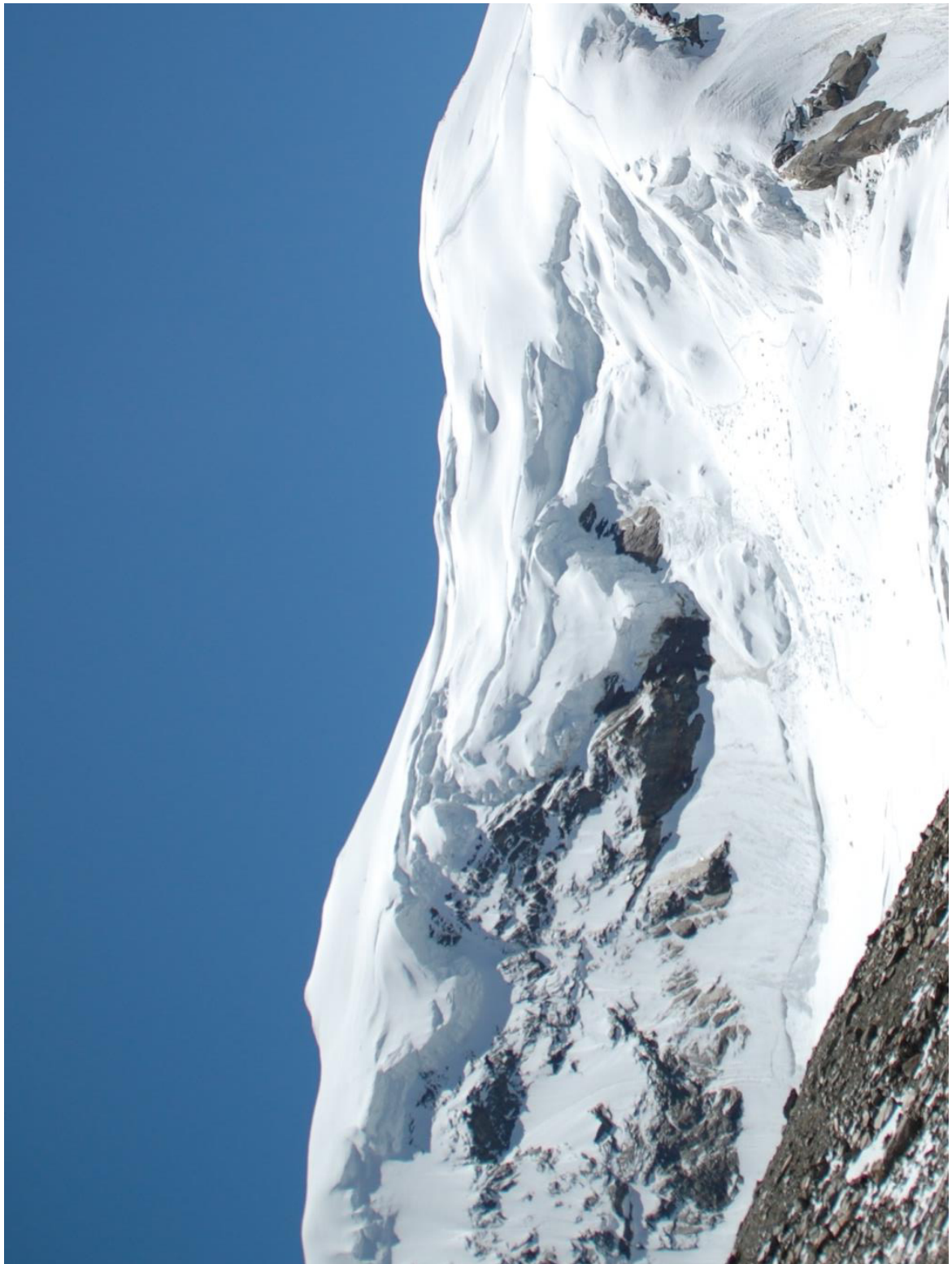


Figure 84: 17.07.2014 © Clemens Walter



Figure 85: 05.08.2014, © Alexandra Bürge



Figure 86: 27.08.2014, © Peter Albert

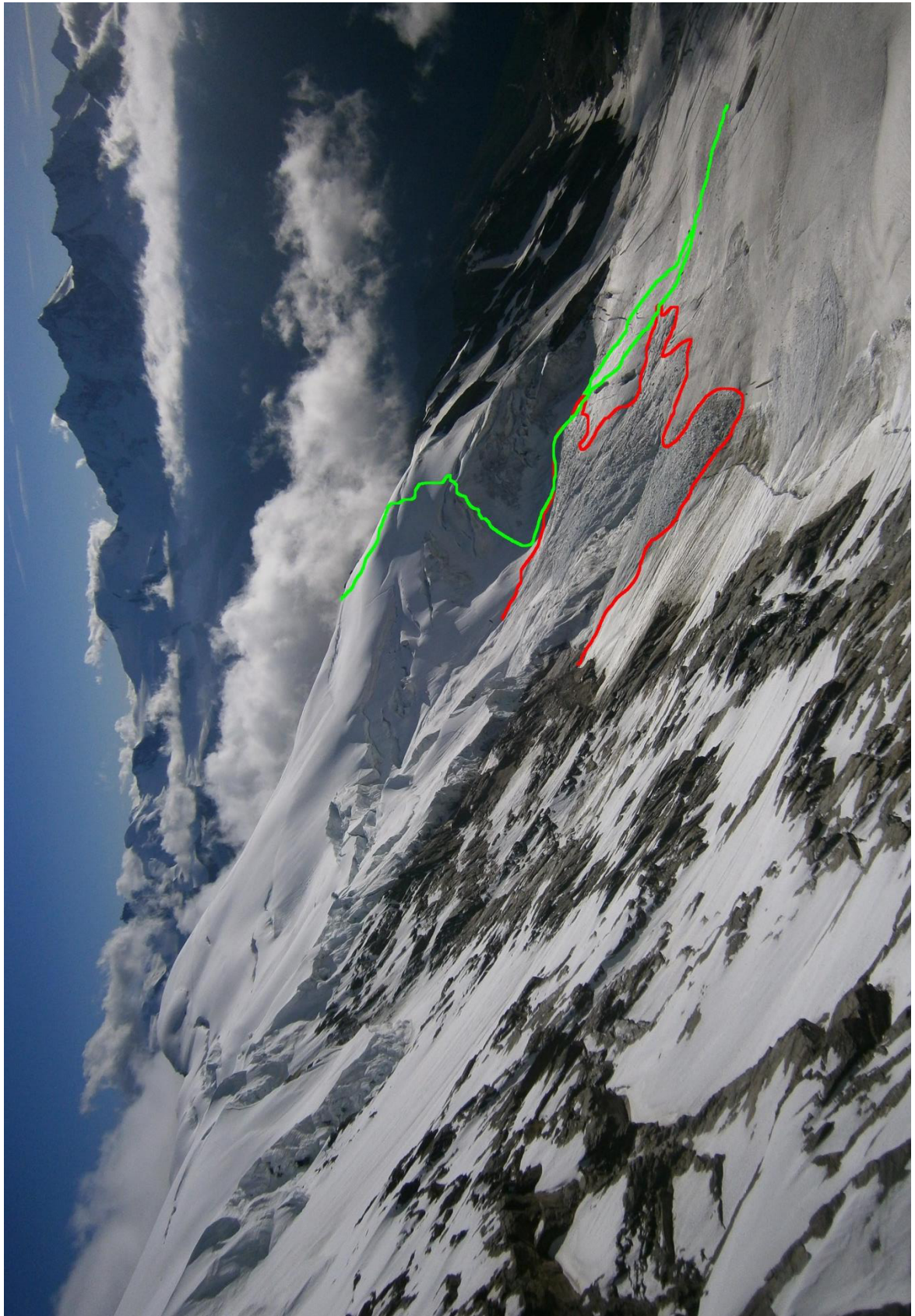


Figure 87: 13.08.2015, ©Alexander Müdespacher



Personal Declaration

I hereby declare that the submitted thesis is the result of my own, independent work. All external sources are explicitly acknowledged in the thesis.

Unterengstringen, 29.09.2016

Michael Peneder